GAS PHASE STUDIES OF *N*-HETEROCYCLIC ORGANIC SPECIES USING MASS SPECTROMETRY

by

KAI WANG

A Dissertation submitted to the

Graduate School-New Brunswick

Rutgers, The State University of New Jersey

in partial fulfillment of the requirements

for the degree of

Doctor of Philosophy

Graduate Program in Chemistry and Chemical Biology

written under the direction of

Professor Jeehiun K. Lee

and approved by

_____

_____

_____

_____

New Brunswick, New Jersey

[May, 2014]

ABSTRACT OF THE DISSERTATION

GAS PHASE STUDIES OF *N*-HETEROCYCLIC ORGANIC SPECIES USING MASS SPECTROMETRY

By KAI WANG

Dissertation Director:

Professor Jeehiun K. Lee

This dissertation focuses on the examination of thermochemical properties, including gas phase acidities, proton affinities and tautomerism of two types of *N*-heterocyclic organic species: damaged nucleobases and 1,2,3-triazoles via mass spectrometry methods (bracketing method on FTMS and Cooks kinetics method on LCQ) and theoretical studies (quantum mechanical calculations). Reactivities of *N*-heterocyclic carbenes as organocatalysts were also studied in the gas phase.

3-Methyladenine DNA glycosylase II (AlkA), which is found in *Escherichia coli*, is an enzyme that cleaves a wide range of damaged nucleobases from DNA. Herein we study the 3-methylated AlkA purine substrates, 3-methyladenine, non-substituted purine and and a potential AlkA substrate, 6-chloropurine. We found that the damaged nucleobases are more acidic than normal nucleobases. Resulting from this increasing of acidity, it is expected that damaged nucleobases are easier to be cleaved from the DNA

chain since their conjugate bases should be better leaving groups. We also find that the gas phase acidities correlate with AlkA excision rate. Thus, the results lend support to the theory that AlkA differentiates among substrates by cleaving those nucleobases which are the most facile to remove.

We also focus on studying the gas phase properties of 1,2,3-triazoles, which, compared with their applications, are largely unknown. The gas phase acidities and proton affinities of benzotriazole, 4-phenyl-1,2,3-triazole, substituted 4-phenyl-1,2,3-triazoles are discussed herein. Moreover, the tautomerism prevalence of 4-phenyl-1,2,3-triazole is acertained by ion-molecule reaction coordinate analysis and H/D exchange studies.

In order to study the reaction mechanism of *N*-heterocyclic carbenes catalyzed reactions such as benzoin condensation, we synthesized a thiazolium catalyst with ethyl sulfonyl group on C4 position of five-membered thiazolium ring. Upon deprotonation, the thiazolium-based carbene is given a negative charge, which renders the visibility for both the carbene and reaction intermediates via mass spectrometry. We herein isolate and study the fragmentation pattern of both free carbene and reaction intermediates using ESI-MS/MS technique. As comparison, we also employ an imidazolium-based NHC to study the benzoin condensation via mass spectrometry and characterize the catalyst as well as the intermediates.

DEDICATION

To my parents, Taishun Wang and Changqing Guo, and to my wife, Ying Pan, for the endless love and support.

ACKNOWLEDGEMENTS

First and foremost, I would like to express my sincere gratitude to Dr. Jeehiun Katherine Lee, for her mentoring, guidance and support in the past five and half years.

I would also like to thank my committee members, Dr. Ralf Warmuth, Dr. Karsten Krogh-Jespersen and Dr. Brian Buckley for their valuable time, attention and help for my research.

I also want to thank Dr. Alexei Ermakov for his wonderful expertise on Mass Spectrometry, thank Dr. Xiaodong Shi from West Virginia University for collaboration, thank my best friend Mu Chen for the friendship and help, thank Xuejun Sun, Min Liu, Anna Zhachkina Michelson, Sisi Zhang, Hao Zeng, Yuan Tian, Yijie Niu, Landon Green for the friendship, share of knowledge and generous support.

I would like to thank my parents, Taishun Wang and Changqing Guo, for their endless love and support; to my parents-in-law, Baoming Pan and Suqin Qin, for their love and understanding. I also want to thank my grandmother, Caihua Zhang, my aunt, Chang-E Guo, my uncle's family, Changrui Guo, Donglian Li and my cousins, Hong Guo and Zhen Zhao for their love and kindness.

Finally, but most importantly, I wish to thank my wife, Ying Pan, who has not just been the most wonderful wife, but also the greatest friend a person could ever have. I could not have completed my research without her support, love, patience and faith in me.

TABLE OF CONTENTS

LIST OF FIGURES

LIST OF TABLES

Chapter 1 Introduction

1.1 Overview

1.1.1 DNA, normal nucleobases and damaged nucleobases

Deoxyribonucleic acid (DNA) is a molecule that restores all the genetic information for the function of all living organisms. DNA is composed of two polymeric chains that are complementary to each other. Each of the chain is further comprised of monomeric units called nucleotides. Each monomer unit, the nucleotide, contains a nucleobase (could be adenine (A), guanine (G), cytosine (T) or thymine (T)) which is attached to the deoxyribose molecule by an *N*-glycosidic bond. A phosphate group is also linked to the sugar via a phosphodiester bond.

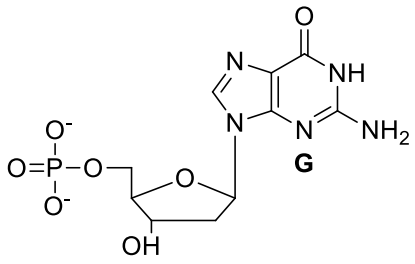

Figure 1.1. Nucleotide structure (with guanine as nucleic base).

Normal nucleobases include adenine (A), guanine (G), cytosine (C) and thymine (T). Both exogeneous agents (environmental mutagens, such as various chemicals, UV light, nucleic radiation) and endogeneous (cellular metabolites) constantly attack DNA, and cause nucleic base modification, thus jeopardizing the integrity of DNA and the

genetic information encoded within it, which may further interfere with DNA replication and transcription and lead to permanent changes in DNA sequence and their biological effects and finally mutation, carcinogenesis and aging.[1-3] There are several kinds of damage to the nucleobases, the most common ones are oxidation, deamination and alkylation. These modifications result in the so called "damaged nucleobases" and selected examples along with normal nucleobases are shown in Figure 1.2.

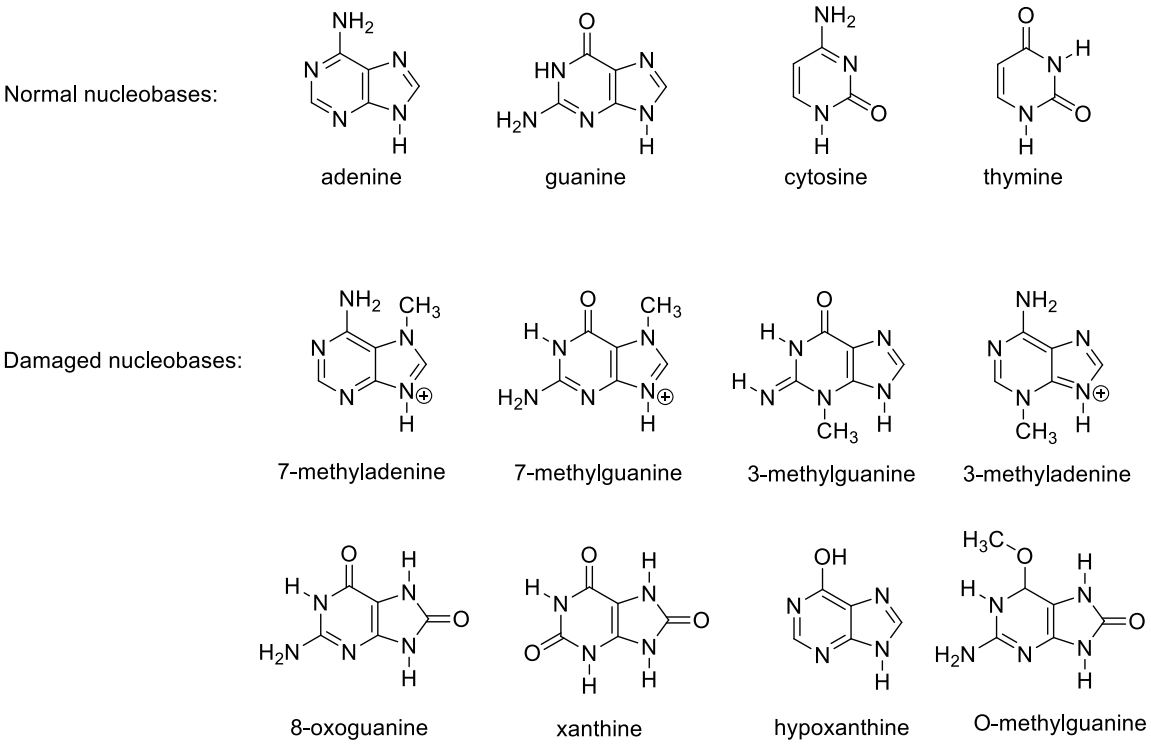

Figure 1.2. Normal nucleobases and selected damaged nucleobases.

1.1.2 DNA glycosylases and base excision repair pathway

Base excision repair pathway (BER), which is a cellular mechanism found in a lot of organisms, repairs damaged nucleobases from DNA. Other than glycosylases which

recognize and remove the damaged nucleobase, there are other types of enzymes functioning in the base excision repair pathway such as "AP endonuclease" which cleaves an AP site to yield a 3'-hydroxyl group next to a 5'-deoxyribosephosphate (dRP); "end processing enzymes" which facilitate the formation of hydroxyl group on 3' end and phosphate group on 5' end; "DNA polymerases" and "ligase" which fill the resulting vacancy.

We are extremely intrigued by the first step of the BER pathway, the removal of damaged nucleobases by glycosylases. Specifically, DNA glycosylases has the ability to recognize the damaged nucleobases, followed by flipping them out of the double helix, and cleaving the *N*-glycosidic bond of the damaged base to leave an abasic site (AP site) while leaving the normal bases untouched. Different organisms have their own glycosylases. The glycosylases found in *Escherichia coli* might be different from those found in human. 3-Methyladenine DNA glycosylase II (AlkA), which can be found in *Escherichia coli,* is an enzyme that cleaves a wide range of damaged bases from DNA including 7-methyladenine (7-MeA), 7-methylguanine (7-MeG), 3-methyladenine (3-MeA), 3-methylguanine (3-MeG), purine (P), xanthine, hypoxanthine, oxanine, etc.[4-8] Normal nucleobases might also be cleaved by AlkA but with much lower efficiency.[8,9] The reason why AlkA has the broad specificity on damaged nucleobases against normal ones remains unclear. It is reasonable to argue that the rate of excision of damaged nucleobases is dependent on the reactivity of the N-glycosidic bond which is related to its stability.[8] The mechanism of the cleavage of *N*-glycosidic bond is believed to occur via S_N1 mechanism, where the leaving of the leaving group happens first.[3] (Figure 1.3)

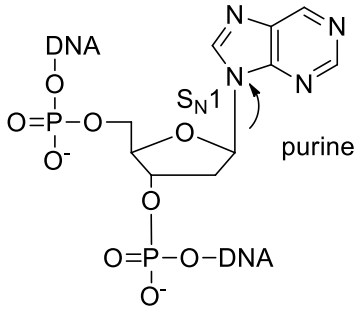

Figure 1.3. Mechanism of the cleavage of *N*-glycosidic bond

Our group previously hypothesized that a similarly functioned enzyme found in human body, alkyl adenine glycosylase (AAG) which also possesses the broad specificity, provides a hydrophobic site that enhances the *N*-glycosidic bond stability difference between damaged nucleobases and normal ones.[10-13] We hypothesized the AlkA accomplished the work similarly. Since it is accepted that alkylated nucleobases and other AlkA substrates have decreased *N*-glycosidic stability compared to normal nucleobases, and therefore can be easily excised, studying the gas phase properties of damaged nucleobases in the gas phase, which is the ultimate nonpolar environment, will be very useful.[10-14]

Therefore, we try to clarify how the AlkA removes such a broad range of damaged nucleobases while leave the normal ones untouched.

1.1.3 Gas phase acidity and proton affinity

The gas phase acidity ΔH_{acid}, unlike the acidity in condensed phases, is defined as the enthalpy change for the deprotonation reaction of AH at 298 K (Eq. 1.1). On the other

hand, the proton affinity (PA) is the negative value of the enthalpy change of protonation reaction at 298 K (Eq. 1.2).[15]

$$HA \rightarrow H^+ + A^- \qquad \textbf{Eq. 1.1}$$

$$B + H^+ \rightarrow HB^+ \qquad \textbf{Eq. 1.2}$$

The gas phase acidities range between 300 to over 400 kcal mol^{-1}, while the proton affinities varies from 130 kcal mol^{-1} (methane) to over 250 kcal mol^{-1} (super base). Selected gas phase proton affinities and acidities values are shown in Table 1.1 and Table 1.2, respectively.

Table 1.1. Selected values of gas phase acidities[15]

Name of molecules	Molecular formula	ΔH^{o}_{acid} (kcal mol^{-1})
Ethane	C_2H_6	420.1
Methane	CH_4	416.6
Ethylene	C_2H_4	407.5
Benzene	C_6H_6	400.7
Water	H_2O	390.7
Iodomethane	CH_3I	386.0
Acetylene	C_2H_2	377.8
Acetonitrile	CH_3CN	372.9
Acetone	CH_3COCH_3	369.1
Nitromethane	CH_3NO_2	357.6

Phenol	PhOH	349.2
Acetic acid	CH_3COOH	348.6
Benzoic acid	PhCOOH	340.2
Iodoacetic acid	IC_6H_4COOH	334.7
Trifluoroacetic acid	CF_3COOH	324.4

Table 1.2. Selected values of gas phase proton affinities[15]

Name of molecules	Molecular formula	PA (kcal mol^{-1})
Methane	CH_4	130.2
Ethane	C_2H_6	142.7
Acetylene	C_2H_2	153.3
Ethylene	C_2H_4	162.6
Water	H_2O	165.2
Formaldehyde	CH_2O	170.4
Benzene	C_6H_6	179.3
Acetic acids	CH_3COOH	187.3
Acetone	CH_3COCH_3	197.2
Diethyl ether	$CH_3CH_2OCH_2CH_3$	200.2
Ammonia	NH_3	204.0
Aniline	$C_6H_5NH_2$	210.9
Dimethylacetamide	$CH_3CON(CH_3)_2$	217.0

Piperidine	$C_5H_{11}N$	228.0
1,5-Diazabicyclo[4.3.0]non-5-ene	$C_7H_{12}N_2$	248.2

1.1.4 Triazoles

The cycloaddition of azides and alkynes to yield triazoles was first disclosed by Huisgen in 1967.[16] However, the reaction did not draw much attention due to the harsh reaction conditions and lack of regioselectivity. Since the discovery of copper-catalyzed version of Huisgen cycloaddition, the copper-catalyzed-azide-alkyne-cycloaddition (CuAAC, also referred as "click chemistry"), 1,2,3-triazoles have become very popular due to their unique properties and applications.[17-31] Click chemistry, on the other hand, is a modular approach that only utilizes the most reliable and practical transformations and CuAAC falls into this particular category.[32] Click chemistry was first described by Barry Sharpless, Valery Fokin and M. G. Finn in 2001.[17] It is not a specific reaction, but an idea to mimic the nature to join small molecules together.

Huisgen thermal cycloaddition

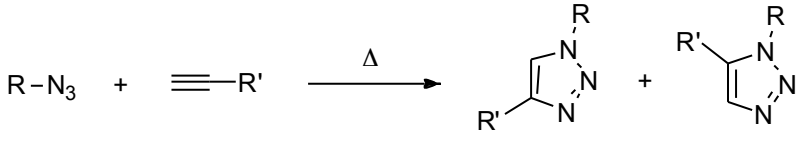

Copper-catalyzed-azide-alkyne cycloaddition (CuAAC)

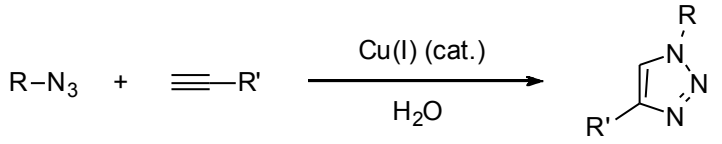

Figure 1.4. Huigen thermal cycloaddition and Copper-catalyzed-azide-alkyne cycloaddition (CuAAC)

Huisgen thermal cycloaddition yields a mixture of C4 and C5 substituted triazoles, while CuAAC gives only C4 substituted triazole. In 2008, ruthenium was also used to catalyze the cycloaddtion reaction and C5 substituted triazole was obtained.[33] Our collaborator, Xiaodong Shi from West Virginia University developed one-pot cascade synthetic method for the synthesis of 4,5-disubstituted triazoles. Through post-triazole alkylation and arylation of NH triazoles, efficient synthetic methods for N2 alkyl- and aryl- substituted 1,2,3-triazoles were developed.[34-36] (Figure 1.5)

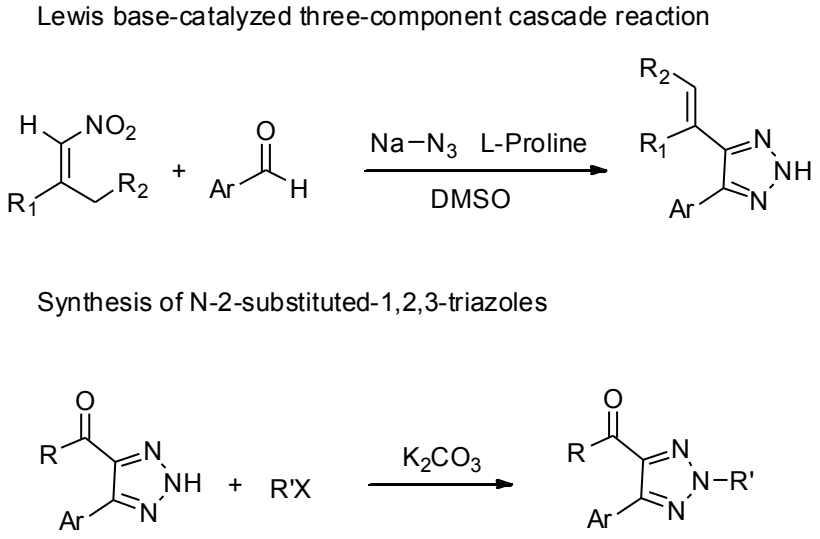

Figure 1.5. Lewis base-catalyzed three-component cascade reaction and synthesis of N-2 substituted 1,2,3-triazoles by Dr. Xiaodong Shi

1,2,3-Triazoles are able to coordinate with transition metals such as ruthenium (Rh) and gold (Au) to form triazole-Rh(I) and triazole-Au(I) complexes, the latter of which is a catalyst with improved stability and efficiency for electrophilic activation of alkynes

compared with traditional cationic Au(I) catalysts.[37-45] NH triazoles can be used as both neutral ligands and anionic ligands. On the other hand, N-substituted triazoles can only coordinate as neutral ligands.

The fundamental thermochemical properties of these compounds, on the other hand, are little-known. [46-52] Furthermore, Abboud and coworkers gave some ambiguous results for the gas phase proton affinity and tautomerism about 4-phenyl-1,2,3-triazole.[47] Therefore, we try to disclose the fundamental properties of 1,2,3-triazoles in the gas phase using both computational and experimental methods.

1.1.5 Benzoin condensation, N-Heterocyclic carbenes

Stable *N*-heterocyclic carbenes (NHCs) were first reported by Arduengo and coworkers in 1991 and have demonstrated broad applications in various areas[53]. However, the idea of stable carbene was proposed long before that. In 1958, Breslow proposed a thiazolium-based carbene to catalyze the benzoin condensation.[54-57]

The coupling of two benzaldehyde catalyzed by cyanide, the benzoin condensation, was first reported by Liebig in 1832.[58] Kinetics of this reaction has been studied by Bredig and coworkers in 1904.[59] This reaction is further carefully reviewed by Lachman in 1923 who found that benzaldehyde and benzoin are able to convert to each other when the reaction is catalyzed by cyanide ion in alcoholic-H_2O solution.[60] The reversibility of this reaction was also studied experimentally by Buck in 1931, Sumrell in 1956, Kuebrich in 1971; and theoretically by Yamabe in 2009.[61-64]

In 1958, Breslow proposed reaction mechanism of benzoin condensation catalyzed by thiazolium and imidazolium salts. Breslow mechanism (Figure 1.6) features the formation of C2-ylide **II**, generated *in situ* from the deprotonation of parent thiazolium

salts **I** with mild bases. Subsequent nucleophilic addition to a benzaldehyde, after deprotonation, yields a resonance-stablized intermediate **IV** (**V**), which is also referred as "Breslow intermediate". A second benzaldehyde adding to the intermediate **IV** gives diphenylhydroxy thiazolium adduct **VI**, which eventually releases the benzoin and re-generates thiazolium ylide **II**.

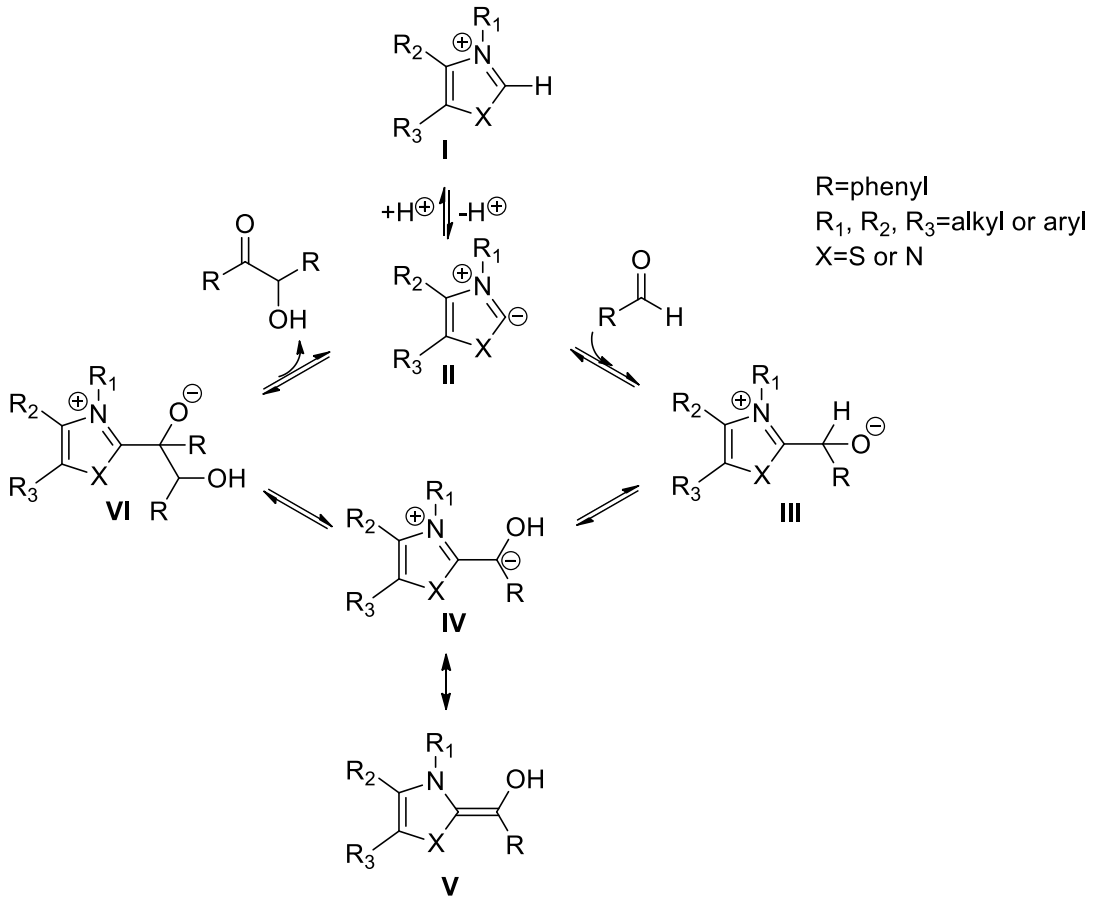

Figure 1.6. Mechanism of benzoin condensation catalyzed by thiazolium- or imidazolium-based carbene proposed by Breslow.

In 1960, Wanzlick proposed that the carbene generated from vacuum pyrolysis is in equilibrium with its dimer, which he believed, only acts as the carbene reservoir.[65-68]

Challenges to Breslow mechanism and Wanzlick equilibrium by Lemal, and later by Winberg claimed that the carbene dimer is actually catalytically active in the catalytic circle.[69,70] Since the late 1980s, Castells and coworkers proposed alternative dimer mechanism.[71-77] Later, controversial results on Castells dimer mechanism were reported.[78,79] Up till today, Breslow mechanism has still been the dominant and well-accepted mechanism for benzoin condensation.

In the past half century, scientists have been taking efforts to develop chiral thiazolium catalysts in order to give enantioselective benzoin condensation reaction. The selected examples have been summarized in Table 1.3, and the catalysts shown in Table 1.3 are listed in Figure 1.7.

Table 1.3 . Benzoin condensation catalyzed by thiazolium catalysts

Entry	Thiazolium catalyst	Author	Year	Yield	e.e.	Reaction condtions
1	1a[80]	Sheehan	1966	9%	22%	MeOH; Et_3N; Ambient temperature
2	1b[81]	Sheehan	1974	6%	52%	MeOH; Et_3N; 30 ^oC
3	1c[81]	Sheehan	1974	78%	7.8%	MeOH; Et_3N; 30 ^oC
4	1d[82]	Tagaki	1980	20%	35%	H_2O; Et_3N; 0.5M phosphate buffer (PH8)Room Temperature
5	1d[82]	Tagaki	1980	trace	N/A	MeOH; Et_3N; 0.5M phosphate buffer (PH8)

						Room Temperature
6	1e[82]	Tagaki	1980	82%	0.8%	H_2O; Et_3N; 0.5M phosphate buffer (PH8) Room Temperature
7	1f[73]	Calahorra	1993	11.5%	27%	MeOH; Et_3N; 30 ^oC
8	1f[73]	Calahorra	1993	20.6%	26%	MeOH; Et_3N; 0 ^oC
9	1g[83]	Leeper	1997	34%	20%	MeOH; Et_3N; 20 ^oC
10	1h[83]	Leeper	1997	50%	20.5%	EtOH; Et_3N; 80 ^oC
11	1i[84]	Rawal	1998	18%	30%	MeOH-H_2O (1:2.5); Et_3N; Ambient temperature

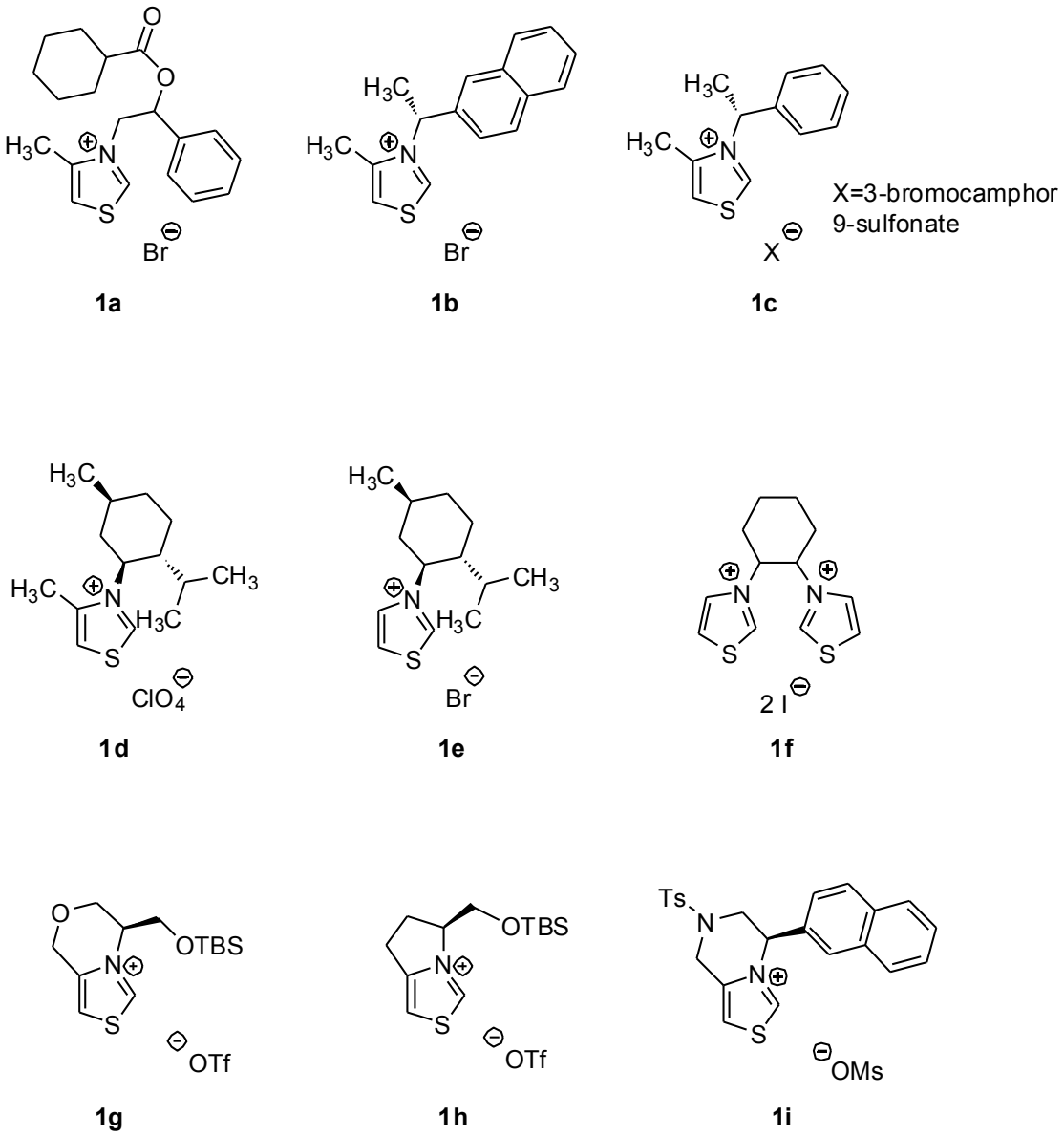

Figure 1.7. Thiazolium-based catalysts from Table 1.3.

Imidazolium-based NHCs have become more and more popular since the first isolation of NHC by Arduengo in 1991.[53,85-89] Benzoin condensation catalyzed by imidazolium-based catalysts also have became popular since then and selected references are summarized in Table 1.4.

Table 1.4. Imidazolium catalyzed benzoin condensation

Entry	Imidazolium catalyst	Author	Year	Yield	ee	Reaction condtions
1	2a[90]	Miyashita	1994	79%	Not reported	MeOH; NaOH; Room Temperature
2	2b[90]	Miyashita	1994	54%	Not reported	MeOH; NaOH; Room Temperature
3	2c[91]	Gao	2002	91%	Not reported	THF; NaOH; Refluxing
4	2d[92]	Xu	2005	86%	Not reported	CH_2Cl_2; K_2CO_3; Room temperature
5	2d[93]	Estagar	2006	97%	Not reported	Solvent free; MeONa; 150 ^oC; microwave
6	2a[94]	Iwamoto	2006	0%	Not reported	H_2O; Et_3N; Room temperature
7	2f[94]	Iwamoto	2006	99%	Not reported	H_2O; Et_3N; Room temperature
8	2g[94]	Iwamoto	2006	98%	Not reported	H_2O; Et_3N; Room temperature

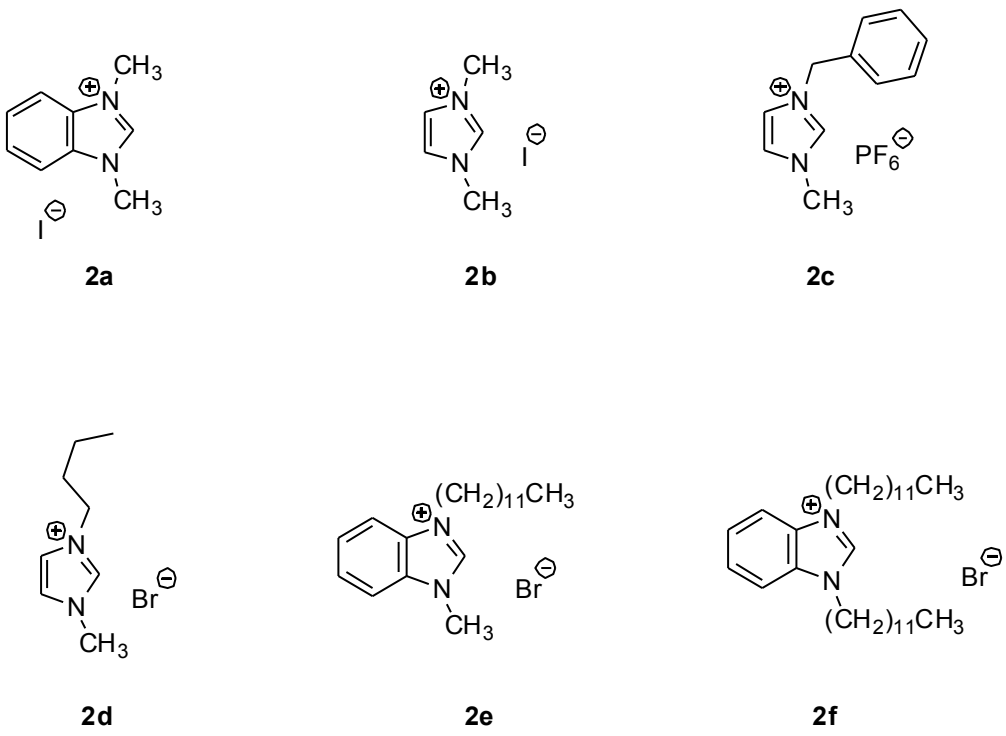

Figure 1.8. Imidazolium-based catalysts from Table 1.4.

Other than thiazolium and imidazolium catalysts, 1,2,4-triazolium-based catalysts also received great attention and developed significantly over the years.[95-102]

Neutral carbenes are undetectable by mass spectroscopy, and intermediates are usually unstable and have the propensity of fragmentation. Introducing a charged handle to NHC will address the first issue while using a "soft" electrospray ionization tendem mass spectrometry (ESI-MS/MS) will help the latter.[103] ESI-MS/MS has achieved recognition as a tool to probe the reaction mechanisms over the years.[104-106] Thus, we apply this method to characterize a novel thiazolium NHC with sulfonate group as charged handle in an effort to develop a useful method to monitor the reaction via mass spectrometry. A related imidazolium catalyst was also used to study the mechanism, which has previously been described by Lalli and coworkers.[107]

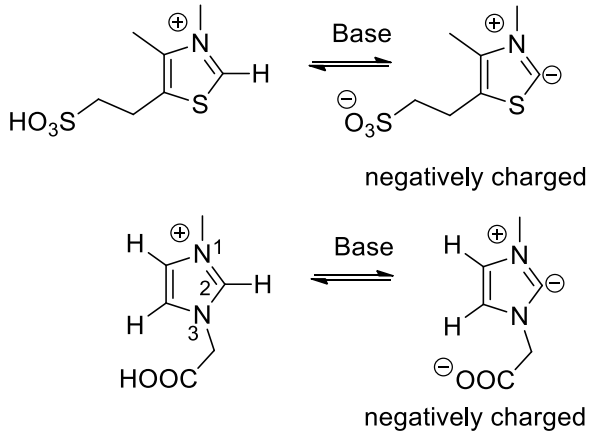

Figure 1.9. Thiazolium and imidazolium catalysts with charged handle.

1.2 Instrumentation

1.2.1 FTMS

Fourier Transform Ion Cyclotron Resonance (FT-ICR), also known as Fourier Transform Mass Spectrometry (FTMS), is a unique type of mass spectrometry to analyze the mass-to-charge ratio of charged species. FTMS has been known to yield excellent resolution and accuracy and out-perform most of the other mass spectrometers.[108] In the mean time, high maintenance is required for FTMS.[109,110] Fourier transform mass spectrometry evolved from ion cyclotron resonance (ICR) spectrometry, which was first developed in 1930s by Lawrence.[111] In 1974, inspired by the development of FT-NMR technique, Comisarow and Marshall applied the Fourier transform method to ICR-MS, and built the very first FTMS instrument.[109,112]

A superconducting magnet, accompanied by high-vacuum system, cell(s) and data-processing system compose the FTMS.[109] The magnet is kept cold by cryogens (liquid helium and liquid nitrogen); high vacuum is achieved by diffusion pumps and mechanical pumps. Our customized dual-cell Finnigan 2001 FTMS, equipped with a 3.3 Tesla superconducting magnet and vacuum system (mechanic and diffusion pumps), is able to pump to pressure as low as 10^{-9} Torr. Two adjacent 2-inch cubic cells are placed collinearly with each other (also referred as the "source cell" (closer to solids probe) and "analyzer cell (right cell when looking toward the control panel), see Figure 1.10. We use batch inlets, pulsed valves, leak valves and solids probe to introduce compounds into the cells, and conduct the gas phase studies. Solids probe only introduces solid samples while pulsed valves, leak valves and batch inlets are able to send in liquid samples. Our FTMS is also equipped with an ESI source (Figure 1.11) which is able to ionize the chemicals softly.

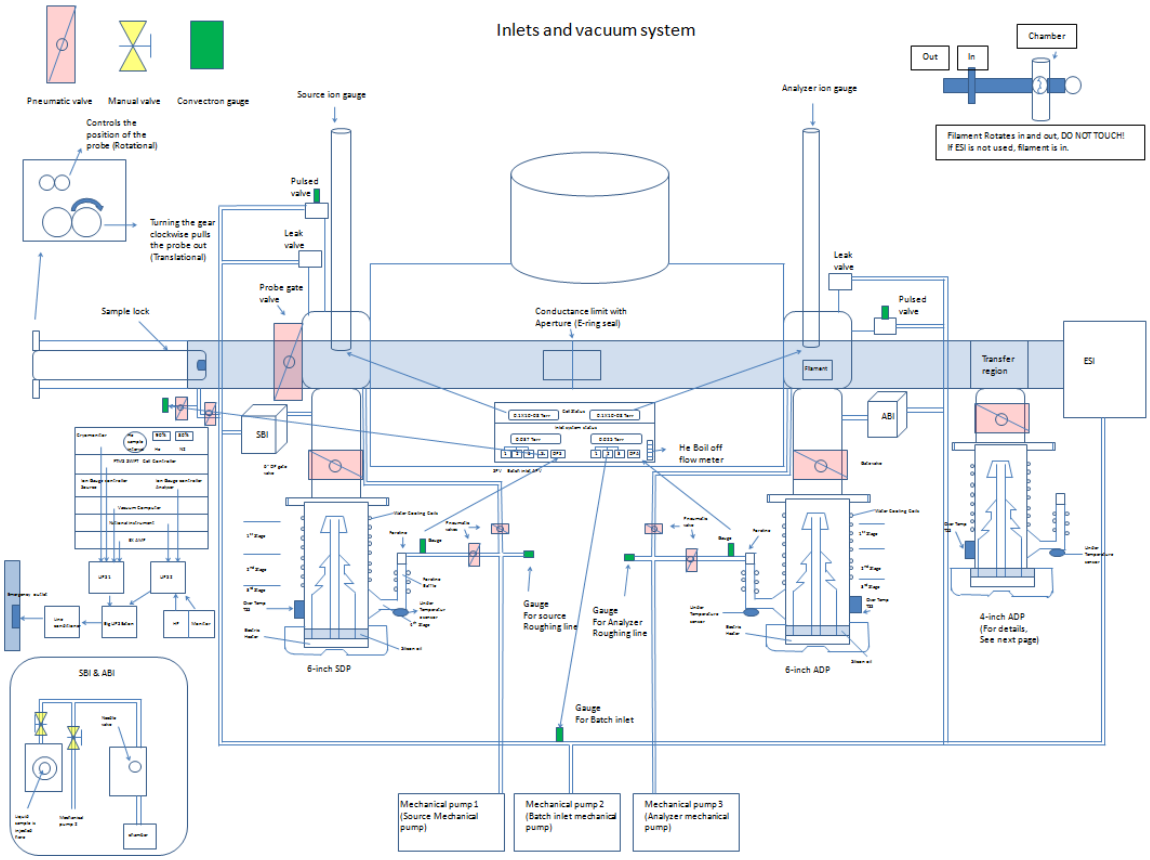

Figure 1.10 Detailed scheme of our FTMS (Finnigan 2001).

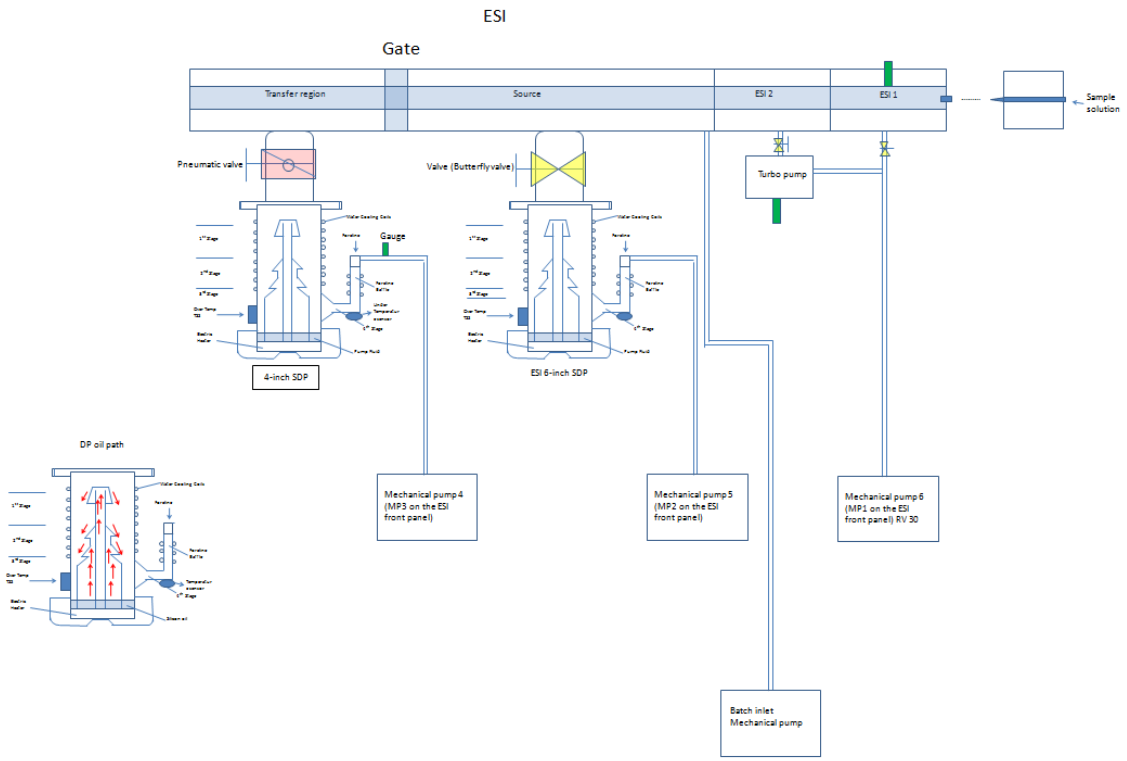

Figure 1.11 Detailed scheme for transfer region and ESI of FTMS (Finnigan 2001).

1.2.2 Electrospray ionization and quadrupole ion trap mass spectrometer

Electrospray ionization (ESI) is a special way to generate ions in the gas phase. It relies on the electronic repulsion to produce the liquid drops. Since it is conducted in the atmospheric pressure, it belongs to the atmospheric pressure ionization (API) sources. The advantage of using ESI is that it could give minimum fragmentation upon ionization of analytes. Therefore, it is especially useful when conducting mechanism studies such as generating “fragile” ions. As a soft ionization method, it could also be employed when studying mechanisms by generating reaction intermediates from reaction aliquot.

When using ESI, volatile solvent is often used such as methanol, acetonitrile and water. Chemicals dissolved in such solvents will be evaporated and electrosprayed into a heating capillary under a flow rate of 1 μL/min~1 mL/min.

An ion trap is a setup that is able to "trap" the ions in certain areas by applying different electric field. The 3D quadrupole ion trap was invented by Wolfgang Paul in 1989, which rendered him the Nobel Prize in the same year.[113] Therefore, the 3D quadrupole ion trap is also called Paul trap. It is extremely intriguing by providing the possibility of conducting tandem mass analyzing. [114] Our group utilized a quadrupole ion trap spectrometry to conduct structural elucidation studies as well as thermochemical property measurements via collision-induced fragmentation (CID).

1.3 Methodology

1.3.1 Bracketing method

As described previously, we have a dual cell setup for our FTMS. The cells are called the source cell and the analyzer cell, individually. Essentially, these two cells are the same and there is a 2 mm hole in the center of the trapping plate for ions to move from one to the other. The pressure of the cells has to be pumped down to 1×10^{-9} torr as appropriate vacuum needs to be achieved for ion detection. This is accomplished by a diffusion pump-mechanical pump setup. Excited ions can be cooled by Argon. There are different ways to introduce chemicals into the cells such as a heated solids probe to introduce solid samples, heated batch inlets for liquid samples, or pulsed valves or leaking valves.

The protocol for bracketing experiments has been described in detail by our lab previously.[10-12,14,115] Briefly, when conducting acidity bracketing experiments, hydroxide ions are produced through chemical ionization in the FTMS cells by sending an electron beam (8 eV, 6 μA) through the cell from a heated filament to ionize the water. The hydroxide ions then deprotonate neutral molecules "HA" (either unknowns or reference acids) to give the conjugate base, A^- ions. The A^- ions are transferred to the other cell and initiate proton transfer reaction with either the unknown or reference. The reactions for both directions are conducted and efficiencies calculated (Figure 1.12a and 1.12b), by which we can assess the occurrence and non-occurrence of the proton transfer, which also reflects whether the reaction is exothermic or endothermic. The same procedure is used for proton affinity bracketing, while different electron energies (20 eV, 6 μA) are used.

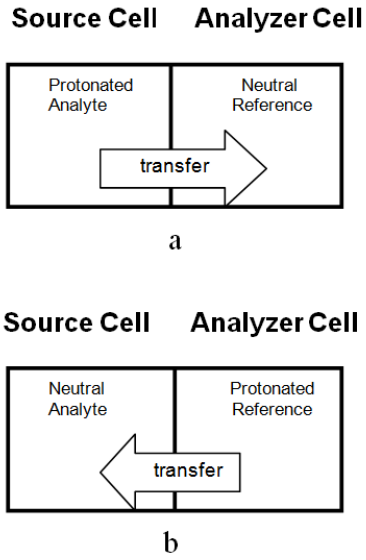

Figure 1.12. Scheme of FT-ICR dual cell bracketing experiments: (a) S->A; (b) A->S

Again, reaction efficiency is used to determine the occurrence (exothermicity) or non-occurrence (endothermicity) of a proton transfer reaction (Eq. 1.1); If the calculated value is higher than 10%, we assume the reaction occurs, and *vice versa*. The k_{exp} value is obtained from experiments while k_{coll} is calculated using Average Dipole Orientation (ADO) program.[116,117]

$$Efficiency = \frac{k_{\exp}}{k_{coll}} \times 100\% \qquad \textbf{Eq. 1.1}$$

The experimental rate constant k_{exp} is calculated from Eq. 1.2:

$$k_{\exp} = \frac{-slope}{P_{neutral} \times \Theta} \qquad \textbf{Eq. 1.2}$$

In Eq. 1.2, Θ is a conversion factor of 3.239×10^{16} molecule·cm^{-3}·torr^{-1}; The slope is a parameter that reflects the decrease of reactant ions over time under pseudo-first-order reaction conditions. Also, we need to eliminate the effects of neutral by dividing the neutral pressure.

Other than measuring the "most" acidic (basic) site of analytes, our group previously developed a method to study the second most acidic (basic) sites using bracketing method.[12,14] We call it the "less" site measurements. Different from "most" acidic (basic) site bracketing, reactant ions will be transferred from source cell to analyzer cell immediately upon generation and react will the reference acid (base). The purpose of removing the reactants immediately is to prevent from isomerization of the reactant ions to maintain the existence of ions with deprotonated (protonated) "less" site. In the "less"

site measurements, the 10% cutoff is no longer used. In this case, the observation of the proton transfer determines the exothermicity of the reaction.

1.3.2 Cooks kinetic method

We also used the Cooks kinetic method (LCQ) to measure the acidities and proton affinities of compounds.[118-122] Briefly, we first need to isolate the proton-bound dimer between the unknown and reference. Collision-induced dissociation (CID) is applied and results in the formation of protonated (deprotonated) unkown and neutral reference, or the protonated (deprotonated) reference with neutral unkown. The ratio of the protonated (deprotonated) unkown versus the protonated (deprotonated) references is related to the difference of proton affinity (acidity) between the unknown and reference.

1.3.3 Computational method

We also employ computational methods to quantify the gas phase acidities and proton affinities of chemicals.

The Gaussian 03 and Gaussian 09 programs were used with B3LYP as method and 6-31+G(d) as basis set.[123,124] All the geometries are fully optimized and frequencies are calculated and used. No scaling factor is applied. All the values used herein are in kcal mol^{-1} at 298K.

Note: Adapted with permission from: Michelson, Anna Zhachkina; Chen, Mu; Wang, Kai; Lee, Jeehiun K. *J. Am. Soc. Chem.* **2012**, *134*, 9622-9633.

Chapter 2 Gas Phase Studies of Purine 3-Methyladenine DNA Glycosylase II (AlkA) Substrates

2.1 Introduction

As we discussed in the first chapter, alkylation damage threatens proper cell function and intervene with gene replication and expression.[1-3] Damaged nucleobases are repaired through base excision repair (BER) mechanism. The *E-coli* 3-methyladenine DNA glycosylase II (AlkA) is an enzyme that removes a series of damaged bases from DNA.[4-7] AlkA is extrememly intriguing due to its ability to excise a vast variety of damaged bases, in despite of size and structure.

We have previously proposed that for a similar enzyme, alkyladenine DNA glycosylase (AAG) which is found in human body, differentiates among substrates by cleaving those nucleobases which are the most facile to remove. We postulate that the AlkA functions in a similar way. The rate of excision of damaged nucleobases by AlkA is related how good the leaving groups (conjugate bases) are, which are ultimately related to the gas phase acidities at the *N*-glycosidic position of the nucleobases. Our theory is that damaged nucleobases are better leaving groups than normal bases, thus, are more acidic than normal nucleobases. Moreover, we propose that the difference of leaving group

ability between normal and damaged nucleobases are enhanced in the nonpolar enviroment, by which the AlkA is able to exhibit its broad specificity.

Our goal here is to test and verify our theory. Meanwhile, the damaged bases are of interest in its own right. Studying the gas phase properties (gas phase acidites, proton affinities and tautomerism) will lend us insight of fundamental properties of these heterocyclic compounds. Therefore, one of the most fundamental structure, the unsubstituted purine which is also a substrate of AlkA, is studied herein firstly. Moreover, we will lay our eyes on two interesting nucleobases, 6-chloropurine and 3-methyladenine, the former of which is a potential substrate for AlkA and the latter potentially could either be a positively charged substrate or a neutral one.

2.2 Experimental

All the chemicals were commercially available and were used as received.

2.2.1. Bracketing method

Acidity and proton affinity bracketing measurements were conducted via a Fourier Transform Ion Cyclotron Resonance Mass Spectrometer (FTMS) with a dual cell setup, which has been described in the first chapter.[10-14,115] There are two adjoining 2-inch cubic cells positioned collinearly in the 3.3 T superconducting magnet. The pressure of the dual cell is pumped down to less than $1x10^{-9}$ Torr by a diffusion pump-mechanical pump setup. Solid purines are introduced into the cell via a heatable solids probe, which are then protonated or deprotonated by hydroxide or hydronium ions, depending on whether it is acidity measurement or PA measurement. Hydroxide or hydronium ions are

generated from water pulsed into the cell, and ionized by an electron beam (typically 8 eV (for OH^-), or 20 eV (for H_3O^+) and 6 μA, ionization time 0.5 s). Liquid reference acids or bases are introduced through a batch inlet system or a leak valve, and allowed to react with either hydroxide (for acidity measurement) or hydronium ions (for proton affinity (PA) measurement). Ions are generated from reference acids/bases or purine, selected, transferred to another adjoining cell through a 2-mm hole in the center of the central trapping plate, cooled by a pulse of argon, and allowed to react with neutral purine or reference/base. Proton transfer reactions are conducted in both directions. The occurrence of proton transfer is regarded as evidence that the reaction is exothermic ("+" in the Tables).

The bracketing experiments were conducted under pseudo-first order conditions, where the amount of the neutral substrate is in much excess relative to the reactant ions. Reading the pressure from an ion gauge is often unreliable, both because of the gauge's remote location as well as varying sensitivity for different substrates.[125,126] Therefore, we first evaluate the pressure by a controlled reaction. Briefly, we first calculate the rate constant of reaction between hydroxide and neutral compound. We assume the reaction proceed with theoretical rate since hydroxide is very basic.[116,117] We then could exclude the influence of pressure.[10-14,115,126]

2.2.2. Cooks kinetic method

We also used the Cooks kinetic method in a quadrupole ion trap (LCQ) mass spectrometer to measure the gas phase acidities and proton affinities of purines and substituted purines.[118-121]

The theory of Cooks kinetic method is related to the formation of a proton-bound dimer of the unknown AH^+ and a reference acid B_iH^+ of known acidity (eq. 2.1).

$$AH^{\oplus} + B_i \xleftarrow{k_1} [A \cdots H^{\oplus} \cdots B_i] \xrightarrow{k_2} A + B_iH^{\oplus} \qquad \textbf{E.q. 2.1}$$

Collision-induced dissociation (CID) is then conducted on the proton-bound dimer. The ratio of rate constants k_1 and k_2 in eq. 2.2 are proportional to the ratio of abundances of A^- and B^-.

$$\ln\frac{k_1}{k_2} = \ln\frac{AH^{\oplus}}{B_iH^{\oplus}} = \frac{\Delta G(B_i) - \Delta G(A)}{RT_{eff}} \approx \frac{\Delta H(B_i) - \Delta H(A)}{RT_{eff}} = \frac{PA(A) - PA(B_i)}{RT_{eff}} \qquad \textbf{Eq. 2.2}$$

R is the gas constant and T_{eff} is the effective temperature of the activated dimer complex.[118-121,127] Cooks method requires the assumptions: (1) dissociation has no reverse activation energy barrier, (2) the dissociation transition state structure is late. The proton-bound dimers mostly fall into this category.[122,128,129] In order to obtain the proton affinity of compound A, the natural logarithm of relative intensity ratios is plotted against the proton affinities of a series of reference bases which could be easily found in NIST. The slope is ($-1/RT_{eff}$) and the y-intercept is ($PA(A)/ RT_{eff}$). The T_{eff} is then obtained from the slope. The proton affinity of compound A, (PA(A)), is calculated from either **Eq. 2.2** or the y-intercept. The same procedure can be applied for acidity measurements (via negatively charged proton bound dimers).

For purine acidity and proton affinity studies, the dimers were produced through ESI and introduced to LCQ. Methanol or water–methanol (20%) solutions are used as solvents. An electrospray needle voltage of ~4 kV and the flow rate of 25 μL/min is

applied. The proton-bound complex ions are isolated and then dissociated using collision-induced dissociation (CID); the complexes are activated for about 30 ms. Finally, the dissociation product ions are detected to give the ratio of the deprotonated (or protonated) analyte and deprotonated (or protonated) reference acid. A total of 40 scans are averaged for the product ions.

2.2.3. Calculations

Calculations are conducted at B3LYP/6-31+G(d) using Gaussian 09.[124,130-132] The geometries are fully optimized and frequencies are calculated. No scaling factor is applied. All the values reported are ΔH at 298 K.

2.3 Results

2.3.1 Purine

i. Calculations: Purine tautomers, acidity, proton affinity.

Purine is a known substrate for AlkA, and is also of interest as it is the most fundamental structure for the species studied herein (thus its name!). There are four possible purine tautomers, of which the most stable one is the canonical structure **1a** (Figure 2.1). The acidity of this tautomer is calculated to be 329.8 kcal mol^{-1} (at the N9-H); the proton affinity is 219.2 kcal mol^{-1} (at N1).

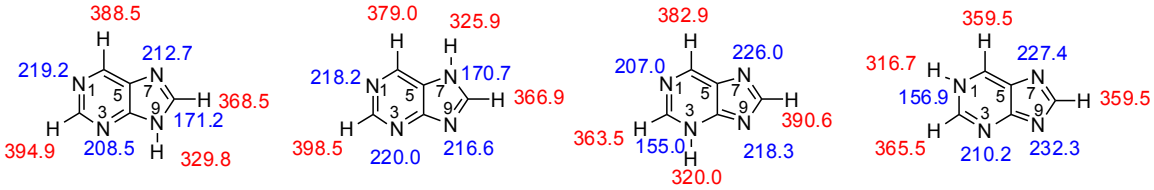

1a
N9H purine
(0)

1b
N7H purine
(3.9)

1c
NH purine
(9.8)

1d
N1H purine
(13.1)

Figure 2.1. Tautomeric structures of purine. Gas phase acidities are in red; gas phase proton affinities are in blue. Relative stabilities are in parentheses. Calculations were conducted at B3LYP/6-31+G(d); reported values are ΔH at 298 K.

ii. Experiments: Purine acidity

We measured the acidity of purine using the bracketing method (Table 2.1). Deprotonated purine can deprotonate perfluoro-*tert*-butanol (ΔH_{acid} = 331.6 ± 2.2 kcal mol^{-1}) but not pyruvic acid (ΔH_{acid} = 333.5 ± 2.9 kcal mol^{-1}). Pyruvate deprotonates purine, but perfluoro-*tert*-butanoxide does not. We therefore bracket the acidity of the more acidic site of purine to be ΔH_{acid} = 333 ± 4 kcal mol^{-1}.

Table 2.1. Summary of results for most acidic site bracketing of purine (**1**).

Reference compound	*ΔH_{acid}*[a]	*Proton transfer*[b]	
		Ref. acid	*Conj. base*
2,4-pentanedione	343.8 ± 2.1	–	+
α,α,α-trifluoro-*m*-cresol	339.2 ± 2.1	–	+
pyruvic acid	333.5 ± 2.9	–	+

perfluoro-*tert*-butanol	331.6 ± 2.2	+	–
difluoroacetic acid	331.0 ± 2.2	+	–
3,5-bis(trifluoromethyl) phenol	329.7 ± 2.1	+	–
1,1,1-trifluoro-2,4-pentanedione	328.3 ± 2.9	+	–

[a]ΔH_{acid} is in kcal mol^{-1}.[15] [b]A "+" indicates the occurrence and a "–" indicates the absence of proton transfer

The acidity was also measured using the Cooks kinetic method. Five reference acids were used: 3-(trifluoromethyl) benzoic acid (ΔH_{acid} = 332.2 ± 2.1 kcal mol^{-1}), 2-nitro-benzoic acid (ΔH_{acid} = 331.7 ± 2.2 kcal mol^{-1}), perfluoro-*tert*-butanol (ΔH_{acid} = 331.6 ± 2.2 kcal mol^{-1}), difluoroacetic acid (ΔH_{acid} = 331.0 ± 2.2 kcal mol^{-1}), and 3,5-bis(trifluoromethyl) phenol (ΔH_{acid} = 329.7 ± 2.1 kcal mol^{-1}), to yield an acidity of 332 ± 3 kcal mol^{-1}.

Our group also developed a method to measure the "less" acidic/basic site of compound, which has been described in chapter 1. Here, we apply this method to measure the less acidic site of purine (Table 2.2). Deprotonated purine, when transferred to the analyzer cell instantly after being deprotonated, is not able to deprotonate 2-ethyl-1-butanol (ΔH_{acid} = 373.1 ± 2.0 kcal mol^{-1}), but can deprotonate 3-ethylpentane-3-ol (ΔH_{acid} = 370.9 ± 2.8 kcal mol^{-1}). Therefore, we bracket the less acidic site of purine to be 372 ± 4 kcal mol^{-1}, which correspond to C8-H.

Table 2.2. Summary of results for less acidic site bracketing of purine (**1**).

Reference compound	*ΔH_{acid}*[a]	*Proton transfer*[b] *Ref. acid*
methanol	382.0 ± 1.0	–
ethanol	378.3 ± 1.0	–
1-butanol	375.3 ± 2.0	–
2-butanol	374.1 ± 2.0	–
dimethyl sulfoxide	373.5 ± 2.1	–
2-ethyl-1-butanol	373.1 ± 2.0	–
3-ethylpentane-3-ol	370.9 ± 2.8	+
1-hexene-3-ol	369.4 ± 2.1	+
aninline	366.4 ± 2.1	+
2,4-pentadione	343.8 ± 2.1	+

[a]ΔH_{acid} is in kcal mol^{-1}.[15] [b]A "+" indicates the occurrence and a "–" indicates the absence of proton transfer

iii. Experiments: Purine proton affinity.

The proton affinity of purine was bracketed as shown in Table 2.3. For the reaction of protonated purine and *n*-butylamine (PA = 220.2 ± 2.0 kcal mol^{-1}) and that of protonated *n*-butylamine and purine, proton transfer is observed in both directions, yielding a bracketed PA of 220 ± 3 kcal mol^{-1}. This value is consistent with a previous equilibrium measurement.[133]

Table 2.3. Summary of results for proton affinity bracketing of purine (**1**).

Reference compound	*PA*[a]	*Proton transfer*[b]	
		Ref. base	*Conj. acid*
3-picoline	225.5 ± 2.0	+	–
pyridine	222.0 ± 2.0	+	–
N-ethylaniline	221.0 ± 2.0	+	–
n-butylamine	220.2 ± 2.0	+	+
N-methylpropionamide	220.0 ± 2.0	–	+
propylamine	219.4 ± 2.0	–	+
benzylamine	218.3 ± 2.0	–	+
dimethylacetamide	217.0 ± 2.0	–	+
m-toluidine	214.1 ± 2.0	–	+

[a]PA is in kcal mol^{-1}.[15] [b]A "+" indicates the occurrence and a "–" indicates the absence of proton transfer

For the Cooks PA measurement of purine, nine reference bases were used: cyclohexylamine (PA = 223.3 ± 2.0 kcal mol^{-1}), ethanolamine (PA = 222.3 ± 2.0 kcal mol^{-1}), octylamine (PA = 222.0 ± 2.0 kcal mol^{-1}), isobutylamine (PA = 221.0 ± 2.0 kcal mol^{-1}), *L*-phenylalanine (PA = 220.6 ± 2.0 kcal mol^{-1}), *n*-butylamine (PA = 220.2 ± 2.0 kcal mol^{-1}), propylamine (PA = 219.4 ± 2.0 kcal mol^{-1}), benzylamine (PA = 218.3 ± 2.0 kcal mol^{-1}), and dimethylacetamide (PA = 217.0 ± 2.0 kcal mol^{-1}), to yield a PA of 221 ± 3 kcal mol^{-1}.

2.3.2 6-Chloropurine

i. Calculations: 6-Chloropurine tautomers, acidity, proton affinity.

6-Chloropurine has not been experimentally tested as an AlkA substrate. We chose to study this as a potential substrate, based on the assumption that the chloride group would render the compound quite acidic at N9 (more in Discussion). 6-Chloropurine has four possible tautomeric structures, of which the N9-H canonical is calculated to be most stable (Figure 2.2). The most acidic site of the canonical tautomer has a calculated ΔH_{acid} of 322.8 kcal mol^{-1} (N9-H); the most basic site, at N1, has a PA of 212.5 kcal mol^{-1}.

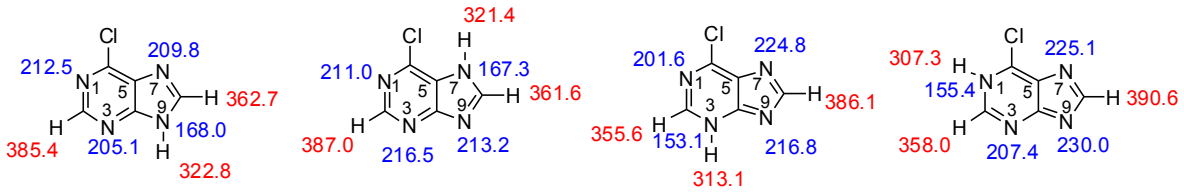

2a
6-Cl-N9H purine
(0)

2b
6-Cl-N7H purine
(2.4)

2c
6-Cl-N3H purine
(10.7)

2d
6-Cl-N1H purine
(16.5)

Figure 2.2. Tautomeric structures of 6-chloropurine. Gas phase acidities are in red; gas phase proton affinities are in blue. Relative stabilities are in parentheses. Calculations were conducted at B3LYP/6-31+G(d); reported values are ΔH at 298 K.

ii. Experiments: 6-Chloropurine acidity.

6-Chloropurine is predicted to be quite acidic (calculated ΔH_{acid} of 322.8 kcal mol^{-1}). Because reference acids in this range are limited, we bracketed an upper limit for the ΔH_{acid} of 6-chloropurine (Table 2.4). The most acidic reference acid we used was 1,1,1-trifluoro-2,4-pentanedione (ΔH_{acid} = 328.3 ± 2.9 kcal mol^{-1}). Deprotonated 6-chloropurine is unable to deprotonate 1,1,1-trifluoro-2,4-pentanedione and acids with

higher ΔH_{acid} values (Table 2.3). Likewise, deprotonated 1,1,1-trifluoro-2,4-pentanedione and stronger bases can deprotonate 6-chloropurine, so we bracket an upper limit of the ΔH_{acid} of 328.3 kcal mol^{-1}.[134]

Table 2.4. Summary of results for acidity bracketing of 6-chloropurine (**2**).

Reference compound	*ΔH_{acid}*[a]	*Proton transfer*[b]	
		Ref. acid	*Conj. base*
2,4-pentanedione	343.8 ± 2.1	–	+
perfluoro-*tert*-butanol	331.6 ± 2.2	–	+
3,5-bis(trifluoromethyl) phenol	329.8 ± 2.1	–	+
1,1,1-trifluoro-2,4-pentanedione	328.3 ± 2.9	–	+

[a]ΔH_{acid} is in kcal mol^{-1}.[15] [b]A "+" indicates the occurrence and a "–" indicates the absence of proton transfer

iii. Experiments: 6-chloropurine proton affinity.

The bracketing of the PA of 6-chloropurine is shown in Table 2.5. For the reaction of protonated 6-chloropurine with both methylamine and *m*-toluidine, proton transfer is observed; the reaction occurs in the opposite direction as well, yielding a 6-chloropurine bracketed PA of 214 ± 3 kcal mol^{-1}.[134]

Table 2.5. Summary of results for proton affinity bracketing of 6-chloropurine (**2**).

Reference compound	*PA*[a]	*Proton transfer*[b]

		Ref. base	*Conj. acid*
pyridine	222.0 ± 2.0	+	–
propylamine	219.4 ± 2.0	+	–
dimethylacetamide	217.0 ± 2.0	+	–
3-chloropyridine	215.9 ± 2.0	+	–
methylamine	214.9 ± 2.0	+	+
m-toluidine	214.1 ± 2.0	+	+
N-methylacetamide	212.4 ± 2.0	–	+
aniline	210.9 ± 2.0	–	+
2,4-pentanedione	208.8 ± 2.0	–	+

[a]PA is in kcal mol^{-1}.[15] [b]A "+" indicates the occurrence and a "–" indicates the absence of proton transfer

2.3.3 3-Methyladenine

i. Calculations: 3-methyladenine tautomers, acidity, proton affinity.

Our group previously reported the calculated the acidity and the relative stabilities of the possible tautomers of 3-methyladenine; these data plus new calculations of PA are shown in Figure 2.5.[12] 3-Methyladenine has five possible tautomers; the three lowest are shown. The most stable is the one with the exocyclic amino group (**3a**), for which the calculated acidity is 346.8 kcal mol^{-1} (for the proton on the amino group). The most basic site has a PA of 234.5 kcal mol^{-1}, at the N7.

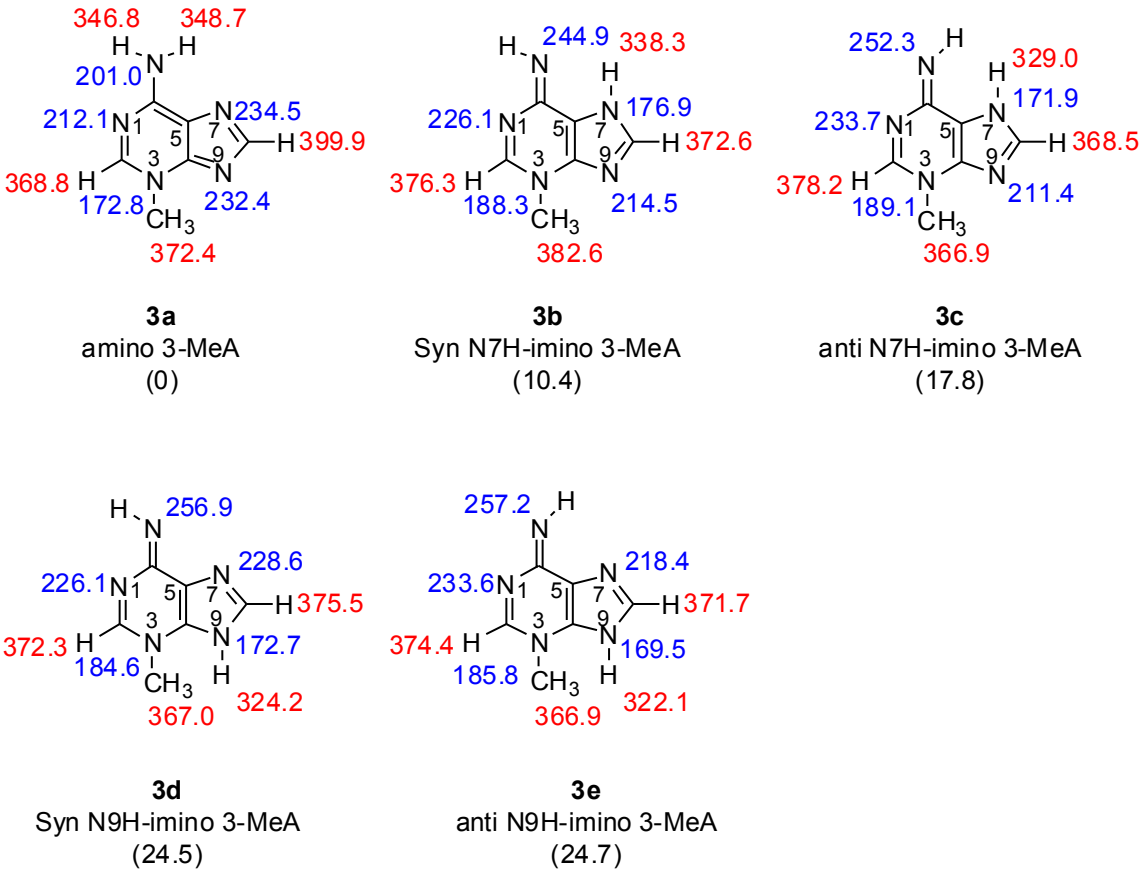

3a
amino 3-MeA
(0)

3b
Syn N7H-imino 3-MeA
(10.4)

3c
anti N7H-imino 3-MeA
(17.8)

3d
Syn N9H-imino 3-MeA
(24.5)

3e
anti N9H-imino 3-MeA
(24.7)

Figure 2.3. Tautomeric structures of 3-methyladenine. Gas phase acidities are in red; gas phase proton affinities are in blue. Relative stabilities are in parentheses. Calculations were conducted at B3LYP/6-31+G(d); reported values are ΔH at 298 K.

ii. Experiments: 3-methyladenine acidity and proton affinity.

The acidity of 3-methyladenine was previously measured by us to be 347 ± 4 kcal mol^{-1}.[12] We bracket the PA of 3meA herein (Table 2.6). Di-*sec*-butylamine (PA = 234.4 ± 2.0 kcal mol^{-1}) can deprotonate protonated 3-methyladenine, but 1-methylpiperidine (232.1 ± 2.0 kcal mol^{-1}) cannot. In the reverse direction, 3-methyladenine deprotonates

protonated 1-methylpiperidine, but not protonated di-*sec*-butylamine. We therefore bracket the PA of 3-methyladenine to be 233 ± 3 kcal mol^{-1}.

Table 2.6. Summary of results for proton affinity bracketing of 3-methyladenine (**3**).

Reference compound	*PA*[a]	*Proton transfer*[b]	
		Ref. base	*Conj. acid*
2,2,6,6-tetramethylpiperidine	235.9 ± 2.0	+	–
trimethylamine	234.7 ± 2.0	+	–
di-*sec*-butylamine	234.4 ± 2.0	+	–
1-methylpiperidine	232.1 ± 2.0	–	+
2,4-lutidine	230.1 ± 2.0	–	+
3-picoline	225.5 ± 2.0	–	+

[a]PA is in kcal mol^{-1}.[15] [b]A "+" indicates the occurrence and a "–" indicates the absence of proton transfer

2.4 Discussion

Biological implications.

As mentioned previously, AlkA is an enzyme with broad specificity that can cleave a variety of substrates disregard of the shape, size and functional groups. [7-9,135-144] However, the reason of its broad specificity has not been deciphered yet. The main hypothesis is that AlkA discriminate damaged nucleobases against normal ones by identifying the intrinsic stabilities of *N*-glycosidic bond. [1,3,8,143] Therefore, since the

stability of *N*-glycosidic bond is related to the leaving group ability, which is ultimately related to the gas phase acidity, we would expect the damaged nucleobases are more acidic than normal nucleobases.

We further postulate that the acidity differences between damaged and normal bases are further enhanced by AlkA through providing a non-polar active site. [10,12,126] Thus, we first compare the gas phase acidities of a series of AlkA substrates with normal nucleobases to see whether damged nucleobases are more acidic. The biological relevant structures are summarized in Figure 2.4.

In Figure 2.4, two types of nucleobases are shown. The first row possesses positive charge, while the rest are neutral species. AlkA is interesting in that it not only cleaves neutral nucleobases, but also excise positively charged nucleobases. The N-glycosidic bond stability is related to N9H acidity of these substrates. Cleaving of positively charged nucleobases result in neutral species while the cleavage of neutral ones will yield anionic species. It is easy to postulate that neutral species are better leaving group than anionic species, which is supported by the calculated gas phase N9H acidity values in Figure 2.4.

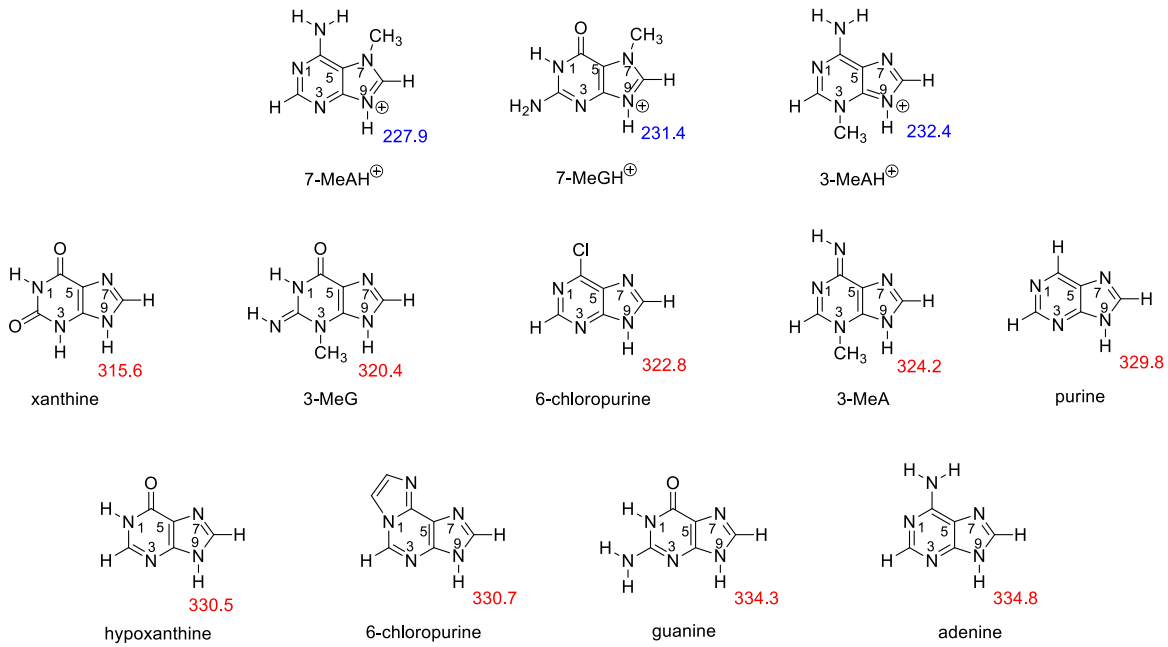

Figure 2.4. Gas phase acidity (ΔH298K, calculated, B3LYP/6-31+G(d), in kcal mol-1) of biologically relevant structures.[10-12]

For neutral species, the gas phase acidities of damaged nucleobases are indeed more acidic than normal ones (adenine and guanine).

To further verify our hypothesis, we summarize the gas phase acidities of nucleobases along with their excision rates.

Table 2.7. Rate constants for excision of various nucleobases by AlkA compared to gas phase acidity.

Substrate	k_{st} (min^{-1})[a,b]	ΔH_{acid} (kcal mol^{-1})[c]
$7meGH^+$	300	231.4
$3meAH^+$(**3H$^+$**)/3meA (**3**)	0.5	232.4/324.2

ethenoadenine	7.5 x 10^{-2}	330.7[d]
purine (**1**)	5.4 x 10^{-2}	329.8
hypoxanthine	2.9 x 10^{-2}	330.5[e]
guanine	6.9 x 10^{-3}	334.3[f]
adenine	5.2 x 10^{-3}	334.8[g]

[a]Reference [8]; [b]k_{st} is single turnover rate constant with saturating AlkA; [c]Calculated ΔH_{acid} values at 298 K (B3LYP/6-31+G(d)); [d]Reference [11]; [e]Reference [10]; [f]Reference [145]; [g]References [12,145]

As can be seen from Table 2.7, the gas phase acidity of N9-H correlate with excision rate very well, which gave further support of our hypothesis. Based on the results, we predict that 6-chloropurine will also be cleaved by AlkA.

2.5 Conclusion

Our experimental and computational study of gas phase properties of AlkA substrates indicate that damaged nucleobases are all more acidic than the normal nucleobases adenine and guanine, by which AlkA is able to discriminate them. The fact that the gas phase acidities tracks the excision rate further supports our hypothesis that AlkA excise the damaged nucleobases based on the intrinsic stability of *N*-glycosidic bond.

Chapter 3 1,2,3-Triazoles: Gas Phase Properties

3.1 Introduction

The 1,3-dipolar cycloaddition reaction between acetylene and azide to give 1,2,3-triazole was first brought into sight by Huisgen and coworkers in 1967.[16] Since the discovery of "click chemistry", the synthesis of substituted 1,2,3-triazoles via copper-catalyzed alkyne–azide 1,3-dipolar addition have come to the forefront .[17-24,30,31,146-150] Thermal Huisgen cycloaddition often yields mixtures of 1,4-substituted and 1,5-substituted regio-isomers, while CuAAC method allows the synthesis of 1,4-disubstituted regio-isomer. Our collaborator, Xiaodong Shi from West Virginia Univeristy, developed a cascade reaction to make 4,5-disubstituted NH-1,2,3-triazoles, which gives us access to the regioselective synthesis of N2-substituted-1,2,3-triazoles.[34,35]

Triazoles can function as neutral and anionic ligands, so we became interested in characterizing their acidity and basicity, using gas phase calculations and experiments to uncover intrinsic properties. Fundamental studies on the properties of 1,2,3-triazoles are scarce.[46-49] Therefore, we here studies the fundamental properties of 4-phenyl-1,2,3-triazole and benzotriazole (parent and 1-phenyl-substituted). We have also found that such triazoles can be used as ligands to produce new cationic Au(I) catalysts that have improved stability and effective reactivity (relative to known catalysts).[38-40,42,44]

Therefore, we not only characterize the fundamental gas-phase properties of all the triazoles, but also focus on effects of substitution on the 1-phenylbenzotriazoles, examining how electron donating and withdrawing groups affect proton affinity and binding to gold. Such studies will aid in the design of catalysts containing triazole ligands bound to metal cations.

3.2 Experimental

3.2.1. Bracketing method

Acidity and proton affinity bracketing measurements of triazoles were conducted using a Fourier Transform Ion Cyclotron Resonance Mass Spectrometer (FTMS) with a dual cell setup, which has been described in chapter 2.

3.2.2. Calculations

For all reported calculated values except for those for the Hammett plot, B3LYP/6-31+G(d) (using Gaussian03 and Gaussian09) was used.[123,124,130-132] Geometries were fully optimized and frequencies were calculated. No scaling factor was applied. All the acidity, proton affinity and relative stability values reported are ΔH at 298 K.

3.3 Results and Discussion.

3.3.1. 4-phenyl-1,2,3-triazole (1)

i. Calculations: 4-phenyl-1,2,3-triazole tautomers, acidity, proton affinity.

We first studied 4-phenyl-1,2,3-triazole (**1**), which had been the subject of a previous study, but with some ambiguous results (*vide supra*).[47] There are eight possible tautomeric structures (five lowest are shown in Figure 3.1). In our experience DFT methods generally yield accurate values for thermochemical properties of heterocyclic rings, so we utilized B3LYP/6-31+G(d) to calculate the relative tautomeric stabilities, acidities (ΔH_{acid}), and proton affinities (PA).[10-12,14,115,126,145] Of the eight possible tautomeric structures, three are within 5 kcal mol^{-1} (**1a**, **1b**, **1c**).

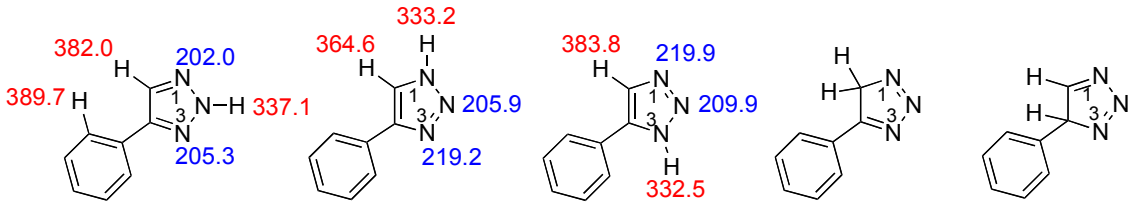

Figure 3.1. The possible tautomers of 4-phenyl-1,2,3-triazole (**1**). Gas phase acidities are in red; gas phase proton affinities are in blue. Relative stabilities are in parentheses. Calculations were conducted at B3LYP/6-31+G(d); reported values are ΔH (kcal mol^{-1}) at 298 K.

ii. Experiments: 4-Phenyl-1,2,3-triazole acidity.

We measured the acidity of 4-phenyl-1,2,3-triazole using acidity bracketing (details in the Experimental Section). The conjugate base of 4-phenyl-1,2,3-triazole deprotonates 2-chloropropionic acid (ΔH_{acid} = 337.0 ± 2.1 kcal mol^{-1}); however, the reaction in the opposite direction (2-chloropropionate with 4-phenyl-1,2,3-triazole) does not take place (Table 3.1). Deprotonated 4-phenyl-1,2,3-triazole is unable to deprotonate α,α,α-trifluoromethyl-*m*-cresol (ΔH_{acid} = 339.3 ± 2.1 kcal mol^{-1}) but the cresolate does deprotonate 4-phenyl-1,2,3-triazole. We therefore bracket the ΔH_{acid} of 4-phenyl-1,2,3-triazole as 338 ± 3 kcal mol^{-1}.

Table 3.1. Summary of results for acidity bracketing of 4-phenyl-1,2,3-triazole (**1**).

Reference compound	ΔH_{acid}[a]	*Proton transfer*[b]	
		Ref. acid	*Conj. base*
methylcyanoacetate	340.80 ± 0.60	–	+
α,α,α-trifluoromethyl-*m*-cresol	339.3 ± 2.1	–	+
2-chloropropionic acid	337.0 ± 2.1	+	–
malononitrile	335.8 ± 2.1	+	–
per-fluoro-tert-butanol	331.6 ± 2.2	+	–

[a] Acidities are in kcal mol^{-1}.[15,151] [b] A "+" indicates the occurrence and a "–" indicates the absence of proton transfer

iii. Experiments: 4-Phenyl-1,2,3-triazole proton affinity.

We find that 3-bromopyridine (PA = 217.5 ± 2.0 kcal mol^{-1}) deprotonates protonated 4-phenyl-1,2,3-triazole; the opposite reaction (4-phenyl-1,2,3-triazole deprotonating protonated 3-bromopyridine) does not occur (Table 3.2). With 3-fluoropyridine (PA = 215.6 ± 2.0 kcal mol^{-1}), the reference base does not deprotonate protonated 4-phenyl-1,2,3-triazole, but 4-phenyl-1,2,3-triazole does deprotonate protonated 3-fluoropyridine, putting the PA at 217 ± 3 kcal mol^{-1}.

Table 3.2. Summary of results for proton affinity bracketing of 4-phenyl-1,2,3-triazole (**1**).

Reference compound	*PA*[a]	*Proton transfer*[b]	
		Ref. base	*Conj. acid*
pyridine	222.3 ± 2.0	+	–
butylamine	220.2 ± 2.0	+	–
3-bromopyridine	217.5 ± 2.0	+	–
3-fluoropyridine	215.6 ± 2.0	–	+
2-chloropyridine	215.3 ± 2.0	–	+
o-toluidine	212.9 ± 2.0	–	+
aniline	210.9 ± 2.0	–	+
2,4-pentadione	208.8 ± 2.0	–	+

[a] PAs are in kcal mol^{-1}.[15] [b] A "+" indicates the occurrence and a "–" indicates the absence of proton transfer

An examination of the computational versus experimental results indicates some discrepancies (Table 3.3). The most stable tautomer **1a** has a predicted acidity of 337.1 kcal mol^{-1}, which is consistent with the experimentally bracketed value (338 kcal mol^{-1}). In contrast, the calculated PA value for the more stable tautomer **1a**, 205.3 kcal mol^{-1} does not agree with the bracketed PA (217 kcal mol^{-1}). Instead, the measured PA corresponds to the less stable tautomer (**1b** or **1c**). These results seem to imply that in our acidity studies, tautomer **1a** predominates, whereas in our PA studies, tautomer **1b** predominates (or maybe even **1c**, though calculations indicate that **1c** should be even less stable than **1b**).

Table 3.3. Calculated (B3LYP/6-31+G(d); 298 K) and experimental acidity and proton affinity data for 4-phenyl-1,2,3-triazole (**1**).

Substrate	Relative tautomer stability[a]	Calculated value	Experimental value[b]
ΔH_{acid}[a]			
4-phenyl-1,2,3-triazole (**1**)			338
"N2H" tautomer (**1a**)	0.0	337.1	
"N1H" tautomer (**1b**)	3.9	333.2	
"N3H" tautomer (**1c**)	4.6	332.5	
PA[a]			
4-phenyl-1,2,3-triazole (**1**)			217

"N2H" tautomer (**1a**)	0.0	205.3
"N1H" tautomer (**1b**)	3.9	219.2
"N3H" tautomer (**1c**)	4.6	219.9

[a]Values are in kcal mol^{-1}; [b]Experimental value is from bracketing measurement; error is ± 3 kcal mol^{-1}.

The PA of **1** was measured previously by Abboud and coworkers, who obtained a value similar to ours (216 kcal mol^{-1}, using the equilibrium method in an FTMS).[47] The authors were unable to explain why the measured PA corresponded to the less stable tautomer **1b** so they made the assumption that "the phenomenon is a thermodynamic one and involves the most stable neutral tautomer or isomer and the most stable cation, even if these are not directly linked..."[47] This explanation seems unsatisfactory to us; all proton transfers must occur within ion-molecule complexes and reactants and products must in fact be "directly linked." We therefore must explain why the measured acidity points to the predominance of tautomer **1a** yet the proton affinity to the less stable tautomer **1b**.

We first considered the possibility that the calculations are inaccurate. To test the accuracy of the calculations, we examined the methylated derivatives 1-methyl-4-phenyl-1,2,3-triazole and 2-methyl-4-phenyl-1,2,3-triazole (Figure 3.2). These methylated derivatives cannot tautomerize, so we can compare calculated and experimentally measured PA values without the complicating factor of tautomer ambiguity.

Figure 3.2. Computed proton affinities for 1-methyl- and 2-methyl-4-phenyl-1,2,3-triazole. Calculations were conducted at B3LYP/6-31+G(d); reported values are ΔH (kcal mol^{-1}) at 298 K.

Calculations predict that the most basic site of 1-methyl-4-phenyl-1,2,3-triazole is the N3, with a PA of 224.3 kcal mol^{-1}. The bracketing reaction of 1-methyl-4-phenyl-1,2,3-triazole with 3-picoline proceeds in both directions, placing the PA at 226 ± 3 kcal mol^{-1} (Table 3.4).

Table 3.4. Summary of results for proton affinity bracketing of 1-methyl-4-phenyl-1,2,3-triazole.

Reference compound	*PA*[a]	*Proton transfer*[b]	
		Ref. base	*Conj. acid*
piperidine	228.0 ± 2.0	+	–
4-picoline	226.4 ± 2.0	+	–
3-picoline	225.5 ± 2.0	+	+
pyridine	222.3 ± 2.0	–	+

isobutylamine	221.0 ± 2.0	–	+

[a] PAs are in kcal mol^{-1}.[15] [b]A "+" indicates the occurrence and a "–" indicates the absence of proton transfer

The most basic site of 2-methyl-4-phenyl-1,2,3-triazole is predicted to be the N3, with a calculated PA of 210.8 kcal mol^{-1}. Bracketing experiments indicate a "crossover" point between 210.9 and 212.4 kcal mol^{-1} (Table 3.5). *N*-Methylacetamide is able to deprotonate protonated 2-methyl-4-phenyl-1,2,3-triazole, but 2-methyl-4-phenyl-1,2,3-triazole cannot deprotonate protonated *N*-methylacetamide. Aniline does not deprotonate protonated 2-methyl-4-phenyl-1,2,3-triazole, but the opposite reaction does occur. We therefore bracket the PA of 2-methyl-4-phenyl-1,2,3-triazole as 212 ± 3 kcal mol^{-1}.

Table 3.5. Summary of results for proton affinity bracketing of 2-methyl-4-phenyl-1,2,3-triazole.

Reference compound	*PA*[a]	*Proton transfer*[b]	
		Ref. base	*Conj. acid*
m-toluidine	214.1 ± 2.0	+	–
o-toluidine	212.9 ± 2.0	+	–
N-methylacetamide	212.4 ± 2.0	+	–
aniline	210.9 ± 2.0	–	+
isopropyl sulfide	209.5 ± 2.0	–	+
2,4-pentadione	208.8 ± 2.0	–	+

[a] PAs are in kcal mol^{-1}.[15] [b]A "+" indicates the occurrence and a "–" indicates the absence of proton transfer

The studies with the methylated derivatives indicate that our DFT calculations should be quite accurate (for 1-methyl-4-phenyl-1,2,3-triazole the computed versus experimental PA is 224 versus 226 kcal mol^{-1}; for the 2-methyl derivative, it is 211 versus 212 kcal mol^{-1}).

If we trust our calculations, we still have a mystery. The acidity measurement is consistent with structure **1a**: our experimental ΔH_{acid} of 338 kcal mol^{-1} is closer to that calculated for **1a** (337 kcal mol^{-1}) than that for **1b** (333 kcal mol^{-1}), Table 3.3). However, the experimental PA is consistent with **1b**: the measured PA is 217 kcal mol^{-1}, which is much closer to the calculated PA for **1b** (219.2 kcal mol^{-1}) than for **1a** (205.3 kcal mol^{-1}, Table 3.3).

First let us consider proton affinity. In the bracketing experiment, two reactions are conducted: protonated reference base (BH^+) with the triazole, and protonated triazole with the neutral reference base (B).

For the reaction of the protonated B (BH^+) with **1** (column with header "Conj. acid" in Table 3.2 (fourth column)), 4-phenyl-1,2,3-triazole can deprotonate protonated 3-fluoropyridine (PA = 215.6 kcal mol^{-1}) and any protonated base with a PA lower than 215 kcal mol^{-1}. We believe that these data could be consistent with the presence of **1a**, **1b** or some mixture thereof. If only **1b**, or a mixture of **1b** and **1a** were present, then certainly we would bracket a value close to 217 kcal mol^{-1}, which we do. However, if only **1a** were present, then the triazole should not be able to deprotonate any protonated reference base above 205 kcal mol^{-1}. However, the reaction depicted in Figure 3.3 could be taking place. In Figure 3.3, the protonated reference base BH^+ first forms an ion-

molecule complex with triazole **1a**, which is roughly 20 kcal mol^{-1} exothermic (to form ***A***).[152-154] Proton transfer between the most basic site of **1a** (N3, calculated PA = 205 kcal mol^{-1}) and BH^+ is endothermic (to form complex ***B***), but allowed energetically since the complex is still less than the total energy of the system (indicated by the dotted line).[153] Now the reference base B can access the N2-H proton (exothermic by 5 kcal mol^{-1}) to form the **1c** tautomer of the triazole (complex ***C***). The N1 of **1c** is basic enough to deprotonate the protonated BH^+ (to form complex ***D***), which can then lead to the observable products, B and protonated triazole, in an overall thermoneutral reaction. The structure of the protonated triazole would not be that of $\mathbf{1aH^+}$ but instead, that of $\mathbf{1bH^+}$ (or $\mathbf{1cH^+}$ - these have the same structure). By mass spectrometry, however, one only tracks the m/z ratio, so the presence of any protonated triazole yields the "+" in Table 3.2. Computationally, the path in Figure 3.3 would be predicted to be accessible for any base with a PA of about 215 kcal mol^{-1} or lower, which is what we observe experimentally (Table 3.2).

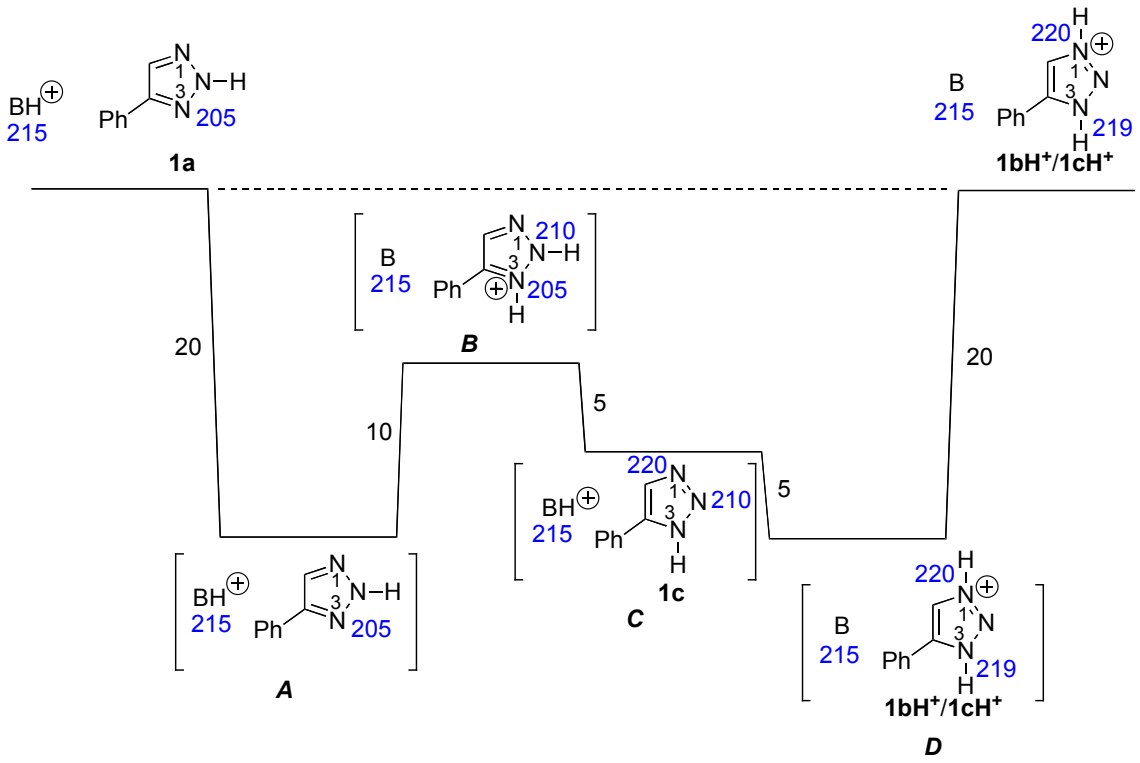

Figure 3.3. Pathway by which a protonated reference base BH^+ could react with the N2H tautomer of 4-phenyl-1,2,3-triazole (**1a**). Values are in kcal mol^{-1}. Blue values are PAs; for the triazole, values are calculated at B3LYP/6-31+G(d)(ΔH).

Thus, from the results for the proton transfer in this direction, we can only conclude that we may have **1a**, **1b** or a mixture.

What about the opposite direction? When B is allowed to react with protonated **1**, we find that reference bases with PAs below that of 3-bromopyridine (PA = 217.5 kcal mol^{-1}) do not appear to deprotonate protonated triazole (Table 3.2, third column). This would imply that only $\mathbf{1bH^+}$ (which has the same structure as $\mathbf{1cH^+}$) is present. However, does this mean that the initial vaporized triazole was only structure **1b**?

In our experiment, we sublime the neutral triazole into the gas phase via the solids probe. Hydronium ion (H_3O^+) is then used to protonate the triazole. Because crystal structures of the neutral triazole indicate that **1a** is the most stable structure in the solid state, we would expect the initially vaporized neutral triazole to be the more stable structure **1a**.[47] However, after protonation to form **1aH**$^+$, further reaction with neutral **1a** can take place to form the thermodynamically more stable protonated structure **1bH**$^+$ (Figure 3.4). Essentially, by the time we form protonated **1** and transfer it to the second cell for reaction (see Methods for details), the **1H**$^+$ ions are predominantly **1bH**$^+$.

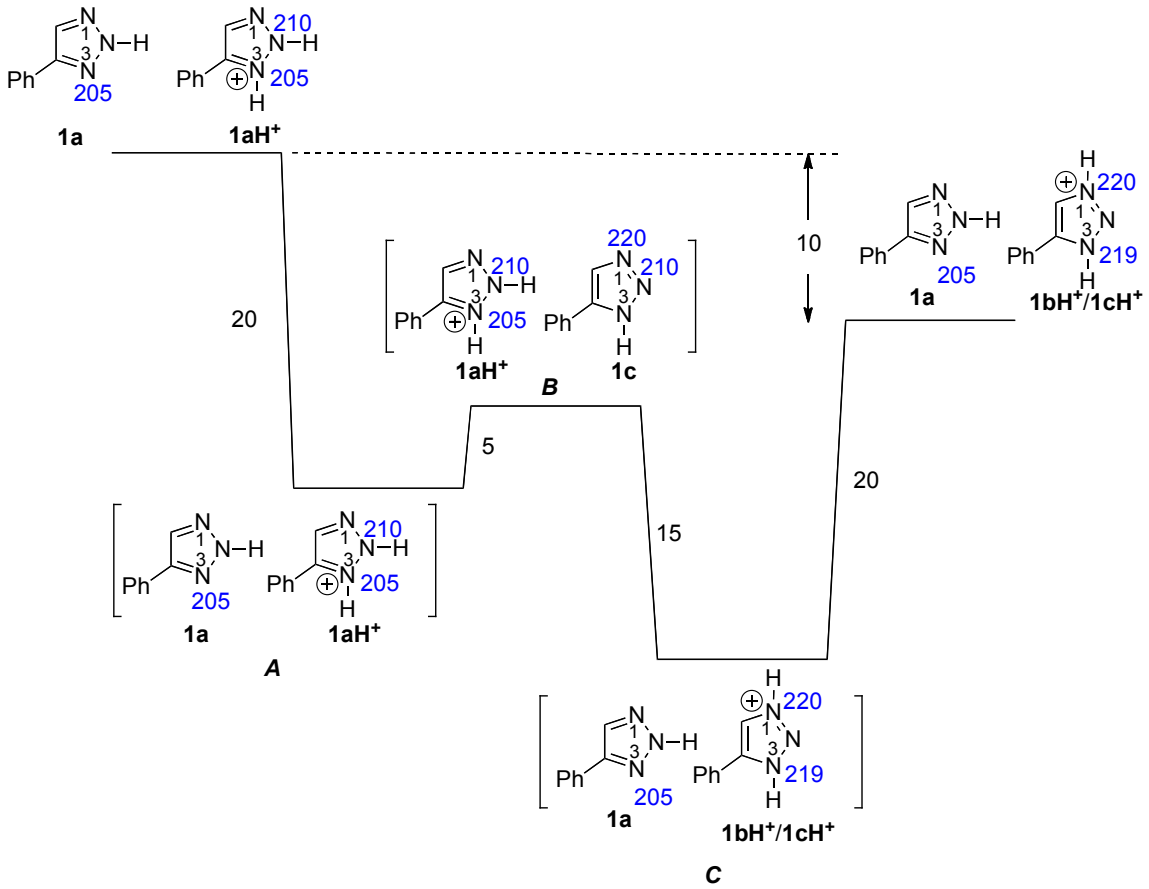

Figure 3.4. Pathway for reaction of neutral and protonated forms of the N2H tautomer of 4-phenyl-1,2,3-triazole (**1a** with $\mathbf{1aH^+}$). Values are in kcal mol^{-1}. Blue values are PAs; for the triazole, values are calculated at B3LYP/6-31+G(d) (ΔH).

Thus, in the direction where we bracket protonated triazole with reference bases B, we probably have only $\mathbf{1bH^+}$ (although we may have started under our gas phase conditions with some amount of, if not all, **1a**). To probe this possibility and our theory that $\mathbf{1aH^+}$ could be isomerizing to $\mathbf{1bH^+}$, we performed the protonation of **1** under conditions that would minimize isomerization: we remove the protonated **1** from the neutral **1** environment as quickly as possible. First, we vaporize **1** into the gas phase via a heated solids probe. Second, we allow hydronium to protonate **1** and form $\mathbf{1H^+}$. At this point, we transfer protonated triazole out of the neutral triazole environment, to the second adjoining cell of our FTMS, to allow it to react with reference bases.

Our theory is that if we do generate $\mathbf{1aH^+}$, exposure to neutral **1** (which is constantly being vaporized from the solids probe) in the first cell will cause isomerization to $\mathbf{1bH^+}$. Therefore, we varied the time that we waited after protonation and before transfer out of the neutral triazole environment. We then measured the efficiency of proton transfer between the protonated triazole and aniline, which has a PA of 211 kcal mol^{-1}. With a PA of 211, aniline will only be protonated if $\mathbf{1aH^+}$ is present. As can be seen from Table 3.6, as the time before transfer decreases, the efficiency of the reaction by which aniline deprotonates protonated triazole increases. That is, when the protonated triazole is taken out of the neutral triazole environment more quickly, we see more proton transfer with aniline. This implies that more $\mathbf{1aH^+}$ is present. We therefore believe that under our

normal conditions (4 seconds before transfer), isomerization from **1aH**$^+$ to **1bH**$^+$ occurs. Thus, by the time we add the reference base, we are only seeing results with **1bH**$^+$.

Table 3.6. Efficiencies of reactions between protonated 4-phenyl-1,2,3-triazole (**1H**$^+$) and aniline as a function of time before transferring protonated 4-phenyl-1,2,3-triazole from neutral triazole environment.

Time before transfer (seconds)	Efficiency of proton transfer from **1H**$^+$ to aniline (PA = 211 kcal mol^{-1})
4	1.2%
0.2	7.0%
0.05	11.4%

Another way to test this theory is through the use of an appropriately chosen deuterated reference base. Ethylene glycol-O-d_2 has a PA of 195 kcal mol^{-1}. If allowed to react with **1aH**$^+$, we would expect exchange of a proton for a deuteron, resulting in a unit increase in the mass-to-charge ratio (*m/z* 146 to *m/z* 147, Figure 3.5). This reaction should be thermoneutral.

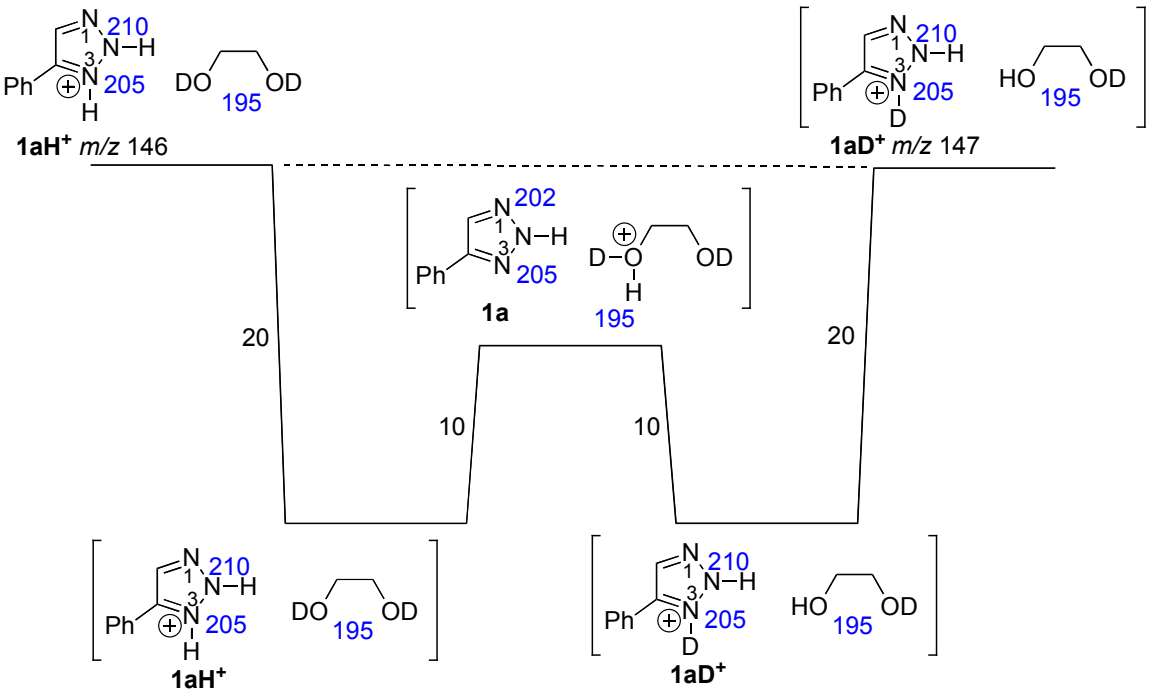

Figure 3.5. Pathway for reaction of protonated N2H tautomer of 4-phenyl-1,2,3-triazole (**1aH**$^+$) with ethylene glycol-O-d_2. Values are in kcal mol^{-1}. Blue values are PAs; for the triazole, values are calculated at B3LYP/6-31+G(d)(ΔH).

In contrast, because of its higher PA, **1bH**$^+$ should not be able to exchange its proton (Figure 3.6).

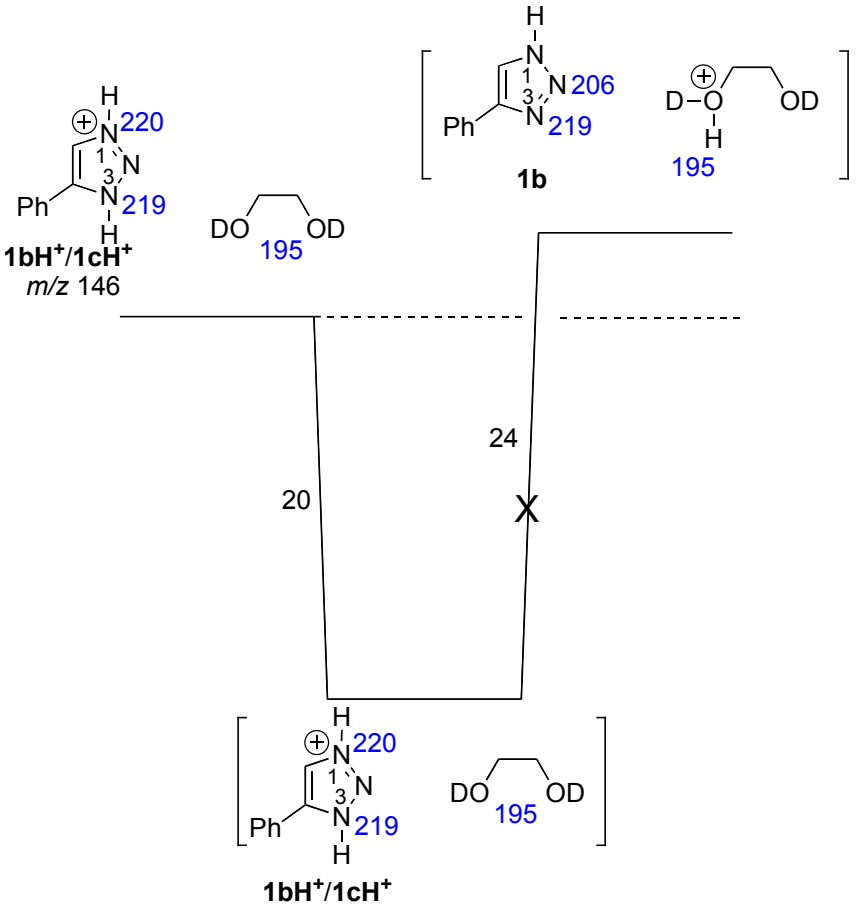

Figure 3.6. Pathway for reaction of protonated N1H tautomer of 4-phenyl-1,2,3-triazole (**1bH**$^+$) with ethylene glycol-O-d_2. Values are in kcal mol^{-1}. Blue values are PAs; for the triazole, values are calculated at B3LYP/6-31+G(d)(ΔH).

Again, we varied the time in which the protonated triazole remained in the neutral triazole environment (before transfer to the second cell for reaction with deuterated ethylene glycol). The longer we wait after the protonation step (and before transfer out of the neutral triazole environment), the more neutral-triazole-catalyzed isomerization should occur (to transform **1aH**$^+$ to **1bH**$^+$). We find that at shorter times before transfer (1s and 2s), we do in fact see *m/z* 147, indicating that H/D exchange takes place. For 4 s and higher, we no longer see an appreciable amount of *m/z* 147. This would indicate that

at shorter times before transfer, we have **1aH**$^+$, which is capable of undergoing H/D exchange. At longer times before transfer, the ion population has isomerized to **1bH**$^+$ and reaction with deuterated ethylene glycol does not effect H/D exchange. This lends further evidence to our theory that our vaporized triazole definitely has **1a** present, which when protonated forms **1aH**$^+$, which, given enough time in a neutral triazole environment, will isomerize to **1bH**$^+$. Although we know that **1a** must be present, we cannot know whether **1b** is or is not present.

Can our acidity experiments shed more light on this puzzle? The bracketed value of 338 kcal mol^{-1} is consistent with the calculated acidity value of **1a** (337 kcal mol^{-1}). Does this indicate the presence of **1a** only? First, let us consider the reaction of deprotonated triazole with reference acids (third column in Table 3.1). Whether we have **1a** or **1b** present, deprotonation results in the same structure, so one will bracket in this direction to the most basic site, which is the N2.

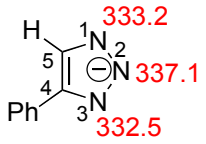

deprotonated **1**

In the opposite direction, conjugate bases of reference acids are allowed to react with **1** (Table 3.1, rightmost column). If **1b** (ΔH_{acid} (calculated) = 333 kcal mol^{-1}, Figure 3.1) were present, one would expect the conjugate bases of 2-chloropropionic acid (ΔH_{acid} = 337.0 kcal mol^{-1}) and malononitrile (ΔH_{acid} = 335.8 kcal mol^{-1}) to effect proton transfer, but they do not ("–" in rightmost column of Table 3.1). This result certainly implies that

little to no **1b** is present. There is always the possibility that a base with PA higher than the acidity of **1b** follows the path shown in Figure 3.7, though it seems unlikely that ion-molecule complex B would *never* decomplex to give deprotonated triazole (indicating proton transfer). Because of this possible path, however, we cannot fully discount the presence of **1b** though we consider it unlikely.

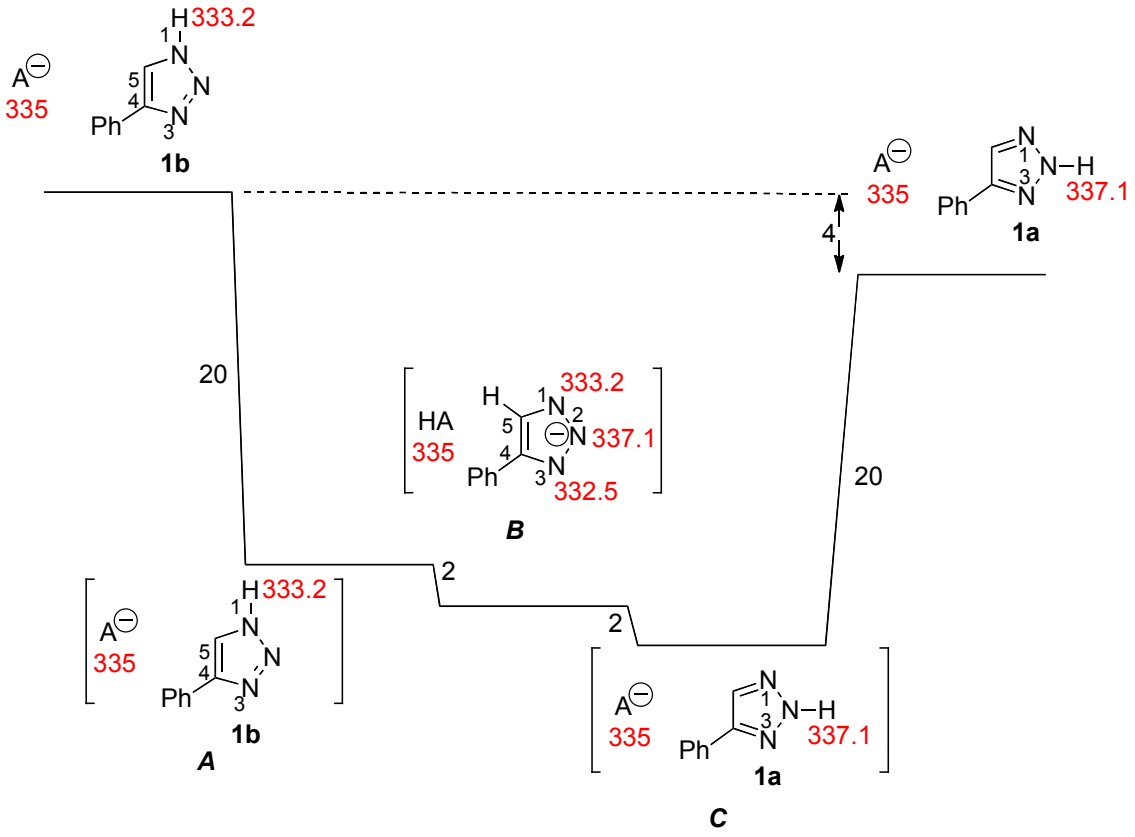

Figure 3.7. Pathway by which conjugate bases of reference acids could react with **1b**. Values are in kcal mol^{-1}. Red values are ΔH_{acid} values; for the triazole, values are calculated at B3LYP/6-31+G(d)(ΔH).

Thus, our results indicate the certain presence of **1a**, with a possibility of some **1b**, under our gas phase conditions. This is consistent with the calculations, which indicate that **1a** is the most stable structure.[155]

Benzotriazoles: parent and 1-phenyl-substituted.

3.3.2. Benzotriazole (parent, 2)

i. Calculations: benzotriazole tautomers, acidity, proton affinity.

Benzotriazole has two possible tautomeric structures (Figure 3.8). The most stable tautomer "N1H" (**2a**) is calculated to be only 0.2 kcal mol^{-1} more stable than the "N2H" tautomer **2b**. We also calculated the acidities and basicities of both tautomers. The most acidic site of **2a** is predicted to be the N1-H (ΔH_{acid} = 334.0 kcal mol^{-1}). (One C-H acidity was calculated to show that those sites will be less acidic than the N-H sites). The most basic site of tautomer **2a** is the N3 (PA = 217.5 kcal mol^{-1}). For the N2H tautomer **2b**, the N-H has a ΔH_{acid} of 333.8 kcal mol^{-1}. For **2b**, the N1 and N3 are equivalent and have a calculated PA of 205.0 kcal mol^{-1}.

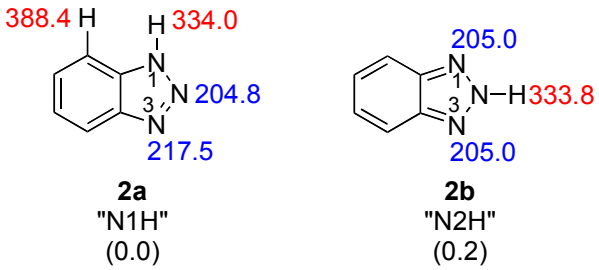

Figure 3.8. The two possible tautomeric structures of benzotriazole (**2**). Gas phase acidities are in red; gas phase proton affinities are in blue. Relative stabilities are in parentheses. Calculations were conducted at B3LYP/6-31+G(d); reported values are ΔH (kcal mol^{-1}) at 298 K.

ii. Experiments: Benzotriazole acidity.

We measured the acidity of benzotriazole using acidity bracketing (Table 3.7). The conjugate base of benzotriazole deprotonates 2-chloropropionic acid (ΔH_{acid} = 337.0 ± 2.1 kcal mol^{-1}); the reaction in the opposite direction (2-chloropropionate with benzotriazole) also occurs (Table 3.7). We therefore bracket the ΔH_{acid} of benzotriazole as 337 ± 3 kcal mol^{-1}.

Table 3.7. Summary of results for acidity bracketing of benzotriazole (**2**).

Reference compound	ΔH_{acid}[a]	*Proton transfer*[b]	
		Ref. acid	*Conj. base*
2,4-pentadione	343.8 ± 2.1	–	+
methylcyanoacetate	340.8 ± 2.1	–	+
a,a,a-trifluoromethyl-*m*-cresol	339.3 ± 2.1	–	+
2-chloropropionic acid	337.0 ± 2.1	+	+
malononitrile	335.8 ± 2.1	+	–
pyruvic acid	333.5 ± 2.9	+	–
per-fluoro-tert-butanol	331.6 ± 2.2	+	–
difluoroacetic acid	331.0 ± 2.2	+	–
1,1,1-trifluoro-2,4-pentadione	328.3 ± 2.9	+	–

[a] Acidities are in kcal mol^{-1}.[15,151] [b] A "+" indicates the occurrence and a "–" indicates the absence of proton transfer.

iii. Experiments: Benzotriazole proton affinity.

In bracketing the PA of benzotriazole, we find that 3-chloropyridine (PA = 215.9 ± 2.0 kcal mol^{-1}) deprotonates protonated benzotriazole; the opposite reaction (benzotriazole deprotonating protonated 3-chloropyridine) also occurs (Table 3.8). We therefore bracket the PA of benzotriazole to be 216 ± 3 kcal mol^{-1}.

Table 3.8. Summary of results for proton affinity bracketing of benzotriazole (**2**).

Reference compound	*PA*[a]	*Proton transfer*[b]	
		Ref. base	*Conj. acid*
pyridine	222.3 ± 2.0	+	–
propylamine	219.4 ± 2.0	+	–
dimethylacetamide	217.0 ± 2.0	+	–
3-chloropyridine	215.9 ± 2.0	+	+
methylamine	214.9 ± 2.0	–	+
m-toluidine	214.1 ± 2.0	–	+
aniline	210.9 ± 2.0	–	+
2,4-pentadione	208.8 ± 2.0	–	+

[a] PAs are in kcal mol^{-1}.[15] [b] A "+" indicates the occurrence and a "–" indicates the absence of proton transfer

We also examined the "locked" tautomer 1-methylbenzotriazole (**3**, Figure 3.9), to assess the accuracy of the calculations (since there is no tautomer ambiguity for this compound). We bracket a gas phase acidity of 379 ± 3 kcal mol^{-1} (calculated value is 379.1 kcal mol^{-1}) and a gas phase proton affinity of 223 ± 3 kcal mol^{-1} (calculated value is 222.4 kcal mol^{-1}), indicating that the calculations do appear to be accurate.[156]

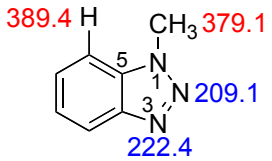

3

Figure 3.9. Calculated properties of 1-methylbenzotriazole (**3**). Gas phase acidities are in red; gas phase proton affinities are in blue. Calculations were conducted at B3LYP/6-31+G(d); reported values are ΔH (kcal mol^{-1}) at 298 K.

Thus, the experimental acidity of the *parent* benzotriazole **1** is measured to be 337 ± 3 kcal mol^{-1}. This value is consistent with an earlier measurement by Taft and coworkers (338 ± 2 kcal mol^{-1}).[157] Because the calculated acidity of the N1H and N2H tautomers is roughly the same (334 kcal mol^{-1}), the experimental acidity value cannot be used to differentiate which structure(s) exist in the gas phase under our conditions. The experimental proton affinity is 216 ± 3 kcal mol^{-1}. This value is consistent with the N1H tautomer **2a** (calculated PA = 217.5 kcal mol^{-1}) but not the N2H tautomer **2b** (PA = 205.0 kcal mol^{-1}). Because the calculations predict that **2b** should be only minimally less stable (0.2 kcal mol^{-1}) than **2a**, one might expect experimental evidence for the presence of **2b**. However, this system would have the same caveats that the 4-phenyl-1,2,3-triazole

system has, wherein protonated bases can cause tautomerization, and so we cannot be sure of the structures present under our conditions: it could be **2a**, **2b**, or some mixture thereof. Previous gas phase studies (UV, FTIR) give conflicting results as to which tautomer predominates, although solid state and aqueous studies point to the N1H tautomer **2a.**[50-52,158-165]

3.3.3. 4'-Substituted-4-phenyl-1,2,3-triazoles

We also probe the substituent effect on gas phase properties of 4-phenyl-1,2,3-triazole. In the unsubstituted 4-phenyl-1,2,3-triazole studies, we found the discrepancy between calculated and experimental proton affinity values. Studying the substituted analogues is interesting also because we can compare their calculated gas phase acidities/proton affinities with experimental values as well to see whether their calculated PA values track their experimental values.

4'-Fluoro-4-phenyl-1,2,3-triazole (5)

i. Calculations: 4'-fluoro-4-phenyl-1,2,3-triazole tautomers, acidity, proton affinity.

2',4'-Dinitro-1-phenylbenzotriazole has eight possible tautomers, five of which are listed in Figure 3.10. Of the eight tautomers, three are within 5 kcal mol^{-1}.

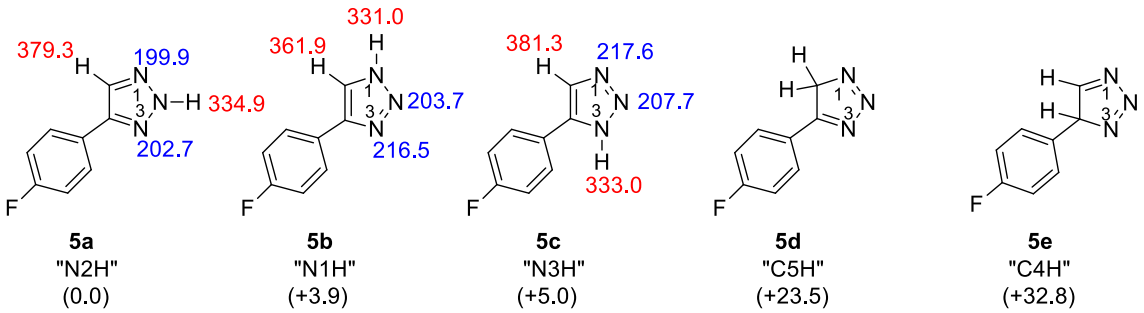

Figure 3.10. The possible tautomers of 4'-fluoro-4-phenyl-1,2,3-triazole (**5**). Gas phase acidities are in red; gas phase proton affinities are in blue. Relative stabilities are in parentheses. Calculations were conducted at B3LYP/6-31+G(d); reported values are ΔH (kcal mol^{-1}) at 298 K.

ii. Experiments: 4'-fluoro-4-phenyl-1,2,3-triazole proton affinity.

We find that *N*-methylacetamide (PA = 212.4 ± 2.0 kcal mol^{-1}) deprotonates protonated 4'-fluoro-4-phenyl-1,2,3-triazole; the opposite reaction (4'-fluoro-4-phenyl-1,2,3-triazole deprotonating protonated *N*-methylacetamide) also occurs (Table 3.9). Therefore, we bracketed the PA at 212 ± 3 kcal mol^{-1}.

Table 3.9. Summary of results for proton affinity bracketing of 4'-fluoro-4-phenyl-1,2,3-triazole (**5**).

Reference compound	*PA*[a]	*Proton transfer*[b]	
		Ref. base	*Conj. acid*
butylamine	220.2 ± 2.0	+	–
dimethylacetamide	217.0 ± 2.0	+	–

3-chloropyridine	215.9 ± 2.0	+	–
m-toluidine	214.1 ± 2.0	+	–
N-methylacetamide	212.4 ± 2.0	+	+
aniline	210.9 ± 2.0	–	+
2,4-pentadione	208.8 ± 2.0	–	+

[a] PAs are in kcal mol^{-1}.[15] [b] A "+" indicates the occurrence and a "–" indicates the absence of proton transfer

4'-Methyl-4-phenyl-1,2,3-triazole (6)

i. Calculations: 4'-methyl-4-phenyl-1,2,3-triazole tautomers, acidity, proton affinity.

The calculated values of 4'-methyl-4-phenyl-1,2,3-triazole are listed in Figure 3.11. Similar to the parent compound 1 and fluoro substituted triazole 5, 4'-methyl-4-phenyl-1,2,3-triazole has eight possible tautomers. Three of the tautomers are within five kcal mol^{-1}.

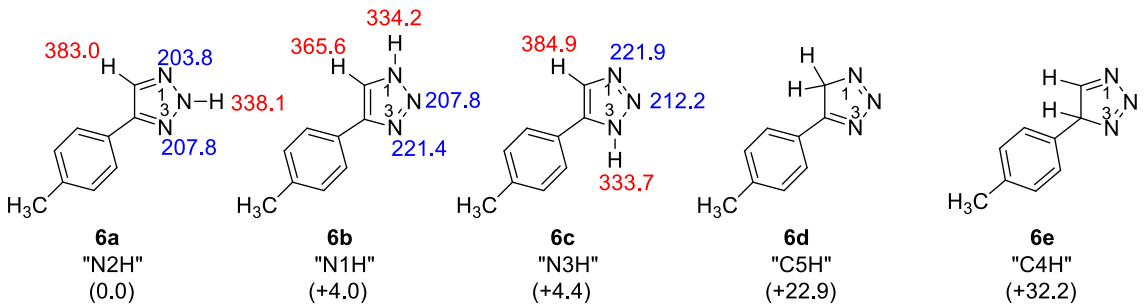

Figure 3.11. The possible tautomers of 4'-methyl-4-phenyl-1,2,3-triazole (**6**). Gas phase acidities are in red; gas phase proton affinities are in blue. Relative stabilities are in parentheses. Calculations were conducted at B3LYP/6-31+G(d); reported values are ΔH (kcal mol^{-1}) at 298 K.

ii. Experiments: 4'-methyl-4-phenyl-1,2,3-triazole proton affinity.

We measured the PA of 4'-methyl-4-phenyl-1,2,3-triazole. Dimethylacetamide (PA = 217.0 ± 2.0 kcal mol^{-1}) deprotonates protonated 4'-methyl-4-phenyl-1,2,3-triazole; the opposite reaction (4'-methyl-4-phenyl-1,2,3-triazole deprotonating protonated dimethylacetamide) also happens (Table 3.10). Therefore, we bracketed the PA at 217 ± 3 kcal mol^{-1}.

Table 3.10. Summary of results for proton affinity bracketing of 4'-methyl-4-phenyl-1,2,3-triazole (**6**).

Reference compound	*PA*[a]	*Proton transfer*[b]	
		Ref. base	*Conj. acid*
cyclohexylamine	223.3 ± 2.0	+	–
pyridine	222.3 ± 2.0	+	–
butylamine	220.2 ± 2.0	+	–
propylamine	219.4 ± 2.0	+	–
dimethylacetamide	217.0 ± 2.0	+	+
2-chloropyridine	215.9 ± 2.0	–	+
2-chloropyridine	215.2 ± 2.0	–	+

[a] PAs are in kcal mol^{-1}.[15] [b] A "+" indicates the occurrence and a "–" indicates the absence of proton transfer

4'-Methoxy-4-phenyl-1,2,3-triazole (7)

i. Calculations: 4'-methoxy-4-phenyl-1,2,3-triazole tautomers, acidity, proton affinity.

4'-Methoxy-4-phenyl-1,2,3-triazole also has eight tautomers, five of which are shown in Figure 3.12. N2H tautomer is the most stable one, which is more stable than N1H tautomer by 3.9 kcal mol^{-1}. N3H tautomer is 4.4 kcal mol^{-1} less stable than N2H tautomer. The other five tautomers are much less stable than these three tautomers.

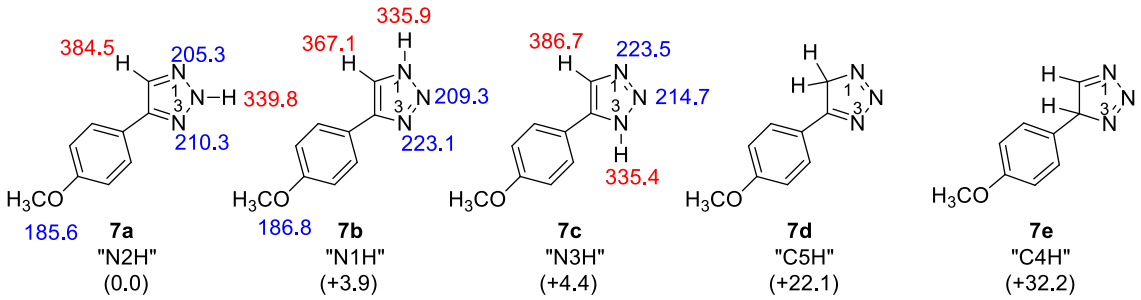

Figure 3.12. The possible tautomers of 4'-methoxy-4-phenyl-1,2,3-triazole (**7**). Gas phase acidities are in red; gas phase proton affinities are in blue. Relative stabilities are in parentheses. Calculations were conducted at B3LYP/6-31+G(d); reported values are ΔH (kcal mol^{-1}) at 298 K.

ii. Experiments: 4'-methoxy-4-phenyl-1,2,3-triazole proton affinity.

We measured the PA of 4'-methoxy-4-phenyl-1,2,3-triazole. Dimethylacetamide (PA = 217.0 ± 2.0 kcal mol^{-1}) does not deprotonate protonated 4'-methoxy-4-phenyl-1,2,3-triazole; the opposite reaction (4'-methyl-4-phenyl-1,2,3-triazole deprotonating protonated dimethylacetamide) occurs (Table 3.11). On the other hand, butylamine (PA =

220.2 ± 2.0 kcal mol^{-1}) deprotonate protonated 4'-methoxy-4-phenyl-1,2,3-triazole; the opposite reaction (4'-methyl-4-phenyl-1,2,3-triazole deprotonating protonated dimethylacetamide) does not happen (Table 3.18).Therefore, we bracketed the PA at 219 ± 4 kcal mol^{-1}.

Table 3.11. Summary of results for proton affinity bracketing of 4'-methoxy-4-phenyl-1,2,3-triazole (**7**).

Reference compound	*PA*[a]	*Proton transfer*[b]	
		Ref. base	*Conj. acid*
pyridine	222.3 ± 2.0	+	–
butylamine	220.2 ± 2.0	+	–
dimethylacetamide	217.0 ± 2.0	–	+

[a] PAs are in kcal mol^{-1}.[15] [b] A "+" indicates the occurrence and a "–" indicates the absence of proton transfer

Both calculated and experimental proton affinities of 4-phenyl-1,2,3-triazoles are summarized in Table 3.12.

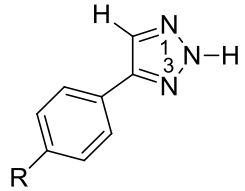

Table 3.12. Summary of results for proton affinity of 4-phenyl-1,2,3-triazoles.

Substituent R	Tautomer	Most basic site (calculated, kcal mol^{-1})	Most basic site (experimental, kcal mol^{-1})
fluoro	N2H (**5a**)	202.7	212 ± 3
	N1H (**5b**)	216.5	
H	N2H (**1a**)	205.3	217 ± 3
	N1H (**1b**)	219.2	
methyl	N2H (**6a**)	207.8	217 ± 3
	N1H (**6b**)	221.4	
methoxy	N2H (**7a**)	210.3	219 ± 4
	N1H (**7b**)	223.1	

Same as unsubstituted 4-phenyl-1,2,3-triazole **1**, the bracketed proton affinities of fluoro, methyl and methoxy substituted 4-phenyl-1,2,3-triazoles are not consistent with either N2H tautomer or N1H tautomer. In order to verify that triazole **5**, **6** and **7** have the same tautomeric situations as triazole 1, we choose one of the triazoles, triazole **6**, to analyze the PA bracketing data (Figure 3.13).

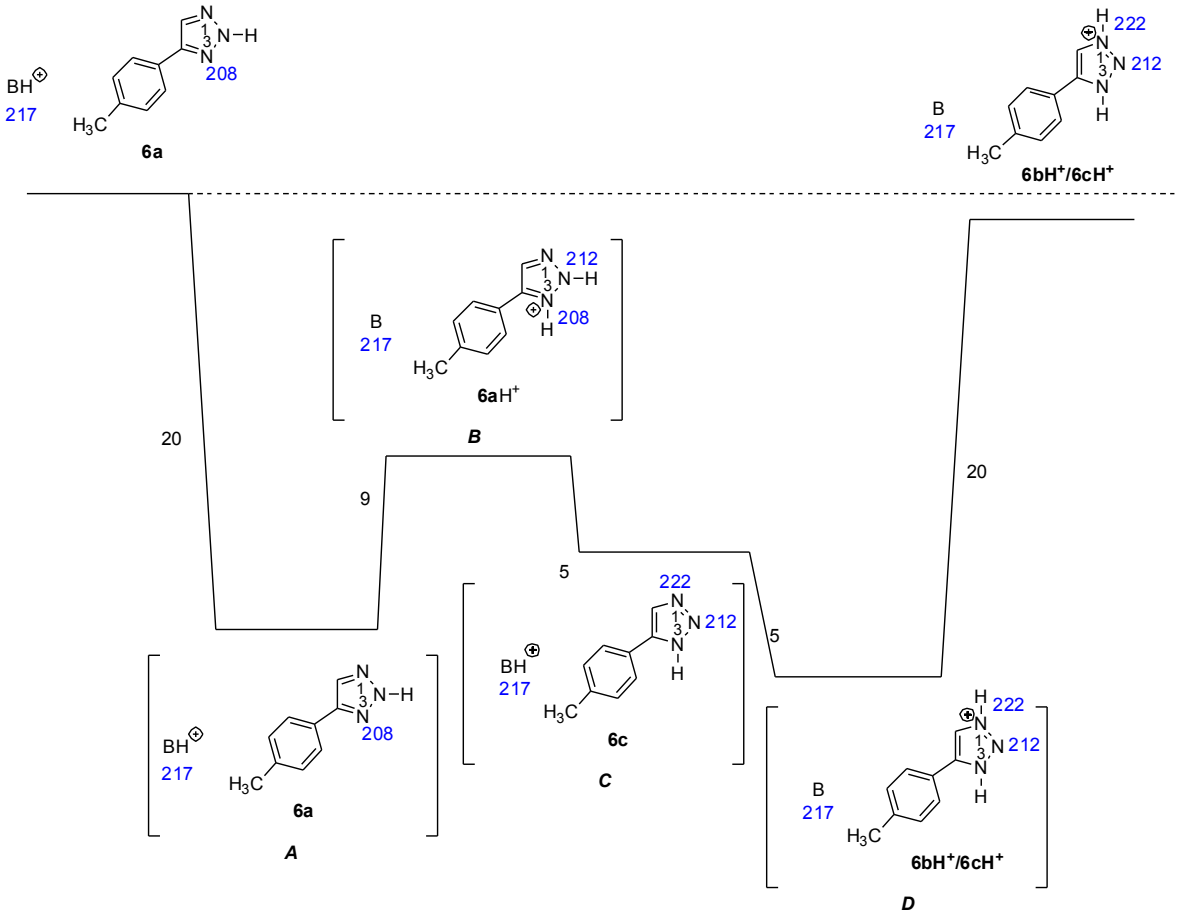

Figure 3.13. Pathway by which a protonated reference base BH^+ could react with the N2H tautomer of 4'-methyl-4-phenyl-1,2,3-triazole (**6a**). Values are in kcal mol^{-1}. Blue values are PAs; for the triazole, values are calculated at B3LYP/6-31+G(d)(ΔH).

The proton affinity of triazole **6** is bracketed to be the same as dimethylacetamide (217.0 ± 2.0 kcal mol^{-1}). If only **6a** were present, then the triazole should not be able to deprotonate any protonated reference base above 217 kcal mol^{-1}. However, the reaction depicted in Figure 3.13 could be taking place. In Figure 3.13, the protonated reference base BH^+ first forms an ion-molecule complex with triazole **6a**, which is roughly 20 kcal

mol^{-1} exothermic (to form ***A***). Proton transfer between the most basic site of **6a** (N3, calculated PA = 208 kcal mol^{-1}) and BH^+ is endothermic (to form complex ***B***), but allowed energetically since the complex is still less than the total energy of the system (indicated by the dotted line). Now the reference base B can access the N2-H proton (exothermic by 5 kcal mol^{-1}) to form the **6c** tautomer of the triazole (complex ***C***). The N1 of **6c** is basic enough to deprotonate the protonated BH^+ (to form complex ***D***), which can then lead to the observable products, B and protonated triazole, in an overall thermoneutral reaction. The structure of the protonated triazole would not be that of $\mathbf{6aH^+}$ but instead, that of $\mathbf{6bH^+}$ (or $\mathbf{6cH^+}$ - these have the same structure). By mass spectrometry, however, one only tracks the m/z ratio, so the presence of any protonated triazole yields the "+" in Table 3.13. Computationally, the path in Figure 3.13 would be predicted to be accessible for any base with a PA of about 217 kcal mol^{-1} or lower, which is what we observe experimentally (Table 3.13). This explains the discrepancy between calculated and experimental results, which further lend support to our theory that the N2H tautomer predominates.

3.4 Conclusions.

We have measured the proton affinity and acidity of 4-phenyl-1,2,3-triazole; the acidity has not heretofore been measured. Together with H/D exchange data, we can establish that under our gas phase conditions, the N2H tautomer **1a** is definitively present. Tautomer **1b** may be present, though it seems unlikely. The parent and substituted 4-phenylbenzotriazoles have also been characterized, with previously unknown acidity and proton affinity values being assessed.

Chapter 4 *N*-heterocyclic Carbene Catalyst with Charged Handle: Benzoin Condensation Studies

4.1 Introduction

It has been known that thiamine and thiazolium salts catalyze benzoin condensation in the presence of mild base since 1943.[166] As an analogous mechanism of catalysis using cyanide ion by Lapworth,[167] Breslow proposed that a persistent carbene acts as a key role in this transformation in the 1950s,[55-57] which has been well accepted ever since. Recently, Berkessel and coworkers isolated the Breslow intermediate for the first time, lending more support in the Breslow mechanism.[168] Imidazolium-based NHCs have become more and more popular since the first isolation of NHC by Arduengo in 1991.[53,85-89] Benzoin condensation catalyzed by imidazolium catalysts has been largely reported ever since.[90-94] Aside from thiazolium and imidazolium based catalysts, triazolium-based catalysts have been proven to effect the benzoin condensation.[95,97-100,102,169]

Breslow mechanism (Figure 4.1) features the formation of C2-ylide **1b**, generated *in situ* from the deprotonation of parent thiazolium salts **1a** with mild bases. Subsequent nucleophilic addition to a benzaldehyde, after deprotonation, yields a resonance-stablized intermediate **1d** (**1e**), which is also referred as "Breslow intermediate". A second benzaldehyde adding to the intermediate **1d** gives diphenylhydroxy thiazolium adduct **1f**, which eventually release the benzoin and re-generate thiazolium ylide **1b**.

In 1960, Wanzlick proposed that the carbene generated from the vacuum pyrolysis is in equilibrium with its dimer, which he believed, only acts as the carbene reservoir.[65,67,68] Challenges to Breslow Mechanism and Wanzlick equilibrium by Lemal, and later by

Winberg claimed that the carbene dimer is catalytically active in the catalytic circle.[69,70] Lemal dimer mechanism (Figure 4.2) is different from Breslow mechanism in that when treated with electrophile (e.g., benzaldehyde), carbene dimer **2d** will attack electrophile rather than carbene monomer, followed by the dissociation to form the adduct **2g** and free carbene **2b**. The free carbene will either react with electrophile, or form the dimer again.

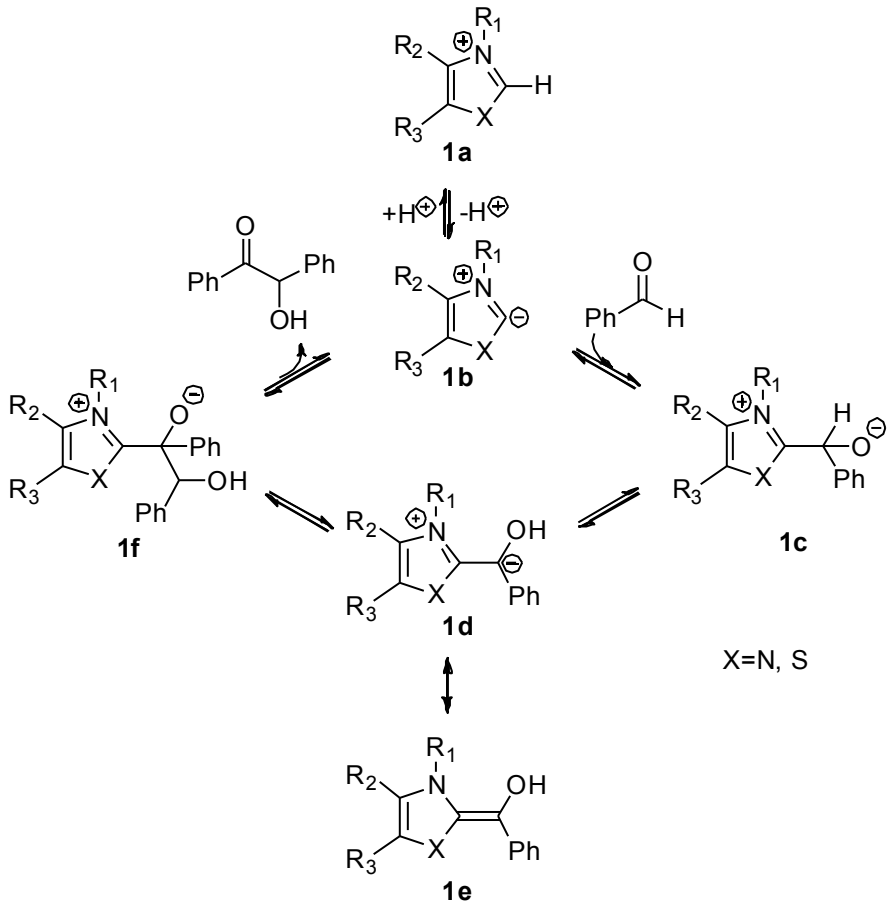

Figure 4.1. Detailed Breslow mechanism for benzoin condensation using thiazolium salt as catalyst.

Since the late 1980s, Castells and coworkers proposed alternative dimer mechanism.[71-76,170] Castells dimer mechanism is different from Lemal dimer mechanism

in that the dimer-electrophile adduct (**3c**) will not undergo dissociation, but rather react with a second electrophile. (Figure 4.3)

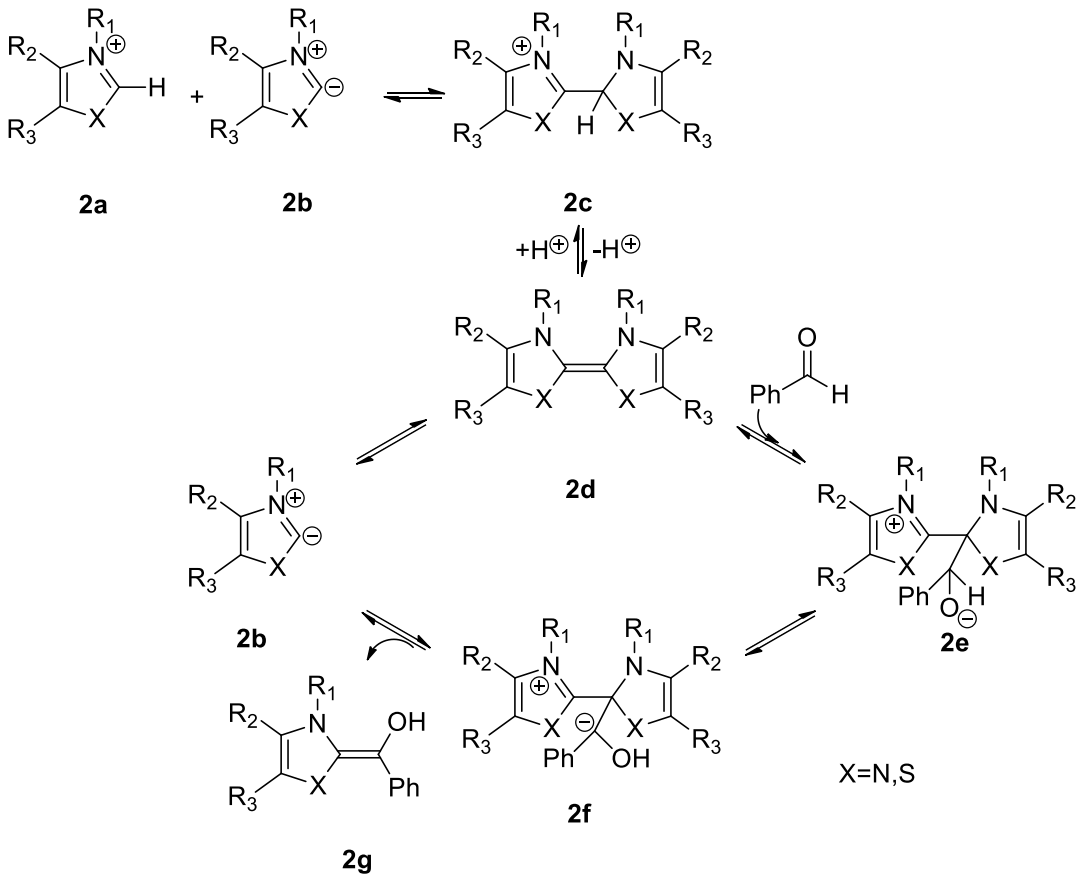

Figure 4.2. Lemal dimer mechanism for benzoin condensation using imidazolium salt as catalyst.

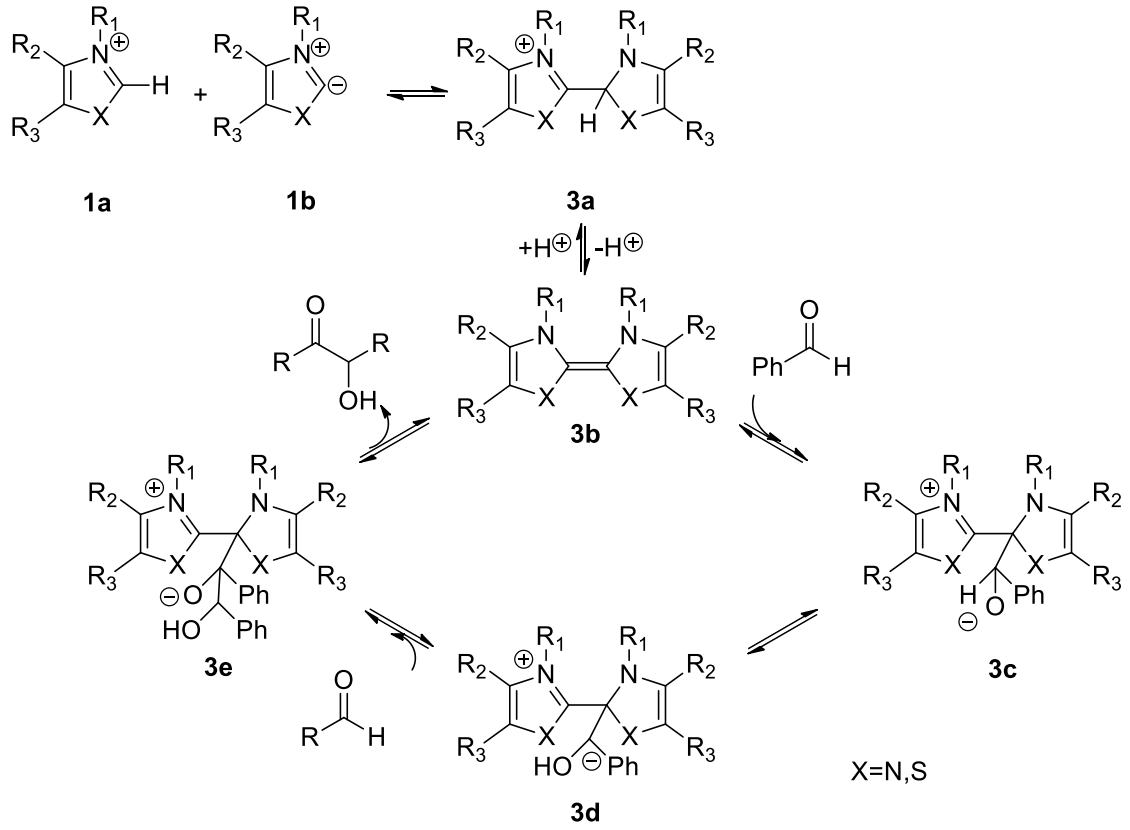

Figure 4.3. Castells dimer mechanism for benzoin condensation using thiazolium salt as catalyst.

Of the three mechanisms, many studies of benzoin condensation point to the the Breslow menchanism.[78,79,168,171,172] Traditional mechanistic studies (kinetic studies) are mainly conducted using NMR.[170-172] Recently, mass spectrometry has been used in many areas. Our group takes an effort to conduct studies of the organic reactions via mass spectrometry. Thus, we start from a well known reaction, benzoin condensation. Neutral carbenes are undetectable by Mass Spectroscopy; and intermediates are usually unstable and have the propensity of fragmentation. Introducing charged handle to NHC will address the first issue while using a "soft" electrospray ionization tandem mass spectrometry (ESI-MS/MS) will help the latter.[173] ESI-MS/MS has achieved recognition

as a tool to probe the reaction mechanisms over the years.[104-106] Therefore, we first apply this method to characterize a novel thiazolium NHC with sulfonate group as charged handle. As a comparison to the thiazolium catalyst, we also employed an imidazolium-based catalyst to track the benzoin condensation reaction. The imidazolium catalyst **5a** has previously been described by Lalli and coworkers.[107]

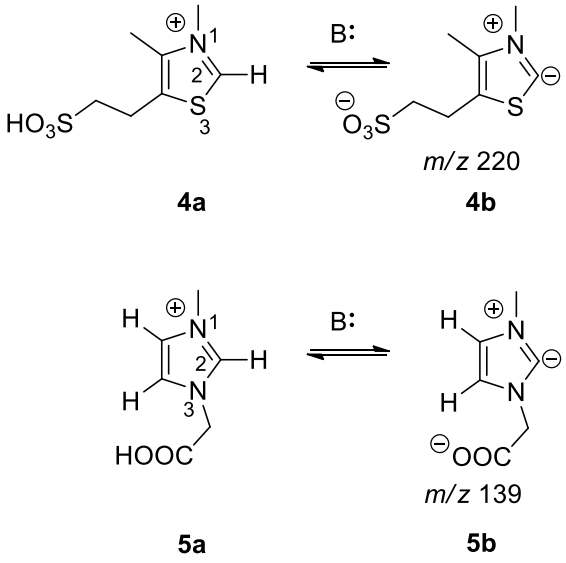

Figure 4.4. Thiazolium catalyst with sulfonate as charged tag.

4.2 Experimental

4.2.1. Chemicals and Materials

1,5-Dimethyl-4-(sulfoethyl) thiazolium iodide (**4a)**[174,175]

A solution of 1,5-dimethyl-4-(hydroxyethyl) thiazolium iodide (1mmol), methylsulfonyl chloride (1.2mmol) and triethylamine (5mmol) in CH_3CN (5ml) was stirred for 2 hrs at 0 ^oC. Reaction was protected by N_2 gas. Then, the potassium

methylthiaoate (1.2 mmol) and ethanol (15 ml) were added to the reaction mixtures and refluxed for 72 hrs. Hydrogen peroxide (8mmol) and formic acid (12 mmol) were then

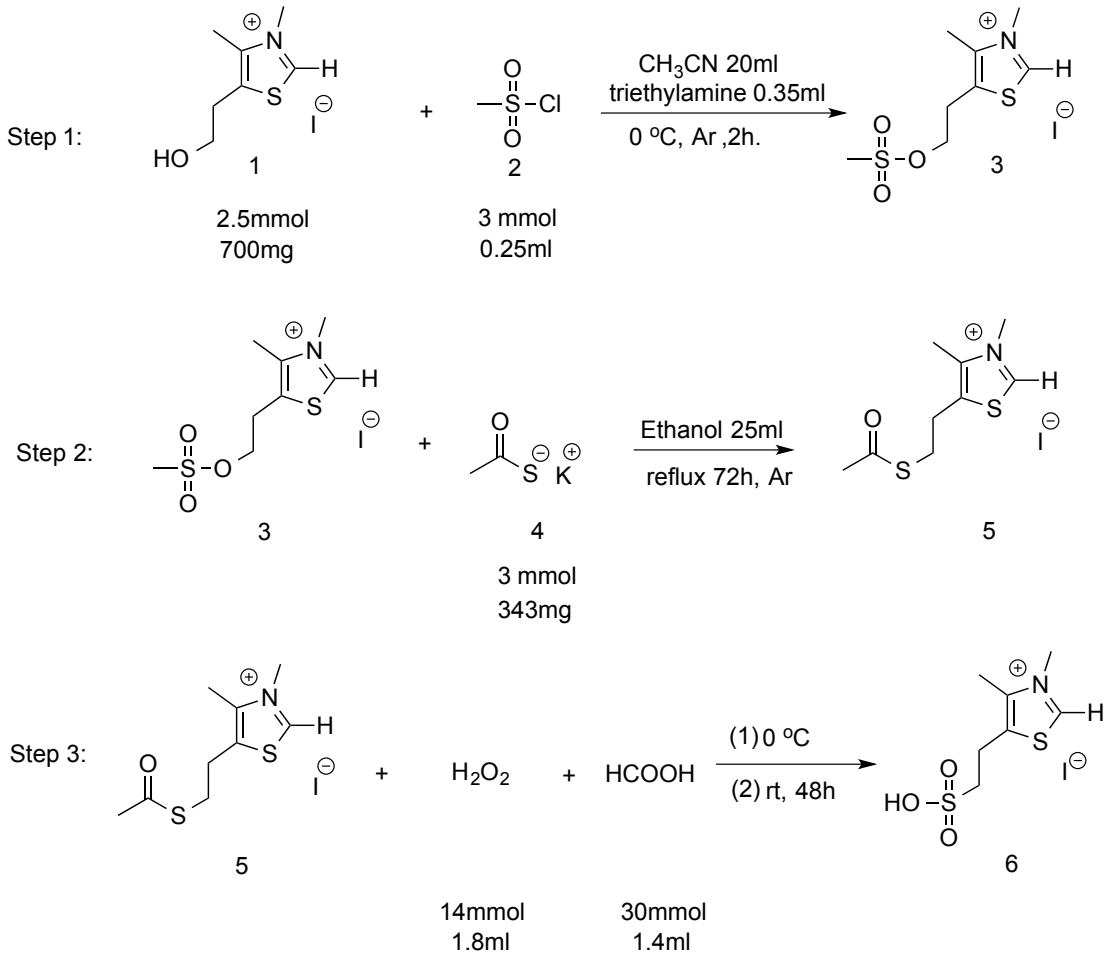

added to the reaction at 0 °C, and let it react at room temperature for 2 hrs. Compound was purified using HPLC.

Figure 4.5. Synthesis route for 1,5-Dimethyl-4-(sulfoethyl) thiazolium iodide (**4a).**

(2) 1-Methyl-3-(carboxylmethyl) imidazolium chloride (**5a)** was purchased from BOC Sciences and used as recieved.

4.2.2. ESI-MS/MS experiments

Catalysts **4a** (**5a)** was dissolved in methanol and diluted to make 100 μM solution. Inert Argon gas was sprayed into the bottle to expel oxygen for 5 mins. 2.5 Equivalents of triethylamine (potassium *tert*-butoxide), along with benzaldehyde (10 equivalents) were added to the catalyst solution. The reaction was kept in a sealed vial for 1 day (1 week when using **5a**). The aliquot was injected and electrosprayed to generate the ions. An electrospray needle voltage of ~4 kV and the flow rate of 25 μL/min was applied. The ions were isolated and then dissociated using collision-induced dissociation (CID); the ions were activated for about 30 ms. Finally, the dissociation product ions were detected, recorded and fragmentation patterns analyzed. A total of 20 scans were averaged for the product ions.

4.3 Results and discussion

4.3.1. Thiazolium carbene 4a

The first step we take is to identify the catalyst using mass spectrometry. In order to obtain negatively charged NHCs, a sulfoethyl group is introduced at C4 position in **4a**. Upon deprotonation, "free" carbene with charged handle is formed and "fished out" to apply colllison-induced dissociation (CID). Surprisingly, the HSO_3^- (*m/z* 81) anion was knocked off from the parent ion, and no other significant fragmentation pathways were observed (See Figure 4.6 and 4.7).

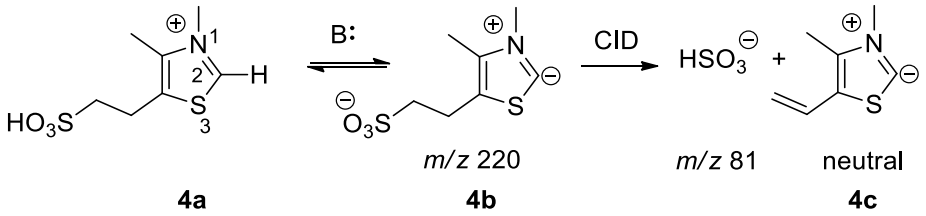

Figure 4.6. Formation of negatively charged NHC via double deprotonation from thiazolium parent ions.

The double bond in the side-chain of daughter product **4c** is resonance-stabilized by the five-membered thiazolium ylide ring, which prevents the formation of SO_3^- radical ion (*m/z* 80) observed by Lalli and coworkers for a similar thiazolium carbene.[107] Moreover, the $HSO3^-$ (*m/z* 81) peak lend us a tool to identify the thiazolium catalyst-bond intermediates. After we fish out the ions with *m/z* corresponding to the intermediates, followed by CID, whether HSO_3^- (*m/z* 81) ion is observed will give us preliminary information whether the desired intermediates were isolated. The MS/MS spectra of thiazolium carbene (*m/z* 220) is shown in Figure 4.7.

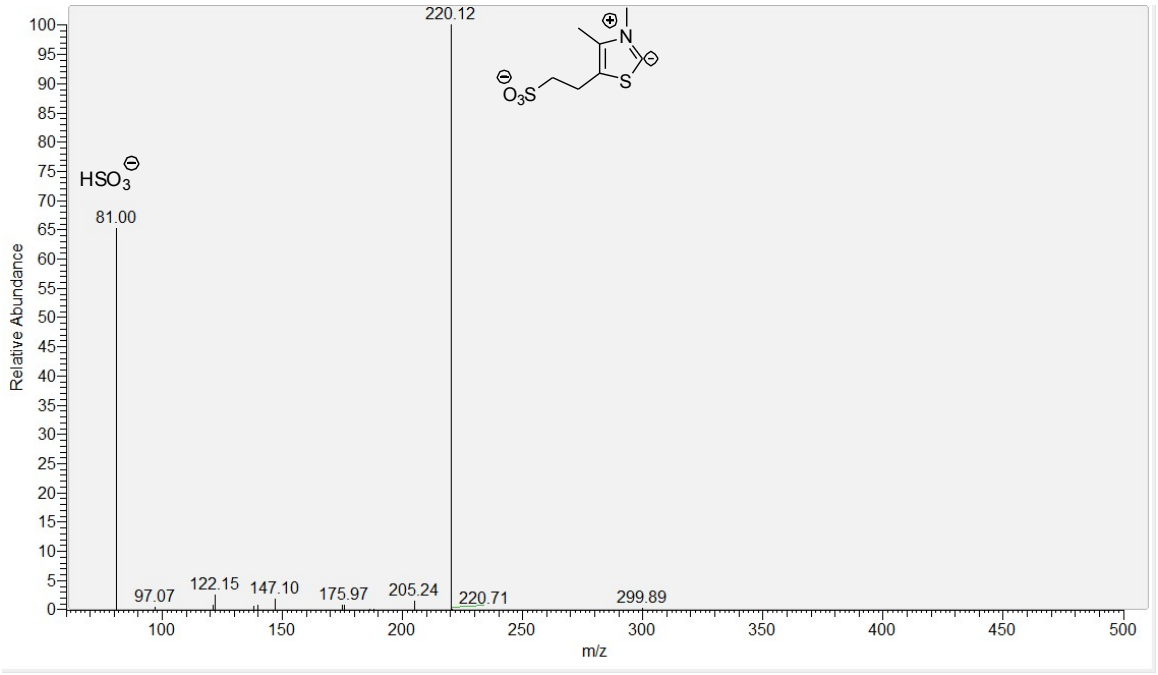

Figure 4.7. ESI-MS/MS spectra of 4b at *m/z* 220.

In order to deprotonate thiazolium catalyst **4a**, we used either NH_4OH or triethylamine as base. Hydroxide and triethylamine are both strong bases, while hydroxide is much more nucleophilic than TEA. Thus, the shortcoming of using a hydroxide is that it could attack the C2 position rather than abstracting C2-H. To verify our postulation, when NH_4OH was used as a base, we trapped the "carbene-water adduct" (**4d**) and apply CID (Figure 4.8), daughter ions with *m/z* 81 and 156 are obtained. Therefore, all the thiazolium-related experiments discussed in chapter 4 employes triethylamine as base.

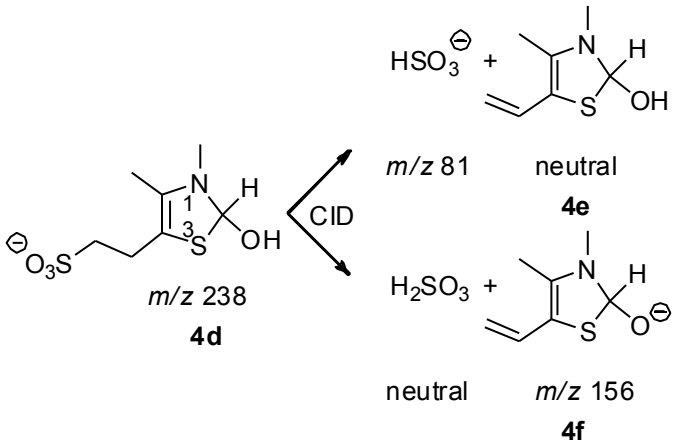

Figure 4.8. Collision-induced dissociation pathways for "carbene-water adduct" **4d**.

4.3.2. Benzoin condensation by thiazolium carbene

Four characteristic intermediates for benzoin condensation are shown in Figure 4.9. **4h** and **4i** have same mass-to-charge ratio, thus it is difficult to differentiate them; same for **4j** and **4k**. Ions with *m/z* 326 and *m/z* 432 were isolated in the ion-trap and CID conducted. The *m/z* 326 (**4h** or **4i**) yields a *m/z* 220 upon CID, indicating a loss of benzaldehyde; other daughter ions *m/z* 311 (loss of CH_3 radical); m/z 308 (loss of H_2O); *m/z* 298 (loss of two CH_3 radicals); *m/z* 244 (loss of H_2SO_4) are also observed (see Figure 4.10). All these fragmentation support the proposed structure of **4h** or **4i**.

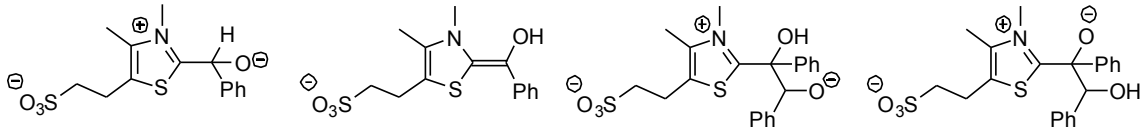

4h *m/z* 326 **4i** *m/z* 326 **4j** *m/z* 432 **4k** *m/z* 432

Figure 4.9. Possible intermediates for benzoin condensation catalyzed by thiazolium **4a**.

The fragmentation pathways of **4h** or **4i** are summarized in Figure 4.10.

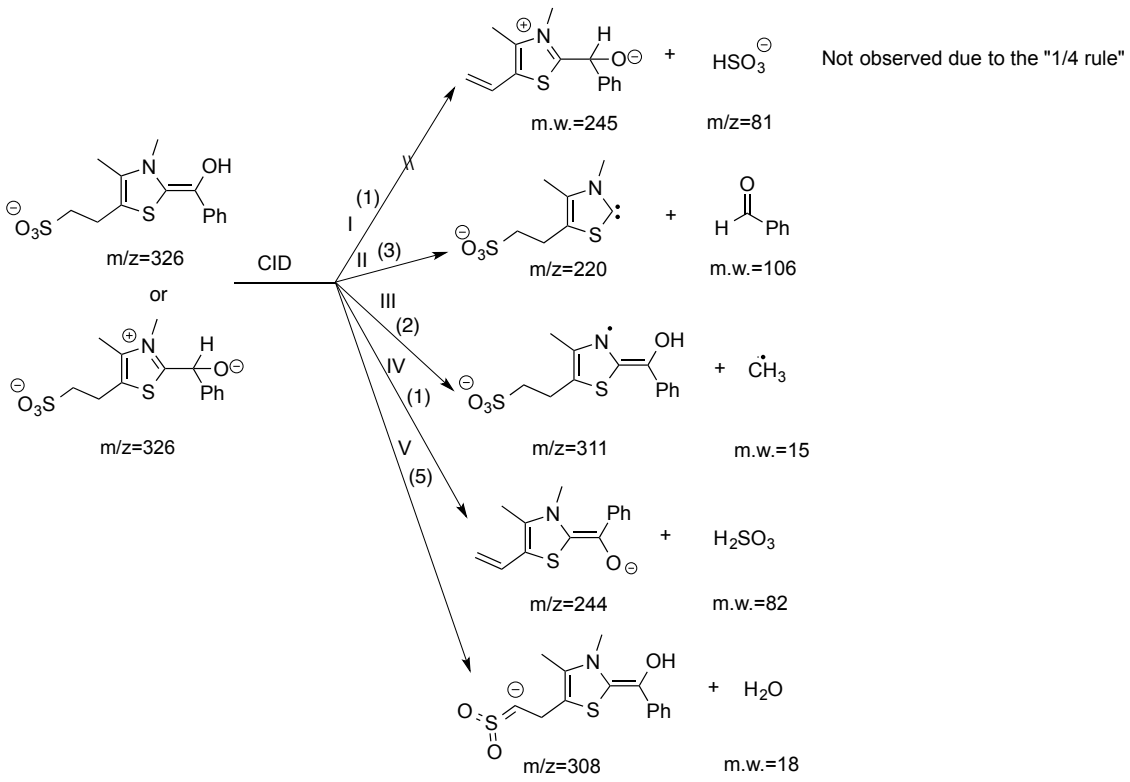

Figure 4.10. Fragmentation pathways of benzaldehyde-thiazolium adduct.

On the other hand, the *m/z* 432 (**4j** or **4k**) yields more complicated fragmentation patterns. Firstly, ions of *m/z* 326 and *m/z* 220 were observed, which correspond to the loss of benzaldehyde and benzoin, respectively. Other peaks such *m/z* 298 (loss of two CH_3 radicals); *m/z* 211 (deprotonated benzoin); *m/z* 163 (di-charged Breslow intermediate

radical) were also seen, which is consistent with the expected structure **4j** or **4k**. The fragmentation patterns are shown in Figure 4.11.

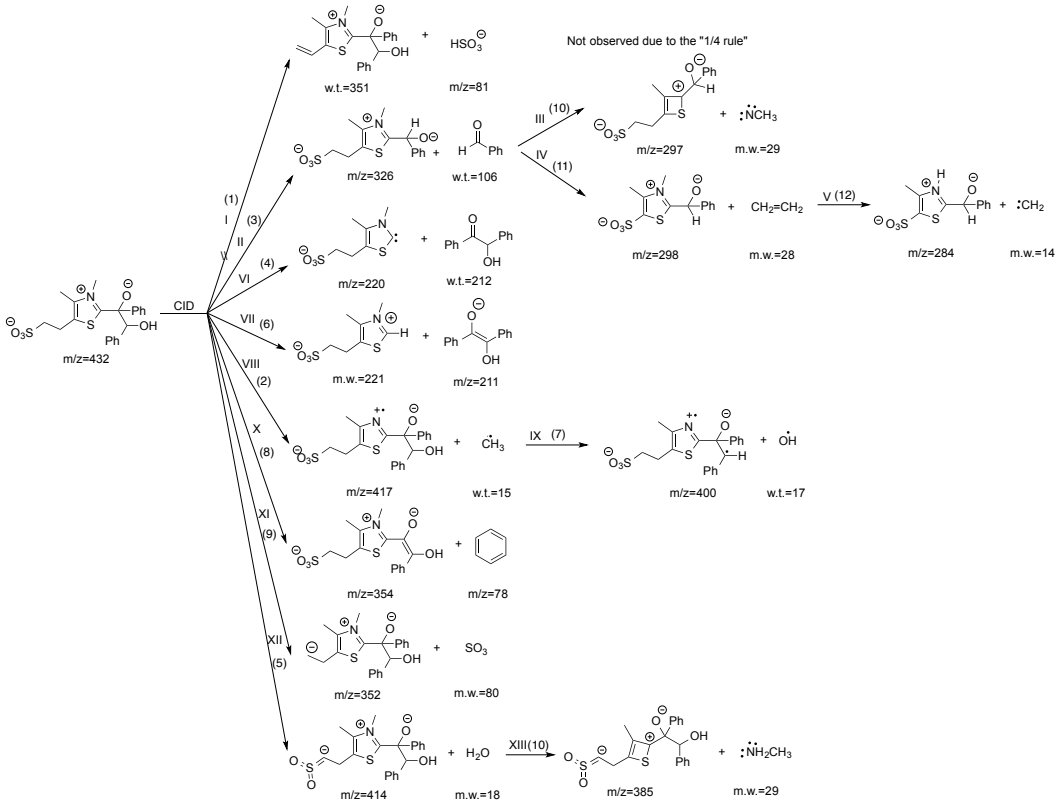

Figure 4.11. Fragmentation pathways of benzaldehyde-thiazolium (2) adduct.

To summarize, we isolate the ion with mass-to-charge ratio that corresponds to the reaction intermediates of Breslow mechanism for benzoin condensation. Fragmentation pathways are consistent with the expected structures of intermediates. Is this method only feasible when using our thiazolium catalyst? Can we use other charged *N*-heterocyclic carbene to conduct the same experiment? In order to further our research, we employed a

imidazolium catalyst with carboxylic group as the charged tag and study on benzoin condensation.

4.3.3. Imidazolium Catalyst 5a

Imidazolium catalysts **5a** with carboxyl group on N3 site, upon double deprotonation and CID, yields a daughter ion **5c** and CO_2 as a main fragmentation pathway (Figure 4.12). There is also another minor daughter peak observed upon CID of 5b (m/z 124). The ion of m/z 124 probably results from the loss of CH_3 radical on N1 site, followed by the abstraction of a H radical (Figure 4.13).

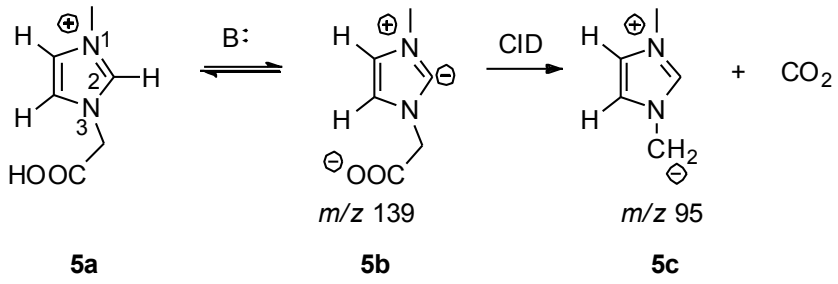

Figure 4.12. Formation of negatively charged NHC via double deprotonation from imidazolium parent ions.

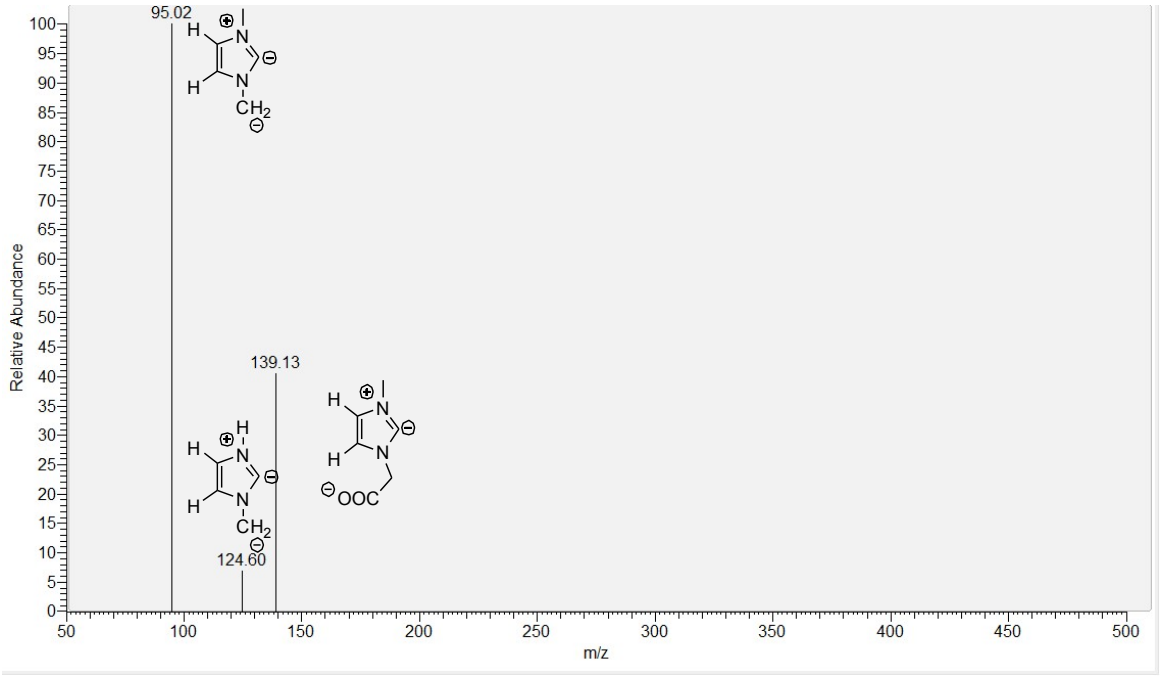

Figure 4.13. ESI-MS/MS spectra of **5b** at m/z 139.

4.3.4. Benzoin Condensation using imidazolium

There are also four expected intermediates of Breslow mechanism for benzoin condensation catalyzed by imidazolium catalyst **5a** (Figure 4.14). Again, **5e** and **5f** have same mass-to-charge ratio, same for **5g** and **5h**. Ion with *m/z* 245 was fished out and underwent dissociation to give *m/z* 201 (loss of CO_2) and *m/z* 139 (loss of benzaldehyde). We also observed daughter ions of *m/z* 231 (loss of CH_3 radical, followed by an abstraction of H radical); *m/z* 230 (loss of CH_3 radical); m/z 227 (loss of H_2O); *m/z* 213 (loss of CH_3 radical and OH radical); m/z 121 (loss of CO_2 and benzaldehyde). The fragmentation pathways are summarized in Figure 4.15.

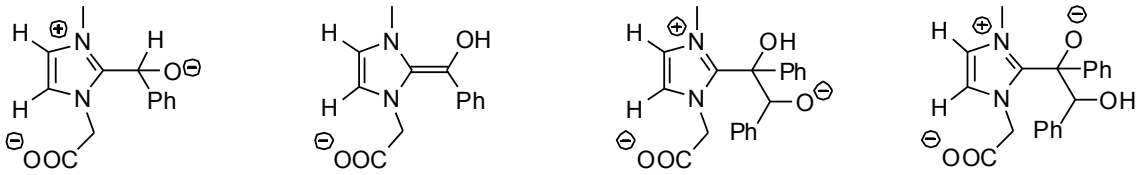

5e m/z=245 **5f** m/z=245 **5g** m/z=351 **5h** m/z=351

Figure 4.14. Characteristic intermediates for benzoin condensation catalyzed by imidazolium **5a**.

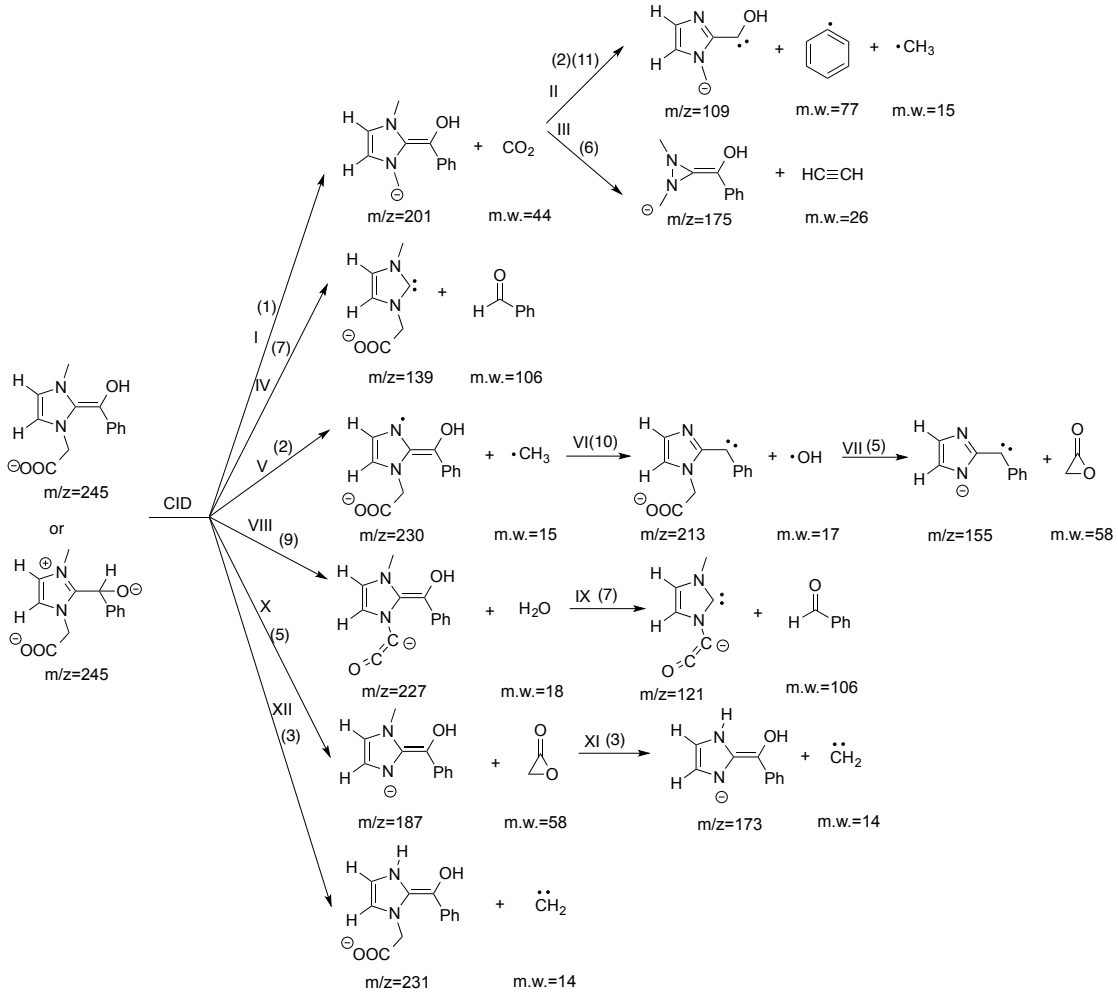

Figure 4.15. Fragmentation pathways of benzaldehyde-imidazolium adduct.

On the other hand, ion of *m/z* 351 (corresponds to imidazolium catalyst with two benzaldehyde) yields *m/z* 307 (loss of CO_2) and *m/z* 245 (loss of benzaldehyde). Other ions such as *m/z* 337 (loss of CH_3 radical, followed by an abstraction of H radical); *m/z* 336 (loss of CH_3 radical); *m/z* 319 (loss of CH_3 radical and H_2O); m/z 213 (loss of H_2O and benzaldehyde); *m/z* 203 (loss of benzaldehyde and C_2H_4N radical resulting from the ring-opening reaction) were also observed. The fragmentation patterns are summarized in Figure 4.16. All these results are consistent with the postulated intermediates (**5e**, **5f**, **5g** and **5h**).

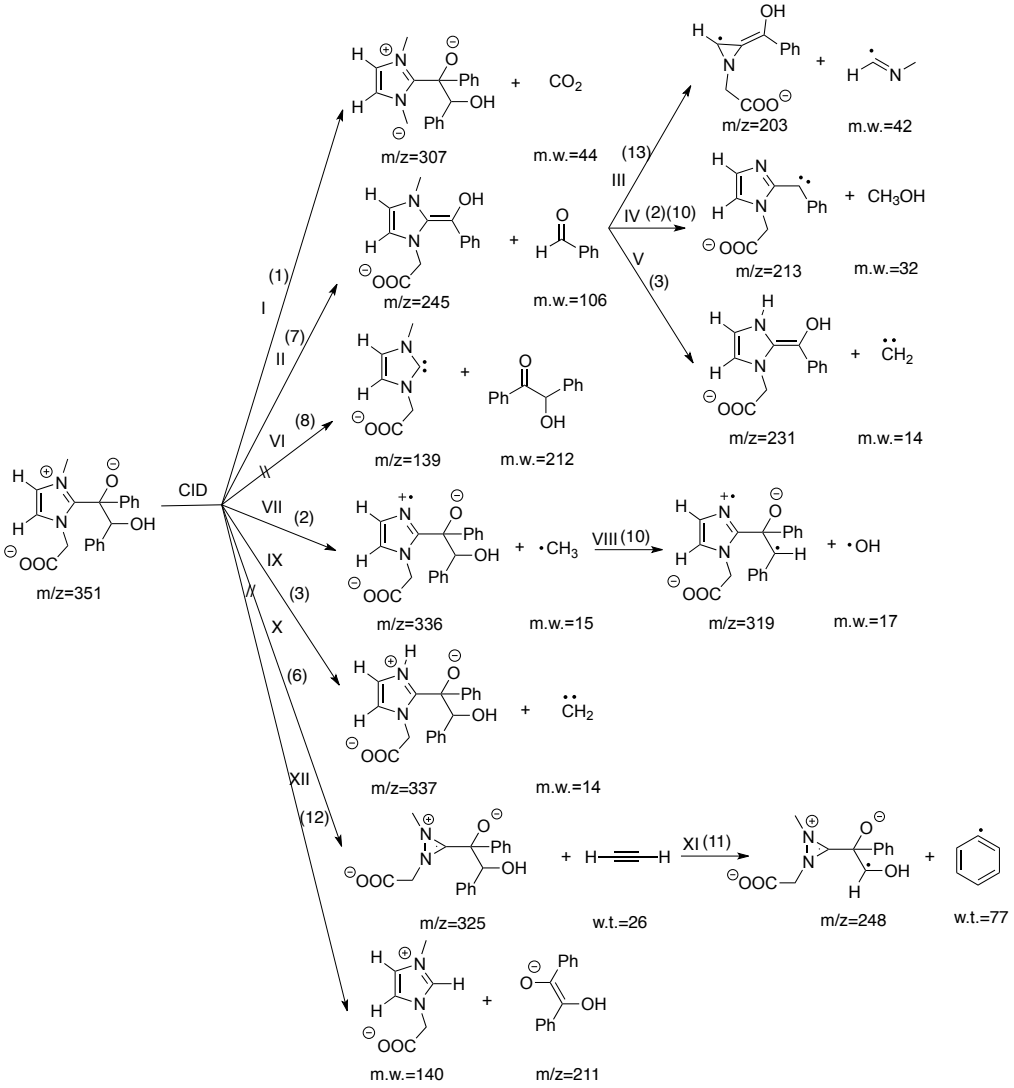

Figure 4.16. Fragmentation pathways of benzaldehyde-imidazolium (2) adduct.

In summary, we found that after deprotonation, the imidazolium catalyst with carboxylic group (**5a**) will undergo double deprotonation to give imidazolium carbene **5b** which is visible on mass spectrometry. CID on **5b** will knock off the CO_2 from the imidazolium carbene and give a charged NHC. We also successfully isolated the ions with m/z ratio corresponds to the reaction intermediates of benzoin condensation catalyzed by imidazolium catalyst. CID on these ions gave various fragmentation pathways which are consistent with the intermediates.

4.4 Conclusion

We have designed a thiazolium salt with negatively charged sidearm, and used it for catalysis analysis. The "charged tag" not only makes the intermediate visible through mass spectroscopy, but also helps us obtain the structural information of intermediates. Free NHCs were characterized by tandem mass spectroscopy and intermediates of Breslow mechanism for benzoin condensation catalyzed by both salts were monitored and analyzed by MS/MS. Intermediates of carbene monomer with one substrate, two substrates were observed and fragmentation pattern studied, respectively. We also extend this method to an imidazolium-based catalyst and successfully characterized the free carbene as well as reaction intermediates via mass spectrometry.

References

(1) Stivers, J. T.; Jiang, Y. L. *Chem. Rev.* **2003**, *103*, 2729-2760.

(2) Stivers, J. T.; Kuchta, R. D. *Chem. Rev.* **2006**, *106*, 213-214.

(3) Berti, P. J.; McCann, J. A. B. *Chem. Rev.* **2006**, *106*, 506-555.

(4) Riazuddin, S.; Lindahl, T. *Biochemistry* **1978**, *17*, 2110-2118.

(5) Karran, P.; Hjelmgren, T.; Lindahl, T. *Nature* **1982**, *296*, 770-773.

(6) Evensen, G.; Seeberg, E. *Nature* **1982**, *296*, 773-775.

(7) Thomas, L.; Yang, C.-H.; Goldthwait, D. A. *Biochemistry* **1982**, *21*, 1162-1169.

(8) O'Brien, P. J.; Ellenberger, T. *J. Biol. Chem.* **2004**, *279*, 26876-26884.

(9) Bowman, B. R.; Lee, S.; Wang, S.; Verdine, G. L. *J. Biol. Chem.* **2010**, *285*, 35783-35791.

(10) Xuejun, S.; Lee, J. K. *J. Org. Chem.* **2007**, *72*, 6548-6555.

(11) Liu, M.; Li, T.; Amegayibor, F. S.; Cardoso, D. S.; Fu, Y.; Lee, J. K. *J. Org. Chem.* **2008**, *73*, 9283-9291.

(12) Sharma, S.; Lee, J. K. *J. Org. Chem.* **2002**, *67*, 8360-8365.

(13) Lee, J. K. *Int. J. Mass. Spectrom.* **2005**, *240*.

(14) Kurinovich, M. A.; Lee, J. K. *J. Am. Soc. Mass. Spectrom.* **2002**, *13*, 985-995.

(15) NIST Chemistry WebBook, NIST Standard Reference Database Number 69; retrieved in 2011. Linstrom, P. J.; Mallard, W. G., Eds.; National Institute of Standards and Technology: Gaithersburg, MD 20899, http://webbook.nist.gov.

(16) Huisgen, R.; Szeimies, G.; Mobius, L. *Chem. Ber.* **1967**, *100*, 2494-2507.

(17) Kolb, H. C.; Fin, M. G.; Sharpless, K. B. *Angew. Chem. Int. Ed.* **2001**, *40*, 2004-2021.

(18) Kolb, H. C.; Sharpless, K. B. *Drug Discovery Today* **2003**, *8*, 1128-1137.

(19) Bock, V. D.; Hiemstra, H.; van Maarseveen, J. H. *Eur. J. Org. Chem.* **2005**, *1*, 51-68.

(20) Whiting, M.; Muldoon, J.; Lin, Y.-C.; Silverman, S. M.; Lindstrom, W.; Olson, A. J.; Kolb, H. C.; Finn, M. G.; Sharpless, K. B.; Elder, J. H.; Fokin, V. V. *Angew. Chem. Int. Ed.* **2006**, *45*, 1435-1439.

(21) Bock, V. D.; Speijer, D.; Hiemstra, H.; van Maarseveen, J. H. *Org. Biomol. Chem.* **2007**, *5*, 971-975.

(22) Ye, C.; Gard, G. L.; Winter, R. W.; Syvret, R. G.; Twamley, B.; Shreeve, J. M. *Org. Lett.* **2007**, *9*, 3841-3844.

(23) Nandivada, H.; Jiang, X.; Lahann, J. *Adv. Mater.* **2007**, *19*, 2197-2208.

(24) Moses, J. E.; Moorhouse, A. D. *Chem. Soc. Rev.* **2007**, *36*, 1249-1262.

(25) Binder, W. H.; Sachsenhofer, R. *Macromol. Rapid Commun.* **2007**, *28*, 15-54.

(26) Zeitler, K.; Mager, I. *Adv. Synth. Catal.* **2007**, *349*, 1851-1857.

(27) Fournier, D.; Hoogenboom, R.; Schubert, U. S. *Chem. Soc. Rev.* **2007**, *36*, 1369-1380.

(28) Moorhouse, A. D.; Moses, J. E. *ChemMedChem* **2008**, *3*, 715-723.

(29) Tron, G. C.; Pirali, T.; Billington, R. A.; Canonico, P. L.; Sorba, G.; Genazzani, A. A. *Med. Res. Rev.* **2008**, *28*, 278-308.

(30) Rostovtsev, V. V.; Green, L. G.; Fokin, V. V.; Sharpless, K. B. *Angew. Chem. Int. Ed.* **2002**, *41*, 2596-2599.

(31) Himo, F.; Lovell, T.; Hilgraf, R.; Rostovtsev, V. V.; Noodleman, L.; Sharpless, K. B.; Fokin, V. V. *J. Am. Chem. Soc.* **2004**, *127*, 210-216.

(32) Kolb, H. C.; Sharpless, K. B. *Drug Discovery Today* **2003**.

(33) Boren, B. C.; Narayan, S.; Rasmussen, L. K.; Zhang, L.; Zhao, H.; Lin, Z.; Jia, G.; Fokin, V. V. *J. Am. Chem. Soc.* **2008**, *130*, 8923-8930.

(34) Chen, Y.; Liu, Y.; Petersen, J. L.; Shi, X. *Chem. Commun.* **2008**, *0*, 3254-3256.

(35) Liu, Y.; Yan, W.; Chen, Y.; Petersen, J. L.; Shi, X. *Org. Lett.* **2008**, *10*, 5389-5392.

(36) Sengupta, S.; Duan, H.; Lu, W.; Petersen, J. L.; Shi, X. *Org. Lett.* **2008**, *10*, 1493-1496.

(37) Duan, H.; Sengupta, S.; Petersen, J. L.; Shi, X. *Organometallics* **2009**, *28*, 2352-2355.

(38) Duan, H.; Sengupta, S.; Petersen, J. L.; Akhmedov, N. G.; Shi, X. *J. Am. Chem. Soc.* **2009**, *131*, 12100-12102.

(39) Duan, H.; Yan, W.; Sengupta, S.; Shi, X. *Bioorg. Med. Chem. Lett.* **2009**, *19*, 3899-3902.

(40) Wang, D.; Ye, X.; Shi, X. *Org. Lett.* **2010**, *12*, 2088-2091.

(41) Chen, Y.; Wang, D.; Petersen, J. L.; Akhmedov, N. G.; Shi, X. *Chem. Commun.* **2010**, *46*, 6147-6149.

(42) Chen, Y.; Wang, D.; Petersen, J. L.; Akhmedov, N. G.; Shi, X. *Chem. Commun.* **2010**, *46*, 6147-6149.

(43) Wang, D.; Zhang, Y.; Harris, A.; Gautam, L. N. S.; Chen, Y.; Shi, X. *Adv. Synth. Catal.* **2011**, *353*, 2584-2588.

(44) Wang, D.; Gautam, L. N. S.; Bollinger, C.; Harris, A.; Li, M.; Shi, X. *Org. Lett.* **2011**, *13*, 2618-2621.

(45) Wang, Q.; Aparaj, S.; Akhmedov, N. G.; Petersen, J. L.; Shi, X. *Org. Lett.* **2012**, *14*, 1334-1337.

(46) Tomas, F.; Abboud, J. L. M.; Laynez, J.; Notario, R.; Santos, L.; Nilsson, S. O.; Catalan, J.; Claramunt, R. M.; Elguero, J. *J. Am. Chem. Soc.* **1989**, *111*, 7348-7353.

(47) Abboud, J.-Luis M.; Foces-Foces, C.; Notario, R.; Trifonov, Rostislav E.; Volovodenko, Anna P.; Ostrovskii, Vladimir A.; Alkorta, I.; Elguero, J. *Eur. J. Org. Chem.* **2001**, *2001*, 3013-3024.

(48) Ichino, T.; Andrews, D. H.; Rathbone, G. J.; Misaizu, F.; Calvi, R. M. D.; Wren, S. W.; Kato, S.; Bierbaum, V. M.; Lineberger, W. C. *J. Phys. Chem. B* **2008**, *112*, 545-557.

(49) Ichino, T.; Kato, S.; Wren, S. W.; Bierbaum, V. M.; Lineberger, W. C. *J. Phys. Chem. A* **2008**, *112*, 9723-9730.

(50) Catalan, J.; Perez, P.; Elguero, J. *J. Org. Chem.* **1993**, *58*, 5276-5277.

(51) Palmer, M. H.; Kurshid, M. M. P.; Rayner, T. J.; Smith, J. A. S. *Chem. Phys.* **1994**, *182*, 27-37.

(52) Fischer, G.; Cao, X.; Purchase, R. L. *Chem. Phys. Lett.* **1996**, *262*, 689-698.

(53) Arduengo, A. J.; Harlow, R. L.; Kline, M. *J. Am. Chem. Soc.* **1991**, *113*, 361-363.

(54) Breslow, R. *Chem. Ind.* **1957**, *26*, 893-894.

(55) Breslow, R. *J. Am. Chem. Soc.* **1957**, *79*, 1762-1763.

(56) Breslow, R. *Chem. Ind.* **1957**, 893-894.

(57) Breslow, R. *J. Am. Chem. Soc.* **1958**, *80*, 3719-3726.

(58) Wöhler, L. *Annalen der Pharmacie* **1832**, *3*, 249-282.

(59) Bredig, H. G.; Stern, E. *Elektrochem* **1904**, *10*, 582-587.

(60) Lachman, A. *J. Am. Chem. Soc.* **1923**, *46*, 708-723.

(61) Buck, J. S.; Ide, W. S. *J. Am. Chem. Soc.* **1931**, *53*, 2350-2353.

(62) Sumrell, G.; Stevens, J. I.; Goheen, G. E. *J. Org. Chem.* **1957**, *22*, 39-41.

(63) Kuebrich, J. P.; Schowen, R. L.; Wang, M.-s.; Lupes, M. E. *J. Am. Chem. Soc.* **1971**, *93*, 1214-1220.

(64) Yamabe, S.; Yamazaki, S. *Org. Biomol. Chem.* **2009**, *7*, 951-961.

(65) Wanzlick, H. W.; Schikora, E. *Angew. Chem.* **1960**, *72*, 494-494.

(66) Wanzlick, H. W.; Schikora, E. *Chem. Ber.* **1961**, *94*, 2389-2393.

(67) Wanzlick, H. W.; Kleiner, H. J. *Angew. Chem.* **1961**, *73*, 493-493.

(68) Wanzlick, H.-W.; Esser, F.; Kleiner, H.-J. *Chem. Ber.* **1963**, *96*, 1208-1212.

(69) Lemal, D. M.; Lovald, R. A.; Kawano, K. I. *J. Am. Chem. Soc.* **1964**, *86*, 2518-2519.

(70) Winberg, H. E.; Downing, J. R.; Coffman, D. D. *J. Am. Chem. Soc.* **1965**, *87*, 2054-2055.

(71) Castells, J.; López-Calahorra, F.; Geijo, F.; Pérez-Dolz, R.; Bassedas, M. *J. Heterocycl. Chem.* **1986**, *23*, 715-720.

(72) Castells, J.; Lopez-Calahorra, F.; Domingo, L. *J. Org. Chem.* **1988**, *53*, 4433-4436.

(73) Martí, J.; Castells, J.; López-Calahorra, F. *Tetrahedron Lett.* **1993**, *34*, 521-524.

(74) Castells, J.; Domingo, L.; López-Calahorra, F.; Martí, J. *Tetrahedron Lett.* **1993**, *34*, 517-520.

(75) Martí, J.; López-Calahorra, F.; Bofill, J. M. *J. Mol. Struct. THEOCHEM* **1995**, *339*, 179-194.

(76) López-Calahorra, F.; Castro, E.; Ochoa, A.; Martí, J. *Tetrahedron Lett.* **1996**, *37*, 5019-5022.

(77) Alder, R. W.; Allen, P. R.; Murray, M.; Orpen, A. G. *Angew. Chem. Int. Ed.* **1996**, *35*, 1121-1123.

(78) Breslow, R.; Kim, R. *Tetrahedron Lett.* **1994**, *35*, 699-702.

(79) Breslow, R.; Schmuck, C. *Tetrahedron Lett.* **1996**, *37*, 8241-8242.

(80) Sheehan, J. C.; Bennett, G. B.; Schneider, J. A. *J. Am. Chem. Soc.* **1966**, *88*, 3455-3456.

(81) Sheehan, J. C.; Hara, T. *J. Org. Chem.* **1974**, *39*, 1196-1199.

(82) Tagaki, W.; Tamura, Y.; Yano, Y. *Bull. Chem. Soc. Jpn* **1980**, *53*, 478-480.

(83) Knight, R. L.; Leeper, F. J. *Tetrahedron Lett.* **1997**, *38*, 3611-3614.

(84) Dvorak, C. A.; Rawal, V. H. *Tetrahedron Lett.* **1998**, *39*, 2925-2928.

(85) Arduengo, A. J.; Dias, H. V. R.; Harlow, R. L.; Kline, M. *J. Am. Chem. Soc.* **1992**, *114*, 5530-5534.

(86) Arduengo, A. J.; Goerlich, J. R.; Marshall, W. J. *J. Am. Chem. Soc.* **1995**, *117*, 11027-11028.

(87) Arduengo, A. J.; Davidson, F.; Dias, H. V. R.; Goerlich, J. R.; Khasnis, D.; Marshall, W. J.; Prakasha, T. K. *J. Am. Chem. Soc.* **1997**, *119*, 12742-12749.

(88) Arduengo, A. J.; Krafczyk, R. *Chemie in unserer Zeit* **1998**, *32*, 6-14.

(89) Arduengo, A. J.; Bannenberg, T. P.; Tapu, D.; Marshall, W. J. *Chem. Lett.* **2005**, *34*, 1010-1011.

(90) Akira, M.; Suzuki, Y.; Iwamoto, K.-i.; Higashino, T. *Chemical & Pharmaceutical Bulletin* **1994**, *42*, 2633-2635.

(91) Gao, G.; Xiao, R.; Yuan, Y.; Zhou, C.-H.; You, J. *Journal of Chemical Research, Synopses* **2002**, 262-263.

(92) Xu, L.-W.; Gao, Y.; Yin, J.-J.; Li, L.; Xia, C.-G. *Tetrahedron Lett.* **2005**, *46*, 5317-5320.

(93) Estager, J.; Lévêque, J.-M.; Turgis, R.; Draye, M. *Journal of Molecular Catalysis A: Chemical* **2006**, *256*, 261-264.

(94) Iwamoto, K.-i.; Hamaya, M.; Hashimoto, N.; Kimura, H.; Suzuki, Y.; Sato, M. *Tetrahedron Lett.* **2006**, *47*, 7175-7177.

(95) Enders, D.; Breuer, K.; Teles, J. H. *Helvetica Chimica Acta* **1996**, *79*, 1217-1221.

(96) Enders, D.; Breuer, K.; Runsink, J.; Teles, J. H. *Helvetica Chimica Acta* **1996**, *79*, 1899-1902.

(97) Enders, D.; Kallfass, U. *Angew. Chem. Int. Ed.* **2002**, *41*, 1743-1745.

(98) Enders, D.; Niemeier, O.; Henseler, A. *Chem. Rev.* **2007**, *107*, 5606-5655.

(99) L. Knight, R.; J. Leeper, F. *Journal of the Chemical Society, Perkin Transactions 1* **1998**, *0*, 1891-1894.

(100) Ma, Y.; Wei, S.; Wu, J.; Yang, F.; Liu, B.; Lan, J.; Yang, S.; You, J. *Adv. Synth. Catal.* **2008**, *350*, 2645-2651.

(101) O'Toole, S. E.; Connon, S. J. *Org. Biomol. Chem.* **2009**, *7*, 3584-3593.

(102) Soeta, T.; Tabatake, Y.; Inomata, K.; Ukaji, Y. *Tetrahedron* **2012**, *68*, 894-899.

(103) Fenn, J. B.; Mann, M.; Meng, C. K.; Wong, S. F.; Whitehouse, C. M. *Science* **1989**, *246*, 64-71.

(104) Santos, L. S.; Pavam, C. H.; Almeida, W. P.; Coelho, F.; Eberlin, M. N. *Angew. Chem. Int. Ed.* **2004**, *43*, 4330-4333.

(105) McCusker, K. P.; Medzihradszky, K. F.; Shiver, A. L.; Nichols, R. J.; Yan, F.; Maltby, D. A.; Gross, C. A.; Galonić Fujimori, D. *J. Am. Chem. Soc.* **2012**, *134*, 18074-18081.

(106) Schrader, W.; Handayani, P. P.; Burstein, C.; Glorius, F. *Chem. Commun.* **2007**, *0*, 716-718.

(107) Lalli, P. M.; Rodrigues, T. S.; Arouca, A. M.; Eberlin, M. N.; Neto, B. A. D. *RSC Advances* **2012**, *2*, 3201-3203.

(108) Scigelova, M.; Hornshaw, M.; Giannakopulos, A.; Makarov, A. *Mol Cell Proteomics* **2011**, *10*, 1-19.

(109) Amster, I. J. *J. Mass Spectrom.* **1996**, *31*, 1325-1337.

(110) Marshall, A. G.; Grosshans, P. B. *Anal. Chem.* **1991**, *63A*, 215-229.

(111) Lawrence, E. O.; Edlefsen, N. E. *Science* **1930**, *72*, 376-377.

(112) Comisarow, M. B.; Marshall, A. G. *Chem. Phys. Lett.* **1974**, *25*, 282-283.

(113) Paul, W. *Angew. Chem.* **1990**, *102*, 780-789.

(114) March, R. E. *Quadrupole ion Trap Mass Spectrometer;* , John Wiley & Sons Ltd: Chichester, 2000.

(115) Michelson, A. Z.; Chen, M.; Wang, K.; Lee, J. K. *J. Am. Chem. Soc.* **2012**, *134*, 9622-9633.

(116) Chesnavich, W. J.; Su, T.; Bowers, M. T. *J. Chem. Phys.* **1980**, *72*, 2641-2655.

(117) Su, T.; Chesnavich, W. J. *J. Chem. Phys.* **1982**, *76*, 5183-5185.

(118) Cooks, R. G.; Kruger, T. L. *J. Am. Chem. Soc.* **1977**, *99*, 1279-1281.

(119) McLuckey, S. A.; Cameron, D.; Cooks, R. G. *J. Am. Chem. Soc.* **1981**, *103*, 1313-1317.

(120) McLuckey, S. A.; Cooks, R. G.; Fulford, J. E. *Int. J. Mass Spectrom. Ion Processes* **1983**, *52*, 165-174.

(121) Brodbelt-Lustig, J. S.; Cooks, R. G. *Talanta* **1989**, *36*, 255-260.

(122) Green-Church, K. B.; Limbach, P. A. *J. Am. Soc. Mass. Spectrom.* **2000**, *11*, 24-32.

(123) *Frisch, M. J. et al.; Gaussian 03. Gaussian, Inc., Wallingford CT, 2004.*

(124) Frisch, M. J. *et al.; Gaussian 09. Gaussian, Inc., Wallingford CT, 2009*.

(125) Bartmess, J. E.; Georgiadis, R. M. *Vacuum* **1983**, *33*, 149-153.

(126) Sharma, S.; Lee, J. K. *J. Org. Chem.* **2004**, *69*, 7018-7025.

(127) Drahos, L.; Vékey, K. *J. Mass Spectrom.* **1999**, *34*, 79-84.

(128) Ervin, K. M. *Chem. Rev.* **2001**, *101*, 391-444.

(129) Gronert, S.; Feng, W. Y.; Chew, F.; Wu, W. *Int. J. Mass. Spectrom. Ion Proc.* **2000**, *196*, 251-258.

(130) Lee, C.; Yang, W.; Parr, R. G. *Phys. Rev. B* **1988**, *37*, 785-789.

(131) Kohn, W.; Becke, A. D.; Parr, R. G. *J. Phys. Chem.* **1996**, *100*, 12974-12980.

(132) Becke, A. D. *J. Chem. Phys.* **1992**, *98*, 5648-5652.

(133) Meot-Ner, M. *J. Am. Chem. Soc.* **1979**, *101*, 2396-2403.

(134) We did not conduct Cooks kinetic method measurements of 6-chloropurine acidity and PA due to experimental difficulties associated with forming proton-bound dimers.

(135) MasaoKa, A.; Terato, H.; Kobayashi, M.; Honsho, A.; Ohyaya, Y.; Ide, H. *J. Biol. Chem.* **1999**, *274*, 25136-25143.

(136) Terato, H.; Masaoka, A.; Asagoshi, K.; Honsho, A.; Ohyaya, Y.; Suzuki, T.; Yamada, M.; Makino, K.; Yamamoto, K.; Ide, H. *Nucleic Acids Res.* **2002**, *30*, 4975-4984.

(137) *DNA Damage and Repair, Vol. 1: DNA Repair in Procaryotes and Lower Eucaryotes;* , Nickoloff, J. A.; Hoekstra, M. F., Eds.; Humana Press, Inc.: Totowa, NJ, 1998.

(138) Guliaev, A. B.; Singer, B.; Hang, B. *DNA Repair* **2004**, *3*, 1311-1321.

(139) Bjelland, S.; Birkeland, N.-K.; Benneche, T.; Volden, G.; Seeberg, E. *J. Biol. Chem.* **1994**, *269*, 30489-30495.

(140) Zhao, B.; O'Brien, P. J. *Biochemistry* **2011**, *50*, 4350-4359.

(141) Hollis, T.; Lau, A.; Ellenberger, T. *Mutation Research* **2000**, *460*, 201-210.

(142) Berdal, K. G.; Johanson, R. F.; Seeberg, E. *EMBO J.* **1998**, *17*, 363-367.

(143) Habraken, Y.; Ludlum, D. B. *Carcinogenesis* **1989**, *10*, 489-492.

(144) Habraken, Y.; Carter, C. A.; Kirk, M. C.; Ludlum, D. B. *Cancer Research* **1991**, *51*, 499-503.

(145) Zhachkina, A.; Liu, M.; Sun, X.; Amegayibor, S.; Lee, J. K. *J. Org. Chem.* **2009**, *74*, 7429-7440.

(146) Binder, W. H.; Kluger, C. *Curr. Org. Chem.* **2006**, *10*, 1791-1815.

(147) Maliakal, A.; Lem, G.; Turro, N. J.; Ravichandran, R.; Suhadolnik, J. C.; DeBellis, A. D.; Wood, M. G.; Lau, J. *J. Phys. Chem. A* **2002**, *106*, 7680-7689.

(148) Sivakumar, K.; Xie, F.; Cash, B. M.; Long, S.; Barnhill, H. N.; Wang, Q. *Org. Lett.* **2004**, *6*, 4603-4606.

(149) Costa, M. S.; Boechat, N.; Rangel, É. A.; da Silva, F. d. C.; de Souza, A. M. T.; Rodrigues, C. R.; Castro, H. C.; Junior, I. N.; Lourenço, M. C. S.; Wardell, S. M. S. V.; Ferreira, V. F. *Bioorg. Med. Chem.* **2006**, *14*, 8644-8653.

(150) Angelos, S.; Yang, Y.-W.; Patel, K.; Stoddart, J. F.; Zink, J. I. *Angew. Chem. Int. Ed.* **2008**, *47*, 2222-2226.

(151) Eyet, N.; Villano, S. M.; Bierbaum, V. M. *Int. J. Mass Spectrom.* **2009**, *283*, 26-29.

(152) Olmstead, W. N.; Brauman, J. I. *J. Am. Chem. Soc.* **1977**, *99*, 4219-4228.

(153) Gronert, S. *Chem. Rev.* **2001**, *101*, 329-360.

(154) DePuy, C. H.; Bierbaum, V. M. *Acc. Chem. Res.* **1981**, *14*, 146-153.

(155) Protonated **1b** and **1c** are the same structure and deprotonated **1a**, **1b**, and **1c** are also the same structure. Calculations indicate less than a 1 kcal mol^{-1} difference between the stabilities of **1b** and **1c**, so arguments that apply to the possible presence of **1b** apply to **1c** as well; that is, either and/or both could be present.

(156) This value was also previously measured by Abboud and coworkers to be 222.6 kcal mol^{-1}. See reference 43.

(157) Catalan, J.; Claramunt, R. M.; Elguero, J.; Laynez, J.; Menendez, M.; Anvia, F.; Quian, J. H.; Taagepera, M.; Taft, R. W. *J. Am. Chem. Soc.* **1988**, *110*, 4105-4111.

(158) Tomas, F.; Catalan, J.; Perez, P.; Elguero, J. *J. Org. Chem.* **1994**, *59*, 2799-2802.

(159) Roth, W.; Spangenberg, D.; Janzen, C.; Westphal, A.; Schmitt, M. *Chem. Phys.* **1999**, *248*, 17-25.

(160) Escande, A.; Galigne, J. L.; Lapasset, J. *Acta Crystallogr B* **1974**, *30*, 1490-1495.

(161) Bigotto, A.; Nand Pandey, A.; Zerbo, C. *Spectrosc. Lett.* **1996**, *29*, 511-522.

(162) Jacoby, C.; Roth, W.; Schmitt, M. *Appl. Phys. B* **2000**, *71*, 643-649.

(163) Fagel, J. E.; Ewing, G. W. *J. Am. Chem. Soc.* **1951**, *73*, 4360-4362.

(164) Jagerovic, N.; Jimeno, M. L.; Alkorta, I.; Elguero, J.; Claramunt, R. M. *Tetrahedron* **2002**, *58*, 9089-9094.

(165) Gaemers, S.; Elsevier, C. J. *Magn. Reson. Chem.* **2000**, *38*, 650-654.

(166) Ugai, T.; Tanaka, S.; Dokawa, S. *J. Pharm. Soc. Jpn.* **1943**, *63*, 269-300.

(167) Lapworth, A. *J. Chem. Soc., Trans.* **1904**, *85*, 1206-1214.

(168) Berkessel, A.; Elfert, S.; Yatham, V. R.; Neudörfl, J.-M.; Schlörer, N. E.; Teles, J. H. *Angew. Chem. Int. Ed.* **2012**, *51*, 12370-12374.

(169) Baragwanath, L.; Rose, C. A.; Zeitler, K.; Connon, S. J. *J. Org. Chem.* **2009**, *74*, 9214-9217.

(170) López-Calahorra, F.; Rubires, R. *Tetrahedron* **1995**, *51*, 9713-9728.

(171) Chen, Y. T.; Jordan, F. *J. Org. Chem.* **1991**, *56*, 5029-5038.

(172) Chen, Y.-T.; Barletta, G. L.; Haghjoo, K.; Cheng, J. T.; Jordan, F. *J. Org. Chem.* **1994**, *59*, 7714-7722.

(173) Fenn, J.; Mann, M.; Meng, C.; Wong, S.; Whitehouse, C. *Science* **1989**, *246*, 64-71.

(174) Marcotullio, M. C.; Campagna, V.; Sternativo, S.; Costantino, F.; Curini, M. *Synthesis* **2006**, *16*, 2760-2766.

(175) Klinman, J. P.; McCusker, K. P. *Tetrahedron Lett.* **2009**, *50*, 611-613.

Title: Gas-Phase Studies of Purine 3-Methyladenine DNA Glycosylase II (AlkA) Substrates

Author: Anna Zhachkina Michelson, Mu Chen, Kai Wang, and Jeehiun K. Lee

Publication: Journal of the American Chemical Society

Publisher: American Chemical Society

Date: Jun 1, 2012

PERMISSION/LICENSE IS GRANTED FOR YOUR ORDER AT NO CHARGE

This type of permission/license, instead of the standard Terms & Conditions, is sent to you because no fee is being charged for your order. Please note the following:

- Permission is granted for your request in both print and electronic formats, and translations.
- If figures and/or tables were requested, they may be adapted or used in part.
- Please print this page for your records and send a copy of it to your publisher/graduate school.
- Appropriate credit for the requested material should be given as follows: "Reprinted (adapted) with permission from (COMPLETE REFERENCE CITATION). Copyright (YEAR) American Chemical Society." Insert appropriate information in place of the capitalized words.
- One-time permission is granted only for the use specified in your request. No additional uses are granted (such as derivative works or other editions). For any other uses, please submit a new request.

Title:	1,2,3-Triazoles: Gas Phase Properties
Author:	Kai Wang, Mu Chen, Qiaoyi Wang, Xiaodong Shi, and Jeehiun K. Lee
Publication:	The Journal of Organic Chemistry
Publisher:	American Chemical Society
Date:	Jul 1, 2013

PERMISSION/LICENSE IS GRANTED FOR YOUR ORDER AT NO CHARGE

This type of permission/license, instead of the standard Terms & Conditions, is sent to you because no fee is being charged for your order. Please note the following:

- Permission is granted for your request in both print and electronic formats, and translations.
- If figures and/or tables were requested, they may be adapted or used in part.
- Please print this page for your records and send a copy of it to your publisher/graduate school.
- Appropriate credit for the requested material should be given as follows: "Reprinted (adapted) with permission from (COMPLETE REFERENCE CITATION). Copyright (YEAR) American Chemical Society." Insert appropriate information in place of the capitalized words.
- One-time permission is granted only for the use specified in your request. No additional uses are granted (such as derivative works or other editions). For any other uses, please submit a new request.